

5-26-2015 12:00 AM

## Biosorption Processes for Removal of Toxic Metals from Wastewaters

Shahram Amirnia, *The University of Western Ontario*

Supervisor: Argyrios Margaritis, *The University of Western Ontario*

A thesis submitted in partial fulfillment of the requirements for the Doctor of Philosophy degree  
in Chemical and Biochemical Engineering

© Shahram Amirnia 2015

Follow this and additional works at: <https://ir.lib.uwo.ca/etd>

 Part of the [Chemical Engineering Commons](#)

---

### Recommended Citation

Amirnia, Shahram, "Biosorption Processes for Removal of Toxic Metals from Wastewaters" (2015).  
*Electronic Thesis and Dissertation Repository*. 2929.  
<https://ir.lib.uwo.ca/etd/2929>

This Dissertation/Thesis is brought to you for free and open access by Scholarship@Western. It has been accepted for inclusion in Electronic Thesis and Dissertation Repository by an authorized administrator of Scholarship@Western. For more information, please contact [wlsadmin@uwo.ca](mailto:wlsadmin@uwo.ca).

# **BIOSORPTION PROCESSES FOR REMOVAL OF TOXIC METALS FROM WASTEWATERS**

(Thesis Format: Integrated Article)

by

Shahram Amirnia

Graduate Program in Chemical and Biochemical Engineering

A thesis submitted in partial fulfillment  
of the requirements for the degree of  
Doctor of Philosophy

The School of Graduate and Postdoctoral Studies  
The University of Western Ontario  
London, Ontario, Canada

© Shahram Amirnia 2015

# Abstract

Excessive and cumulative release of toxic metals from industrial effluents due to rapid industrialization has posed hazard to aquatic ecosystem integrity and environmental/human health. The inadequacy and high cost of traditional metal treatment technologies coupled with the imposition of stricter environmental regulations and guidelines for industrial point source discharges have increased the demand for economically feasible alternative methods.

Application of natural and abundant sorption material known as biosorbents comprising microbial biomass, agriculture waste, and industrial waste biomass, has gained international attention in scientific world as a low-cost and effective method for removal of heavy metals from aqueous solutions. However, this method has not been able to gain the attention of industry for large-scale applications thus far.

This research was aimed to further evaluate the potential of biosorption technique in more realistic conditions appealing to industry by exploiting locally available biosorbents undergoing minimum pretreatment steps, combining living and non-living microbial biosorbents without any heat-inactivation, employing continuous-flow systems, and regenerating the used biomass for recovery of the mixture of heavy metals.

The toxic metals of interest for biosorption in this work were copper, lead, and zinc, and biosorbents selected were cells of *Saccharomyces cerevisiae* as a microbial biomass and *Acer saccharum* tree leaves as an agro-waste. Sorption performances of the biosorbents were evaluated through classical adsorption equilibrium isotherms and kinetics in batch systems, and supplemented by dynamic continuous flow studies, which may serve as a basis for equipment sizing and scale up of the biosorption systems.

Batch sorption studies revealed that pseudo-second order and Langmuir isotherm models were suitable to describe the metals sorption kinetics and equilibrium, respectively. Evaluation of biosorption performance and selection of best biosorbent using the Langmuir isotherm constants correctly were thoroughly discussed based on dynamic equilibrium between the metal species and biosorbents active sites.

Design of experiment technique was used to determine model equations describing the removal efficiencies of mixture of the target metals by *Saccharomyces cerevisiae* with respect to operating conditions such as pH, metal concentration, and biomass dose. The selectivity order of  $\text{Pb}^{2+} > \text{Cu}^{2+} > \text{Zn}^{2+}$  was achieved by yeast cells with  $\text{Pb}^{2+}$  ions removal efficiencies reaching up to 98%. Process optimization helped to evaluate the simultaneous effects of pH, initial metal concentration, and biomass dose on competitive biosorption of metals by yeast cells. Characterization of metal-biomass interactions responsible for biosorption was studied employing zeta potential, BET, FT-IR, and SEM-EDX techniques. The results suggested the involvement of electrostatic interactions, ion exchange, interparticle sequestration, and a weak surface binding in adsorption of the metals by the selected biosorbents.

The use of unmodified yeast cells in a self-contained continuous system was shown to be an effective metal biosorption method by minimizing biomass pretreatment and preparation steps as well as achieving an on-line and concurrent biosorbent production and metal biosorption within the same system.

Biosorptive performance of maple leaves in multiple column sorption-desorption cycles showed no degradation on metal capacity of the biomass (18.3 mg Cu/g) with increasing cycles despite shortening breakthrough times. Biomass regeneration efficiencies up to 98% were achieved using a weak acid as eluent. The presented simplified mass transfer model based on rapid local equilibrium and an apparent dispersion coefficient well simulated the dynamic operation of the packed bed biosorption column.

Research conducted in this thesis can be of value to industries searching for efficient, simple, and green alternative metal treatment methods to meet the regulatory limits for the heavy metals discharges at a lower cost.

**Keywords:** Heavy metals; Biosorption; *Saccharomyces cerevisiae*; *Acer saccharum*; Langmuir isotherm; Sorption kinetics; Batch and column studies; Continuous bioreactor-biosorption system

## Co-Authorship Statement

Publications originating from this thesis and the individual contributions of all members in each article are listed below.

**Chapter 2:** A version of this chapter was published as: “Amirnia S., Margaritis A., Ray M.B., Adsorption of mixtures of toxic metal ions using non-viable cells of *Saccharomyces cerevisiae*, Adsorption Science & Technology, 30, 1 (2012), 43-64”. Experimental work, data analysis and writing of the manuscript were done by Shahram Amirnia under the guidance and supervision of Dr. A. Margaritis and Dr. M.B. Ray who also revised the article and made recommendations and corrections.

**Chapter 3:** A version of this chapter was published as: “Amirnia S., Margaritis A., Ray M.B., Heavy metals removal from aqueous solutions using *Saccharomyces cerevisiae* in a novel continuous bioreactor–biosorption system, Chemical Engineering Journal, 264, (2015) 863–872”. Experimental work, data analysis and writing of the manuscript were done by Shahram Amirnia under the guidance and supervision of Dr. A. Margaritis and Dr. M.B. Ray who also revised the article and made recommendations and corrections.

**Chapter 4:** Amirnia S., Margaritis A., Ray M.B., “Copper Ions Removal by *Acer saccharum* Leaves in a Regenerable Continuous-flow Column”. Experimental work, data analysis, and manuscript preparation were done by Shahram Amirnia under the guidance and supervision of Dr. A. Margaritis and Dr. M.B. Ray who also revised the article and made recommendations and corrections. An article based on this chapter is in preparation for publication.

**Chapter 5:** Amirnia S., Margaritis A., Ray M.B., “Evaluation and Selection of Biosorbents Based on the Use of Langmuir Isotherm Constants”. The data analysis and writing the draft of the manuscript was done by Shahram Amirnia under the supervision of Dr. M.B. Ray and Dr. A. Margaritis who also revised and corrected the manuscript. An article based on this chapter is in preparation for publication.

# Acknowledgements

I wish to express my sincere appreciation and thanks to my thesis supervisors Professor Argyrios Margaritis and Professor Mita Ray for defining this project and their continuous help, supervision, and financial support during this research.

This work could never have been done without the unfailing support of my wife Dr. Neda Alizadeh who was always there for me, and the heavenly smiles of my children Melissa and Benjamin, which were always giving me the energy to work harder.

I am indebted to Dr. Dennis O'Carroll from Civil & Environmental Engineering Department for letting me use the ICP-OES in his lab, and to Tim Stephen who was always ready to offer technical assistance. I would like to extend my thanks and acknowledgements to the Chemical & Biochemical Engineering (CBE) lab technicians, Souheil Afara and Brian Dennis, for their technical assistance during this study. The completion of this thesis would not have been possible without their support.

Finally, I would like to value and remember all who rendered help in completion of this thesis, in particular my dear friends Reyna Gómez Flores, Isabela Reiniati, Cody Bulmer, Dr. Anil Kumar Jhavar, Dr. Kalin Penev, and Dr. Pegah Saremirad for their help, company, and encouragements during this research work. I would also like to thank all current and former CBE department staff who helped me during my PhD: graduate coordinators Ashley Jokhu, Kristen Hunt, and Joanna Blom, as well as administrative officers April Finkenhoefer, Kara Malott, and Sarah Williams.

This research project was supported by NSERC Discovery Grant No. 4388 awarded to Dr. Argyrios Margaritis, and NSERC Discovery Grant awarded to Dr. Mita Ray.



# **Dedication**

To my lovely family Neda, Melissa, Benjamin, my parents Vaji and Yadegar, and my brothers Mehdi and Reza.

# Table of Contents

ABSTRACT .....	II
Co-AUTHORSHIP STATEMENT.....	V
ACKNOWLEDGEMENTS.....	VII
DEDICATION .....	VIII
LIST OF TABLES .....	XII
LIST OF FIGURES .....	XIV
NOMENCLATURE.....	XX
CHAPTER 1.....	1
INTRODUCTION .....	1
1.1. METALS IN THE ENVIRONMENT: THREATS .....	2
1.2. TOXICITY OF HEAVY METALS .....	4
1.3. GLOBAL TOXIC METAL EMISSION INVENTORIES .....	6
1.4. CONVENTIONAL METAL DECONTAMINATION TECHNOLOGIES; DEMERITS .....	7
1.5. BIOSORPTION – BENEFITS AND GAPS .....	7
1.6. BIOSORBENTS .....	10
1.7. RESEARCH OBJECTIVES.....	13
1.8. EXPERIMENTAL METHODOLOGY AND CONFIGURATION .....	15
1.9. REFERENCES.....	20
CHAPTER 2 .....	28
ADSORPTION OF TOXIC METALS MIXTURE USING NON-VIABLE CELLS OF <i>SACCHAROMYCES CEREVISIAE</i> .....	28
ABSTRACT.....	29
2.1. INTRODUCTION .....	29
2.2. MATERIALS AND METHODS .....	31
2.2.1. Biomass preparation.....	31
2.2.2. Biosorption experiments and metal analysis.....	32
2.2.3. Single metal solution chemistry (chemical equilibrium) .....	33
2.2.4. Characterization of yeast surface .....	34
2.2.5. Response surface methodology (RSM) for biosorption optimization .....	34
2.3. RESULTS AND DISCUSSION.....	35
2.3.1. Multi-metal speciation modeling .....	35
2.3.2. Single metal biosorption .....	36
2.3.3. Effect of nutrient composition on biosorption .....	38
2.3.4. Biosorption kinetics and isotherms .....	39
2.3.5. Ternary metal biosorption system.....	41
2.3.6. Competitive metal uptake (ternary metal system of Pb, Cu, and Zn) .....	50
2.3.7. Characterization of yeast-metal interactions (mechanism of biosorption).....	52
2.3.8. Biosorption process optimization .....	56

2.4.	CONCLUSIONS .....	56
2.5.	ACKNOWLEDGEMENT .....	57
2.6.	REFERENCES .....	58
CHAPTER 3 .....		62
REMOVAL OF HEAVY METALS FROM AQUEOUS SOLUTIONS USING <i>SACCHAROMYCES CEREVISIAE</i> IN A CONTINUOUS BIOREACTOR- BIOSORPTION SYSTEM .....		62
ABSTRACT .....		63
3.1.	INTRODUCTION.....	63
3.2.	MATERIAL AND METHODS .....	65
3.2.1.	Biomass Preparation .....	65
3.2.2.	Analytical method .....	67
3.2.3.	Maximum specific growth rate of yeast cells .....	68
3.2.4.	Continuous biosorption operation.....	69
3.2.5.	Adsorption column.....	70
3.2.6.	Adsorption surface area .....	71
3.3.	RESULTS AND DISCUSSION.....	72
3.3.1.	Optimal physicochemical conditions .....	72
3.3.2.	Mixing time.....	74
3.3.3.	Continuous adsorption studies .....	75
3.3.4.	Continuous vs. batch sorption.....	75
3.3.5.	Retention of metal-loaded biomass.....	78
3.3.6.	Effect of mass flowrate .....	79
3.3.7.	Adsorption isotherms .....	81
3.3.8.	Adsorption kinetics .....	83
3.3.9.	Diffusion-based kinetics .....	86
3.3.10.	Biosorption mechanism – further insights .....	91
3.3.11.	Large-scale applicability .....	93
3.4.	CONCLUSIONS .....	94
3.5.	ACKNOWLEDGEMENTS .....	95
3.6.	REFERENCES .....	95
CHAPTER 4 .....		100
COPPER IONS REMOVAL BY <i>ACER SACCHARUM</i> LEAVES IN A REGENERABLE CONTINUOUS-FLOW COLUMN.....		100
ABSTRACT .....		101
4.1.	INTRODUCTION .....	101
4.2.	EXPERIMENTAL.....	104
4.2.1.	Sorbent preparation and analysis .....	104
4.2.2.	Sorbate analysis .....	104
4.2.3.	Biosorption column set-up and operation .....	105
4.2.4.	Column bed void fraction .....	106
4.2.5.	Bed density.....	106
4.2.6.	Column biosorption capacity .....	106
4.2.7.	Characterization of biosorbent.....	108

4.2.8. Modeling error analysis .....	109
4.3. RESULTS AND DISCUSSION .....	109
4.3.1. Batch Studies .....	110
4.3.1.1. Effect of particle size .....	110
4.3.1.2. Biosorption equilibrium isotherms .....	110
4.3.1.3. Biosorption kinetics .....	112
4.3.1.3.1. Effects of MTL dose and Cu(II) concentration.....	112
4.3.1.3.2. Diffusion-based kinetics .....	115
4.3.1.4. Regeneration of MTL (Desorption of Copper form MTL).....	117
4.3.2. Column Studies .....	118
4.3.2.1. Modeling .....	119
4.3.2.2. Column biosorption performance .....	121
4.3.2.3. Desorption .....	125
4.3.2.4. Effect of process parameters .....	126
4.3.3. Characterization of MTL .....	130
4.4. CONCLUSIONS .....	133
4.5. ACKNOWLEDGEMENTS .....	134
4.6. REFERENCES .....	134
CHAPTER 5 .....	140
EVALUATION AND SELECTION OF BIOSORBENTS BASED ON THE USE OF LANGMUIR ISOTHERM.....	140
ABSTRACT .....	141
5.1. INTRODUCTION.....	141
5.2. DISCUSSION.....	143
5.2.1. Derivation of Langmuir Equation Constant.....	146
5.2.2. Estimation of biosorption thermodynamics by Langmuir isotherm constant .....	153
5.3. CONCLUSIONS .....	154
5.4. ACKNOWLEDGEMENTS .....	155
5.5. REFERENCES .....	155
CHAPTER 6 .....	159
CONCLUSIONS AND RECOMMENDATIONS .....	159
6.1. CONCLUSIONS .....	160
6.2. RECOMMENDATIONS FOR FUTURE WORK .....	162
CURRICULUM VITAE.....	164

## List of Tables

Table 1.1. Primary natural and anthropogenic sources of metals in the earth's atmosphere (Nriagu, 1990).....	3
Table 1.2. Permissible levels of heavy metals in drinking water and mining effluents, and adverse health effects of metals on human health.....	5
Table 1.3. Global inputs of heavy metals into aquatic ecosystems (Nriagu, 1990).....	6
Table 1.4. Technology comparisons for heavy metal treatment.....	8
Table 1.5. Typical biosorption capacities of different unmodified natural biomass types for metals.....	12
Table 2.1. Experimental design for multi-metal (Pb, Cu, and Zn) biosorption.....	35
Table 2.2. Parameters of Langmuir isotherm for single metal biosorption.....	40
Table 2.3. Central composite design with codified (x1, x2, x3), real values (X1, X2, X3), and responses for ternary metal biosorption system.....	42
Table 2.4. Statistical analysis (analysis of variance table) results for the experimental design models.....	43
Table 2.5. Ionic properties of tested metals in biosorption by yeast cells.....	52
Table 2.6. FT-IR adsorption bands and suggested corresponding groups of control and Cu-loaded yeast biomass.....	54
Table 2.7. Optimal conditions for removal of a mixture of Pb <sup>2+</sup> , Zn <sup>2+</sup> , and Cu <sup>2+</sup> ions by biosorption using yeast biomass to reach the target of 90% Pb <sup>2+</sup> removal in a ternary metal wastewater stream.....	56

Table 3.1. Metal and biomass concentration fluctuations in the inlet of biosorption tank affected by the flowrate ratio of metal over biomass.....	73
Table 3.2. Langmuir isotherm model parameters for biosorption of metals in continuous system.....	83
Table 3.3. Copper adsorption rate constants associated with pseudo-first-order and the pseudo-second-order kinetics equations.....	85
Table 3.4. External mass transfer and intraparticle diffusion parameters for biosorption of Cu ions on yeast cells (biomass concentration: 1.5 g/l).....	91
Table 4.1. Parameters in the isotherm equations for biosorption of copper with MTL.....	113
Table 4.2. Rate constants and parameters associated with chemical sorption and diffusion-based kinetics for biosorption of Cu (II) ions onto MTL.....	116
Table 4.3. Column biosorption breakthrough parameters for eight sorption-desorption cycles (particle size 500 $\mu\text{m}$ - 1 mm; $\epsilon_b = 0.2621$ ).....	124
Table 4.4. Column performance data at different flowrates and inlet metal concentrations.....	128
Table 4.5. BET surface properties and BJH pore size and volume of ML (particle size < 250 $\mu\text{m}$ ).....	130
Table 5.1. Langmuir model parameters for Cd adsorption by 4 types of algae reproduced from Lodeiro et al. (2005). $q_{10}$ and $q_{200}$ are equilibrium uptake values at 10 and 200 mg/l Cd, respectively.....	152

## List of Figures

Figure 1.1. (a) Optical microscopy of hydrated yeast cells (40x); and (b) scanning electron micrograph of the dried yeast biomass.....	16
Figure 1.2. Fallen roadside maple tree leaves collected and used for biosorption studies as a locally available waste.....	17
Figure 1.3. Experimental set-up used for continuous-flow bioreactor-biosorption system for removal of heavy metals: (a) bioreactor system, (b) nutrients tank for biomass production, (c) biosorption vessel, (d) pH-controller, (e) settling tanks.....	18
Figure 1.4. Experimental set-up for removal of heavy metals by maple leaves biomass in packed-bed columns.....	19
Figure 2.1. Lead, Copper, and Zinc solution chemistry in single-metal solutions obtained by MINEQL+ version 3.01 (metal concentrations 45 mg/l).....	33
Figure 2.2. Zeta potential vs. pH for yeast cells before and after metal biosorption. 1 g/l of biomass and 45 mg/l of each metal in ternary metal solution were used.....	36
Figure 2.3. Percentage of $Pb^{2+}$ , $Zn^{2+}$ , and $Cu^{2+}$ ions in the solutions of 3-metal systems at different metal concentrations.....	37
Figure 2.4. Changes in the capacity of yeast cells to retain single metal ions with solution pH. (concentration of each metal: 45 mg/l).....	38
Figure 2.5. $Cu^{2+}$ Biosorption using yeast cells cultivated in different nutrient compositions (pH=5.50, biomass conc. 4 g/l, initial $Cu^{2+}$ concentration 45 mg/l).....	40
Figure 2.6. Response surface and contour curves showing the interactive effect of pH and biomass dose on percentage removal (RE) of $Cu^{2+}$ , keeping initial metal concentration at its centre level (30 mg/l).....	44

Figure 2.7. Response surface and contour plots showing the interactive effect of pH and initial metal concentration on removal efficiency (RE) of $\text{Cu}^{2+}$ , keeping biomass dose at its centre level (4 g/l).....	45
Figure 2.8. Response surface and contour plots showing the interactive effect of biomass dose and initial metal concentration on percentage removal (RE) of $\text{Cu}^{2+}$ , keeping pH at its centre level (pH=5.0).....	45
Figure 2.9. Response surface and contour curves showing the interactive effect of pH and biomass dose on percentage removal (RE) of $\text{Pb}^{2+}$ , keeping initial metal concentration at its centre level (30 mg/l).....	46
Figure 2.10. Response surface and contour plots showing the interactive effect of pH and initial metal concentration on removal efficiency (RE) of $\text{Pb}^{2+}$ , keeping biomass dose at its centre level (4 g/l).....	46
Figure 2.11. Response surface and contour plots showing the interactive effect of biomass dose and initial metal concentration on percentage removal (RE) of $\text{Pb}^{2+}$ , keeping pH at its centre level (pH=5.0).....	47
Figure 2.12. Experimental vs. predicted data for removal efficiency (RE) of $\text{Pb}^{2+}$ , $\text{Zn}^{2+}$ , and $\text{Cu}^{2+}$ in ternary metal system.....	47
Figure 2.13. Response surface and contour plots showing the interactive effect of pH and biomass dose on percentage removal (RE) of $\text{Zn}^{2+}$ , holding initial metal concentration at its centre level (30 mg/l).....	48
Figure 2.14. Response surface and contour plots showing the interactive effect of pH and initial metal concentration on removal efficiency (RE) of $\text{Zn}^{2+}$ , holding biomass dose at its centre level (4 g/l).....	48
Figure 2.15. Response surface and contour plots showing the interactive effect of biomass dose and initial metal concentration on removal efficiency (RE) of $\text{Zn}^{2+}$ , holding pH at its centre level (pH=5.0).....	49



Figure 2.16. Comparison of uptake of single metals (metal concentration: 50 mg/l; pH 5.50; biomass dose: 4g/l) with uptake of metals in a ternary metal system ( $\text{Pb}^{2+}$ : 50mg/l, $\text{Cu}^{2+}$ : 50mg/l, $\text{Zn}^{2+}$ : 50mg/l; pH: 5.50, biomass load: 4g/l).....	50
Figure 2.17. FTIR spectra of dried yeast biomass (a) before and (b) after metal adsorption.....	53
Figure 2.18. Elemental analyses for (a) untreated biomass; and (b) metal-treated biomass in simultaneous adsorption of $\text{Pb}^{2+}$ , $\text{Cu}^{2+}$ , and $\text{Zn}^{2+}$ .....	55
Figure 3.1. Schematic process flow diagram of the continuous biosorption system (sampling points are shown on the diagram).....	66
Figure 3.2. Schematic diagram of the 2-L double draft tube fluidized adsorption column: (A) liquid level, (B) head space, (C) sampling ports, (D) air jet orifices, (E) air inlet, (F) liquid outlet, (G) jacket (adapted from Bashar et al., 2003).....	67
Figure 3.3. Yeast growth curves in batch and continuous culture. In the continuous system, the growth curve became constant at the biomass concentration of 3 g/l at the end of exponential growth phase.....	70
Figure 3.4. Size of yeast cells observed under optical microscope with 100X magnification.....	71
Figure 3.5. Mixing time comparisons for the airlift and stirred contactors of same volume.....	74
Figure 3.6. Metal uptake (mg/g) and percentage removal (%) plots for biosorption of test metals at different initial concentrations and biomass dose of 1.5 g dry wt./l in continuous biosorption system (data represents an average of three independent experiments).....	76
Figure 3.7. Batch vs. continuous adsorption performance comparisons for Cu (II) and Pb (II) ions under similar environmental conditions (e.g. biomass dose; 1.5 g/l, pH 5.5	

for Cu, and 5.0 for Pb adsorption). Heat-dried non-living cells used in previously studied batch experiments (Amirnia et al., 2012).....	77
Figure 3.8. Comparison of biomass separation efficiency for metal-free biomass and metal-loaded biomass.....	78
Figure 3.9. Comparison of sorption performance of yeast cells for Cu (II) at different biomass concentrations obtained at different metal inlet flowrates into the biosorption vessel.....	80
Figure 3.10. Effect of biomass dose, controlled by metal-biomass flowrates ratios, on percentage removal of $\text{Cu}^{2+}$ by yeast biomass in continuous system.....	81
Figure 3.11. The linearized Langmuir isotherm plots for the adsorption of Cu (II) and Pb (II) ions onto yeast cells in continuous mode.....	82
Figure 3.12. Time course of $\text{Cu}^{2+}$ ions uptake by yeast cells at different metal concentrations (biomass concentration: 1.5 g/l).....	84
Figure 3.13. A pseudo-second-order kinetic model applied to examine the effect of initial metal concentration on rate constant (biomass dose 1.5 g/l).....	86
Figure 3.14 Schematic of the transfer of metals from the bulk liquid phase to a yeast cell.....	87
Figure 3.15. Intraparticle diffusion model for Cu (II) biosorption on yeast cells at different metal concentrations. Multi-linearity of plots (three distinct regions) was observed for metal uptake as the metal-biomass contact time increased.....	88
Figure 3.16. Slopes of second stage intraparticle diffusion plots ( $1 < t^{1/2} < 4$ ) to calculate the $K_I$ coefficient values.....	90
Figure 3.17. Time profile of Cu (II) ions dimensionless concentration $C_t/C_0$ at different initial solute concentrations (biomass dose: 1.5 g/l). The external mass transfer	

constant ( $K_E$ ) for Cu (II) adsorption on yeast cells was obtained from the initial slopes of the plots.....	92
Figure 4.1. Schematic of triple column continuous-flow biosorption system (columns dimensions: 27 cm height and 3.42 cm base diameter).....	107
Figure 4.2. Influence of particle size on removal efficiency of $\text{Cu}^{2+}$ ions by MTL biomass (dose: 1 g/l).....	111
Figure 4.3. $\text{Cu}^{2+}$ biosorption equilibrium data compared to of those predicted by isotherm models.....	112
Figure 4.4. Influence of Cu (II) concentration on the kinetics of biosorption by MTL (biomass dose = 4 g/l). The slopes of the second stage of biosorption ( $q_t$ vs. $t^{0.5}$ ) was used to obtain the intraparticle diffusion rate constants in Eq.(11).....	114
Fig. 4.5 Plot of dimensionless concentration vs. time for obtaining the external diffusion constant in Eq.(12) from the initial slopes for adsorption of Cu (II) ions onto MTL at different biomass doses (metal concentration 50 mg/l).....	117
Figure 4.6. Regeneration of maple leaves with five types of eluents. Concentration of Cu (II) in the biomass (to be desorbed) was 25 ppm for all eluents (contact time: 1 hour).....	118
Fig. 4.7. Concentration profile of Cu (II) at the column outlet as a function of time for eight biosorption cycles ( $C_0 = 55$ mg/l , $F = 21$ ml/min). Effluent concentration of 1 mg/l was used to obtain the column breakthrough time.....	122
Figure 4.8 Metal ions released during the 1st and 2nd cycles of column biosorption. After the 2nd cycle, no significant amount of metal ions release was observed.....	123
Figure 4.9. Cu (II) desorption concentration profile for regeneration cycles 3 to 6 (elute: 0.1N $\text{H}_2\text{SO}_4$ , flowrate: 35 ml/min).....	126

Figure 4.10. Experimental breakthrough curves and the simulated model results for different feed flowrates ( $\text{Cu}^{2+}$ concentration at the inlet =55 mg/l).....	128
Figure 4.11. Plots of normalized $\text{Cu}^{2+}$ concentration at the column outlet vs. time and simulated results at different metal concentrations in the column influent (flowrate: 21 ml/min).....	129
Figure 4.12. FTIR spectra of MTL (a) before and (b) after $\text{Cu}^{2+}$ ions adsorption.....	131
Figure 4.13. SEM images of Maple leaves powder (a) without metal (b) with metal.....	132
Figure 5.1. Langmuir equation plots of metal uptake $q$ versus equilibrium metal concentration with varying coefficient $b$ (0.01 – 5 l/mg) and constant $q_{\text{max}} = 100$ mg/g.....	144
Figure 5.2. Langmuir isotherm model plots for hypothetical biosorbents with constant $b$ (0.05 l/mg) and varying $q_{\text{max}}$ (50 – 200 mg/g). The dashed line values shown on the secondary vertical axis is the dimensionless metal uptake $\theta$ , which overlaps for all range of $q_{\text{max}}$ (50 – 200 mg/g).....	145
Figure 5.3. Performance comparisons of 4 biosorbents in different residual metal concentrations where some biosorbents have not reached their full saturation ( $\theta < 1$ ).....	150
Figure 5.4. Cadmium equilibrium fitted to Langmuir isotherm for five types of algae (2.5 g/l). Data adapted from Lodeiro et al. (2005).....	151

# Nomenclature

$b$ (l/mg)	Langmuir equation constant
$b_0, b_i, b_{ii}$ , and $b_{ij}$	Coefficients of terms of the regression equation (eq .4, chapter 2)
$b_s$	Sips equation constant
$C_i$ (mg/l)	Initial metal concentration in solution
$C_f$ or $C_e$ (mg/l)	Equilibrium metal concentrations
$C_s$ (mg/l)	Metal concetration at the surface of sorbate
$C_t$ (mg/l)	Metal concentration in solution at time $t$
$C_{\text{Biomass}}$ (g/l)	Concentration of biomass at time $t$
$d_c$ (cm)	Packed bed column diameter
$d_p$ ( $\mu\text{m}$ )	Particle diameter
$D$ ( $\text{h}^{-1}$ )	Dilution rate
$D_L$ ( $\text{cm}^2/\text{min}$ )	Axial dispersion coefficient
$F$ (ml/min)	Volumetric flow rate of metal solution (into packed-bed column)
$I$ (mg/g)	Constant related to thickness of diffusion layer (eq. 13, chapter 3)
$k_1$ ( $\text{min}^{-1}$ )	Rate constant of first order adsorption equation (eq. 10, chapter 3)
$k_2$ ( $\text{g} \cdot \text{mg}^{-1} \cdot \text{min}^{-1}$ )	Rate constant of pseudo-second-order adsorption
$k_I$ ( $\text{mg} \cdot \text{g}^{-1} \cdot \text{min}^{0.5}$ )	Inter-particle diffusion rate constant
$k_E$ ( $\text{min}^{-1}$ )	External mass transfer rate constant
$K_f$	Freundlich equation constant
$m_b$ (g)	Biosorbent mass packed in column
$q$ (mg/g)	Metal uptake (mg metal/ g biosorbent)
$q_{\text{max}}$ (mg/g)	Total number of binding sites available for metal biosorption
$q_t$ (mg/g)	Amount of metal adsorbed at any given time $t$
$q_b$ (mg/g)	Total bed biosorption capacity (packed bed column)

RE (%)	Metal removal Efficiency
$R_L$	Dimensionless equilibrium parameter
S (m <sup>2</sup> )	Surface area
t (min)	Time
T (K)	Temperature
$u_z$ (cm/min)	Interstitial velocity of the bulk flow
$V_b$ (cm <sup>3</sup> )	Bed volume (packed-bed column)
$V_V$ (cm <sup>3</sup> )	Void area in packed-bed column
$x_1$ , $x_2$ , and $x_3$	Coded values of pH, biomass dose, and initial metal concentration (eqs. 6-8, chapter 2 )

***Greek symbols***

$\alpha$	Axial design point (chapter 2)
$\varepsilon_b$	Wet-biomass porosity (packed-bed void fraction)
$\mu_{\max}$ (h <sup>-1</sup> )	Maximum specific growth rate of cells
$\rho_b$ (g/l)	Density of bed (in packed-bed column)
$\Delta G$ , $\Delta H$ , and $\Delta S$	Changes in Gibbs free energy, Enthalpy, and Entropy

# **Chapter 1**

## **Introduction** (Literature Review and Objectives)

## **1.1. Metals in the environment: threats**

Metals are a natural part of the environment and an important part of our daily lives. About 600 kg/person of metals including iron-steel, aluminum, copper, lead, zinc, manganese, cadmium and many others are used annually in United States (Jeffery, 2001) to sustain the high standard of living. Metals are used in many simple things we see around us such as batteries, clothes, cars, computers, paints –in short, everywhere in the modern world. This high demand requires a large quantity of metal production through ore mining industries.

The report by Nriagu (1996) shows that metal production and also metal emissions to the environment by human activities has been dramatically increased during the 20<sup>th</sup> century's Industrial Revolution. For instance, mine productions of Cu and Zn have reached to 80 and 65 million metric tons/year, respectively, by the last decade of 20<sup>th</sup> century. Consequently, annual anthropogenic emissions of Cu and Zn to the atmosphere have reached up to 0.5 and 2.7 million metric tons, respectively.

Cumulative anthropogenic release of heavy metals into the environment has disrupted the natural biogeochemical cycles of metals causing increased deposition of heavy metals in soils and aquatic ecosystems. On the other hand, release of these metals from industrial waste streams to the environment without proper treatment has become of a great global environmental concern today (Alluri et al., 2007). Toxic metals persist in the environment and through a process of bioaccumulation, they can further enter into the food chains and pose adverse effects on human and environmental health (Volesky, 2004).

From the environmental point of view, presence and accumulation of those metals that can have a toxic or inhibitory effect on living things are of greatest concern. In global scale, heavy metal ions are detected in the waste streams from mining operations and ore processing, smelters, manufacturing processes such as tanneries, electronics, electroplating and metal-finishing, refineries, power generation, and other metal processing industries (Volesky, 2007; Mishra et al., 2010; Kazemipour et al., 2008).



Pollution from these anthropogenic sources and also natural point sources of metals can easily disperse into different environment compartments and create local conditions of elevated metal concentrations causing disastrous effects on human and environmental health (Nriagu, 1990; Wang, 2010). The predominant sources of natural and anthropogenic metal emissions to the atmosphere, and also the ratio of these emissions (Anthropogenic/Natural) have been summarized in Table 1.1 for comparison.

Table 1.1. Primary natural and anthropogenic sources of metals in the earth's atmosphere (Nriagu, 1990).

Element	Emission Ratio	Natural		Anthropogenic	
	Anthropogenic / Natural	Primary Source	%	Primary Source	%
Sb	1.3	Wind-born soil particles	30	Smelting and refining	41
As	1.6	Biogenic	33	Smelting and refining	65
Cd	6	Volcanoes	59	Smelting and refining	71
Cr	0.7	Wind-born soil particles	63	Manufacturing processes	55
Co	(Only Natural is reported)	Wind-born soil particles	84	(Not reported)	-
Cu	1.2	Volcanoes	34	Smelting and refining	66
Pb	28	Wind-born soil particles	33	Transportation, Batteries	75
Mn	0.12	Wind-born soil particles	70	Manufacturing processes	39
Hg	1.4	Biogenic	56	Energy Production	63
Mo	(Only Natural is reported)	Wind-born soil particles	43	(Not reported)	-
Ni	1.7	Volcanoes	48	Energy Production	81
Se	0.6	Biogenic	84	Energy Production	61
Th	(Only Anth. is reported)	(Not reported)	-	Manufacturing processes	78
Sn	(Only Anth. is reported)	(Not reported)	-	Energy Production	64
V	3	Wind-born soil particles	57	Energy Production	98
Zn	3	Wind-born soil particles	42	Smelting and refining	55

Among the metals listed in Table 1.1, Pb has the highest anthropogenic to natural ratio (28) implying that Pb has the maximum share of anthropogenic fluxes to the atmosphere (Nriagu, 1990). This was mainly because of the leaded gasoline which was

not completely phased out by the time that the data were collected for this report. As shown in Table.1.3, atmospheric fallout is one of the sources of polluting aquatic ecosystems with metals.

Heavy metal pollution in the aquatic ecosystems has also become a serious threat and of great environmental concern (Srivastava & Goyal, 2010), while strict environmental regulations are being implemented all over the world to reduce pollutions. Therefore, the importance of applying inexpensive metal remedial technologies will be increased. This requires a comprehensive research in this field at the moment to find economic solution to metal pollution.

## **1.2. Toxicity of heavy metals**

The term “heavy metals” is widely used in the literature to categorize the group of metals that have potential toxicity (Duffus, 2002). At least 20 out of 70 metals in the periodic table are classified as toxic and half of these are emitted into the environment in quantities that have an environmental adverse effect (Jeffery, 2001). The damaging effects of heavy metals on human being and other habitants are well known.

According to Goldschmidt’s geochemical classification of elements (Goldschmidt, 1954), most of the elements that have toxic properties belong to a group termed as ‘Chalcophiles’ that have affinity to sulfur. This property causes adverse effects in human as the protein molecules in the living things that contain sulfur can bind with these metals so that can prevent replication of DNA and cell divisions (Alluri et al., 2007). Therefore, the toxicity of heavy metal ions mostly owing to their affinity to sulfur, and the metals in Chalcophile group can be considered as heavy metals, or toxic metals (Pb, Hg, Cd, As, Sb, Tl, Zn, Cu, etc.).

The central nervous system is one of the main parts of the human body that can be affected by the presence and accumulation of most of toxic metals (Wang, 2010). Among these elements, mercury, lead and cadmium are termed as ‘the big three’ due to their severe toxicity and their adverse impact on the environment health (Volesky,

1994). Heavy metals that pose risks to environment and human health are also listed in two groups by Wase and Forster (1997): black and grey. Black list contains elements that are very toxic (Hg, Cd) and priority should be given for their elimination from wastewater. The grey list (Pb, Cu, Zn, Ni, Cr) contains metals that are toxic but less harmful than black group.

We chose Pb, Cu, and Zn for this research based on high toxicity and high degree of anthropogenic discharge of Pb into the environment (Tables 1.1, and 1.3), toxicity and high amount of release of Cu to the environment from mining operations in Canada, and Zn for its toxicity and being among the top 10 substances released to water in Canada (Environment Canada, 2011) as well as its high global inputs in aquatic systems (Table 1.3). The maximum allowable concentrations of the 3 heavy metals considered for this study in drinking water in Canada, as well as their concentration limit in metal mining effluents in Canada are presented in Table 1.2. The effects and risks of accumulation of these metals on human health are also summarized in Table 1.2.

Table 1.2. Permissible levels of heavy metals in drinking water and mining effluents, and adverse health effects of metals on human health.

<b>Metal</b>	<b>Effects on Human Health</b>	<b>Acceptable Level* (mg/l)</b>	<b>Metal Mining Effluent Limit (mg/l)**</b>
Cu	Can deposit and damage brain, skin, liver, pancreas and myocardium, convulsions, vomiting, cramps.	1	0.2
Zn	Corrosive effects on skin, damage to nervous membranes, stomach cramps, vomiting, nausea and anemia.	5	0.5
Pb	Encephalopathy, seizures and mental disturbances (memory loss), reproductive disorders, kidney and liver damage.	0.01	0.3
*Health Canada's drinking water guidelines (2014). ** Environment Canada (2012). Sources: Fu and Wang (2011), Igwe & Abia (2006), Alluri et al. (2007), Nordberg (2009), Wang (2010).			

### 1.3. Global toxic metal emission inventories

The fact that man has become the most important agent perturbing natural systems modifying atmosphere, hydrosphere, biosphere, crust, and mantle in a large scale has been very well emphasized by many pioneer researchers such as Fyfe (1981) long time ago. The first inventories of metal emissions, metal sources, and their dispersions into different environmental compartments (air, water, and soils) in global scale were made by Nriagu and Pacyna (1988). Pollution from anthropogenic or natural point sources can easily accumulate and create local conditions of elevated metal concentrations, which could lead to disastrous effects on human and environmental health (Wang, 2010). Table 1.3 shows the inventories of man-made and natural emissions of Cu, Zn, and Pb into the aquatic systems. Coal burning in power plants is one of the major sources of metal emissions to the atmosphere as coal is rich in heavy metals, even more than that in Earth's crust.

Table 1.3. Global inputs of heavy metals into aquatic ecosystems (Nriagu, 1990).

Source	Metals (thousand tons per year)		
	Cu	Zn	Pb
Electric power plant	13	14	0.72
Domestic wastewaters	28	48	6.8
Metal mining and smelting	14	29	7
Manufacturing processes	34	85	14
Atmospheric fallouts	11	40	100
Sewage discharges	12	17	9.4
<b>Total</b>	<b>112</b>	<b>237</b>	<b>138</b>

#### **1.4. Conventional metal decontamination technologies: demerits**

Removal of heavy metals from industrial effluents is usually achieved by using conventional adsorbents, such as activated carbon, polymer resins, synthetic coagulants, and other materials in processes such as chemical precipitation, chemical oxidation or reduction, electrochemical treatment, evaporation, filtration, reverse osmosis, ion exchange, and membrane technologies (Das et al., 2008).

Although very effective, the major disadvantage of precipitation and synthetic coagulants is large volume of sludge production. Ion exchange has high operational costs even though it is often preferred by the industry. Need for resin replacements, membrane clogging, need for special handling and regular cleaning, and periodic replacements are some other disadvantages of this exciting technology for metal removal (Srivastava and Goyal, 2010). A summary of advantages and disadvantages of some metal treatment technologies is presented in Table 1.4. It shows that alternative methods such as biosorption could be a promising substitute to physico-chemical methods for removal of heavy metals.

#### **1.5. Biosorption – Benefits and Gaps**

Biosorption is defined as the property of certain biomaterials to bind and concentrate selected ions or other molecules from aqueous solutions (Volesky, 2007), and it can occur in both living and dead biomass (Tobin et al, 1994; Zouboulis et al.; 2004, Machado et al., 2009). Metal uptake is a combination of a rapid metabolism-independent process, followed by a slower one, associated to metabolism dependent-processes known as bioaccumulation (Wehrheim and Wettern, 1994). Therefore, biosorption of heavy metals can be defined as metal removal by passive linkage in live and dead biomasses from aqueous solutions in a mechanism that is not controlled by metabolic steps. Biosorption process is known as an attractive biotechnological process which employs naturally abundant or waste biomass for removing most types of heavy metals from aqueous solutions. The biosorption is a bioremediation emerging

tool for wastewater treatment that has gained attention in the scientific community over the past three decades.

Table 1.4. Technology comparisons for heavy metal treatment.		
Technology	Strengths	Weaknesses
<b>Ion Exchange</b>	Commercially available, Effective on co-occurring contaminants, Well- understood, Well-accepted by metal industry	Resin regeneration and replacement is costly, Not effective on all metals, Produces metal-laden waste brine, Overall, high capital and operational/maintenance costs
<b>Reverse Osmosis</b>	Effective removal method, Accepted benchmark technology	Capital intensive, Low throughput, Produces Metal-laden waste, Membranes expensive, Easily foul up, Elevated pressure, sensitivity to suspended solids, organics
<b>Chemical Precipitation</b>	Effective, Low capital cost, Simple operation	Inadequate, Requires tight operational controls, Post-treatment needs, Secondary sludge generation
<b>Biosorption</b>	Inexpensive, Metal selectivity, Easy operation, High Efficiency, High versatility, Tolerance to contaminants, Results in low volumes of high-concentration wash solutions suitable for subsequent metal recovery	Not very well understood, difficulty in developing generic technologies
Sources: Fu and Wang (2011), Volesky (2001), Zouboulis et al (2004), Kurniawan et al. (2006), Babel and Kurniawan (2003), Aklil et al. (2004), Kurniawan et al. (2006), Mohammadi et al. (2005), Barakat et al. (2004), Kajitvichyanukula et al. (2005), Volesky (2003).		

The closest analogy for biosorption is represented by ion exchange resins, and biosorbents can be referred to as natural ion exchangers (Volesky, 2004). Biosorption process involves a solid phase biomaterial (sorbent or biosorbent) and a liquid phase (solvent) containing dissolved species like metal ions to be sorbed (sorbate). In biosorption, like every sorption process, binding of sorbate species to biosorbent

continues until equilibrium establishes between the sorbate species in liquid and solid phases. Biosorbents contain some molecular groups that have affinity to sorbates such as metal ions. This technology employs various types of biomass to remove heavy metals from contaminated waters.

The overall incentives of biosorption development for industrial processes are: (a) low cost of biosorbents, (b) great selectivity and efficiency for metal removal at low concentration, (c) potential for biosorbent regeneration and metal valorization, (d) high velocity of sorption and desorption, (e) limited generation of secondary residues, and (f) more environmental friendly life cycle of the material (Robson et al., 2011).

So far, an industrially relevant method for removal of toxic metals has not been achieved yet (Wang and Chen, 2006; Volesky and Naja, 2007; Lesmana et al., 2009). Biosorbents with different degrees of metal adsorption capacities, availability, and selectivity have been shown to be promising for metal removal from aqueous solutions in batch laboratory scale, but it is their applicability in continuous mode that makes this treatment method attractive to industry.

One of the characteristics of a good and useful biosorbent is to be utilized in a continuous system for removing metal ions in aqueous solutions (Lokeshwari and Joshi, 2009; Amirnia et al., 2015). On the other hand, one of the challenges of applying biosorption process for heavy metal removal lies with the separation process of biomass from the metal solution after biosorption is occurred (Tsezos, 1990). We aim to address these issues in this research.

A comparison of biosorption technology with existing methods for metal removal is presented in Table 1.4. In overall, biosorption has been known as a biotechnological innovation as well as a cost effective excellent tool for removing all types of heavy metals from aqueous solutions.

## 1.6. Biosorbents

Generally, biosorbents are prepared from naturally abundant or waste biomass. Few examples of the types of biomaterials that have been tested in different laboratories for metal adsorption are: brown algae, almond hulls, sugarcane bagasse, maize and rice husks, sunflower stalk, tree sawdust, seaweeds, pine barks, wheat bran, shea butter seed husks, banana pith, coconut fiber, sugar-beet pulp nut shells, tea leaves, plant tissues, date stones, activated sludge, and even human hair, etc. Most of these biosorbents are of plant origin and mainly agricultural by-products. Also, many other biosorbents of algal, fungal and bacteria biomass have been employed as biosorbents.

All these biomaterials have been examined for their biosorptive properties and different levels of metal uptakes have been obtained that are high enough yet low-cost, which added to the pool of non-tested biomaterial in the world, warranting further research on biosorption. Recently, there is a great deal of interest in harnessing non-pathogenic microorganisms as a powerful resource in cleaning up of toxic metals from water and wastewater. Yeasts are so far the most commonly used organisms in bioprocess engineering. Of these, *Saccharomyces cerevisiae* strain (studied in Chapter 2 of this work) is recognized by high fermentation rates, wide use in food and beverage production, easy cultivation by inexpensive media, and being by-product or industrial fermentation waste in large quantities that can be used in biosorption processes (Wang and Chen, 2006).

So far, numerous types of biomaterials have been examined by researchers for their metal adsorptive properties and different types of biomass have shown different levels of metal uptakes. A comparison of selected metals uptake with various raw biosorbents on the basis of maximum uptake capacity is summarized in Table 1.5. The results obtained in this research are also listed. The focus of this research was on metal biosorption with minimum pretreatment steps.



It should be noted that the uptake values reported in Table 1.5 represent a typical sorption capacity for the selected biosorbents, and the uptake comparisons would be more meaningful if biosorbents were tested in the same environmental conditions (e.g. pH, biomass and metal concentration range, particle size, temperature, mixing rate, type of metal-biomass contactor, etc.), and they were from the same origin undergoing similar pretreatment steps. For instance, for wheat bran in Table 1.5, copper biosorption capacities between 6.85 to 51.5 mg/g were reported by different studies conducted in different conditions (Farooq et al., 2010).

A wide range of biosorption capacities for *S. cerevisiae* has been reported which implies that high adsorption capacities for metal removal by yeast cells can be achieved using different growth and experimental conditions, sorption surface alterations etc. Studies by Volesky (1994) and Wang and Chen (2006) on metal adsorption properties of *S. cerevisiae* indicate that yeast biomass is a mediocre biosorbent due to fermentation broth residues adhered to the surface of the cells that affects metal uptakes. However, other studies such as Bashar et al. (2003) and Volesky (2003) report high affinity of yeast cells for some cations such as Cd and Pb up to 10% of weight of biomass.

All biosorbents can be manipulated for better efficiency and multiple re-use to increase their economic attractiveness (Vieira and Volesky, 2000). According to Bailey et al. (1999), a biosorbent is assumed as low-cost if it is abundant, or an industrial waste by-product, and requires little processing. Biosorption results in literature show that pretreatment may enhance the sorption capacity of the biosorbents. Biosorbents in both forms of normal grounded or activated carbon have been used by researchers. For instance, activated carbon form of palm shell showed an adsorption capacity of 30.8 mg Cu/g (Issabayeva et al., 2010) and 95.2 mg Pb/g (Issabayeva et al. 2006) at pH 5.

Wan Ngah and Hanafiah (2008) listed the advantages of using untreated plant wastes vs. chemically modified biosorbents as low-cost, selective for metals, simplicity of

process, and easy regeneration, and the disadvantages as mediocre adsorption capacities and release of some soluble organic compounds presented in the plant, which may affect the COD or BOD of the treated water.

Table 1.5. Typical biosorption capacities of different unmodified natural biomass types for metals.			
Metal	Biosorbent	Max Uptake (mg/g)	Reference
<b>Pb</b>	Pomegranate peel	13.87	El-Ashtoukhy et al. (2008)
	Wheat bran	62	Farajzadeh and Monji (2004)
	Sawdust (walnut tree)	15.9	Bulut and Tez (2007)
	<i>Myriophyllum spicatum</i>	55.12	Yan et al. (2010)
	Lichen ( <i>Cladonia furcata</i> )	12.3	Sarı et al. (2007)
	Macrofungus ( <i>Amanita rubescens</i> )	38.4	Sarı and Tuzen (2009)
	Pine bark ( <i>Pinus brutia</i> Ten.)	76.8	Gundogdu et al. (2009)
<b>Zn</b>	Cells of <i>Streptomyces ciscaucasicus</i>	42.75	Li et al. (2010)
	Cocoa pod husk	14.07	Njoku (2014)
	Rapeseed waste	13.858	Paduraru et al. (2015)
	<i>Bacillus cereus</i>	66.6	Joo et al. (2010)
<b>Cu</b>	Potato peels	0.3877	Aman et al. (2008)
	Pomegranate peel	1.3185	El-Ashtoukhy et al. (2008)
	Turkish tea waste	8.64	Çay et al. (2004)
	Chestnut shell	12.56	Yao et al. (2010)
	Wheat bran	15	Farajzadeh and Monji (2004)
	Waste yeast biomass (fermentation )	4.93	Bakkaloglu et al. (1998)
	Commercial yeast biomass (dried at 105°C)	2.59	Cojocarui et al. (2009)
	Free living cells of <i>S. Cerevisiae</i>	23.41	Al-Saraj et al. (1999)
	Maple wood sawdust	9.51	Rahman and Islam (2009)
	Maple wood sawdust	1.79	Yu et al. (2000)
	Cellulose pulp waste	4.98	Ulmanu et al (2003)
	Garden grass	58.34	Hossain et al. (2012)
	Tree fren	11.7	Ho (2003)
	Sphagnum moss peat	16.4	Ho et al. (1994)

Minamisawa et al (2004) compared the adsorption capacities of biosorbents such as coffee residues and tea leaves with conventionally used adsorbents such as activated

carbon and zeolite for  $\text{Cd}^{2+}$  and  $\text{Pb}^{2+}$ . The amounts of metals removed by biosorbents were comparable with those by activated carbon and zeolite; however, the processing of biosorbents was less costly compared to conventional adsorbents and preferable for the economic treatment of wastewater. Despite having much less specific surface areas than activated carbon, biosorbents have the competitive advantage of low-cost and re-usability over activated carbon in remediation of metals from waters (Farooq et al., 2010).

## **1.7. Research Objectives**

Removal of toxic metals from industrial effluents to safe levels is an expensive process although several competing technologies exist for such an operation. Searching for cost-effective and environmentally-sound means of toxic metal removal is a continuous need for the industries with wastewater effluent with metals. Biosorption process has been known as an attractive and feasible alternative to physico-chemical methods for removal of heavy metals from various wastewater streams, and multitude of biosorbents have been examined by researchers for their metal removal performances. However, application of biosorption as a solution to heavy metal pollution has still many challenges to overcome for large scale application.

Although there are many studies in literature involving biosorption, comprehensive studies dealing with environmental conditions for removal of a mixture of metals and continuous-flow operation, which are more applicable to industry, are limited. The purpose of this work is to implement an inexpensive and effective method that uses waste biomass as adsorbent for the removal of mixture of toxic metals from aqueous solutions, and address the issues related to large scale applications of the process.

For commercialization, the main criteria that industry is looking for in selection of any metal clean-up process are (Eccles, 1995): cost effectiveness, compatibility with existing operations, flexibility to handle fluctuations in quality and quantity of effluent feed), reliability to be able to operate continuously, robustness that minimizes supervision and maintenance, selectivity to contaminants (heavy metals), and

simplicity. Thus, comprehensive research is necessary to select the best metal removal method and optimize the process to meet these criteria. The main objective of this work is to implement a method that uses inexpensive waste material, such as fermentation residues or agro-waste, as metal adsorbent and evaluate and optimize the adsorptive performance of the selected adsorbent and the selected system against the above criteria. Overall, the problem formulation and the offered solution in this work are based on the challenges associated with heavy metals in the environment and their proper remediation methods as summarized below:

- Anthropogenic activities have disrupted the natural biogeochemical cycles of metals in the environment.
- If untreated, accumulated levels of toxic heavy metals in the environment can poison the biosphere and threaten our water resources.
- Heavy metals such as lead, copper, and zinc are toxic.
- More stringent environmental regulations are being in force to reduce metal discharge in the environment and avert the adverse health impacts.
- Environmental process costs usually add up to overall costs and minimizing such costs are always desirable.
- Although effective, the traditional metal removal methods appear to be costly and inadequate.
- A preponderance of biosorption data reported in the literature refers to results from batch experiments.
- An industrially relevant biosorption method for removal of toxic metals has not been achieved thus far.

Therefore, economical and efficient removal of heavy metals from industrial effluents before being released to the environment is crucial at the moment. To address the above problems and the associated challenges listed above in removal of heavy metals from aqueous solutions, biosorption was selected and the following steps were taken in implementing this solution to the problem: 1) select waste biomass or species that are locally abundant and test their metal-binding capacities; 2) find out the best

environmental/operational conditions for biosorption; 3) employ innovative and suitable biosorption process designs that are more likely to be used in industrial applications; and 4) apply the sorption equilibrium and dynamic experimental data for modeling of biosorption for possible scaling up. To attain the full potential of biosorption in environmental protection, chemical/biochemical engineering aspects of the process are also taken into account.

## **1.8. Experimental Methodology and Configuration**

In this research, the following biosorption processes were investigated: 1) single and ternary metal solutions removal with non-living cells of *S. Cerevisiae* in a batch system. For this purpose, the capacity of yeast cells to adsorb metal ions was studied with respect to process parameters, namely, pH, sorbent dose, and initial metal concentration; 2)  $\text{Cu}^{2+}$  and  $\text{Pb}^{2+}$  ions treatment by a mixture of living and non-living yeast cells in a self-contained novel continuous system, where biomass generation and metal adsorption are combined; and 3)  $\text{Cu}^{2+}$  ions removal by *Acer saccharum* leaves in a flow-through packed-bed column.

Batch biosorption system in phase (I) of this study provided the basis for tackling the continuous mode systems in the subsequent phases. Large-scale applicability of biosorption relies mostly on the results of continuous-flow systems offered in phase (II) and (III) of this research. In the last chapter of the thesis, conflicting and confusing reports in the literature on the use and interpretation of the Langmuir model constants for quantifying and contrasting the performance of biosorbents were addressed, and Langmuir isotherm was derived based on a dynamic equilibrium between the metal species and biosorbent's active sites for adsorption.

In all experiments, MINEQL+ speciation modeling was used for the tested metals to find out their solution chemistry at different environmental conditions. This ensured us that metal removal was predominantly due to biosorption but not due to any metal precipitation. The optimum process parameters for multi-metal removal were determined using statistical tools such as design of experiment technique (academic

version of Minitab-16). Applying design of experiment in biosorption studies helped to reduce the number of experimental runs considering the interactions among the process parameters (variables), and evaluate the individual and relative importance of the parameters as well as their cumulative effects.

For biomass characterization, the FTIR analysis, EDX spectra, and zeta-potential measurements were performed on untreated and metal-treated biomass, which revealed the chemical environment responsible for biomass-metal interactions. In the column studied in phase (III) of experiments, modeling of biosorption was essential for process design and optimization due to dynamic nature of column sorption where sorption equilibrium, diffusion, and bulk flow coexist.

Figures 1.1 and 1.2 show the biomaterials chosen for biosorption work in this research. High surface-to-volume ratio of the cells of *S. cerevisiae* (Baker's yeast) provided a large metal-biomass contact interface for biosorption.

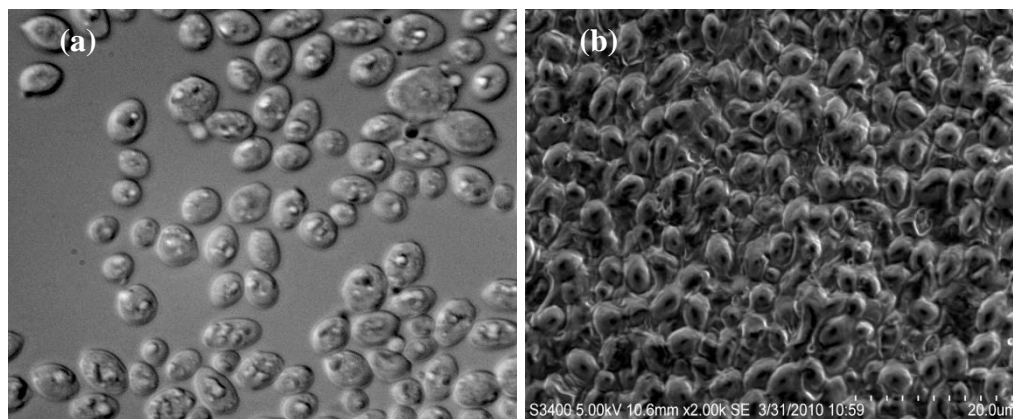


Figure 1.1. (a) Optical microscopy of hydrated yeast cells (40x); and (b) scanning electron micrograph of the dried yeast biomass.



Figure 1.2. Fallen roadside maple tree leaves collected and used for biosorption studies as a locally available waste.

The experimental set-up used in phase (II) of experiments is shown in Figure 1.3. The ability of yeast cells to remove copper and lead ions from aqueous solutions was examined in a continuous system, where biomass is produced using inexpensive medium in a bioreactor to perform on-line metal biosorption in an airlift fluidized column. The unique specification of this set-up was that the biomass production and the metal biosorption were performed in the same system where they were connected in series, and yeast cells were used without any pretreatment of heat-inactivation steps.

Figure 1.4 shows the experimental set-up for the phase (III) of biosorption work using maple tree leaves as biosorbent. Maple tree wood and sap are of high economical value, but maple tree leaves are of none or low economical value (e.g. composting) till now though they have created waste management issues for municipalities.

In this study, we make use of waste maple leaves by evaluating their capability to adsorb heavy metal ions from aqueous solutions. The use of packed-bed columns is one of the most suitable ways for heavy metal treatment as it allows more effective utilization of the biomass capacity by making the best use of concentration difference between sorbent and sorbate known to be the sorption driving force (Sag et al., 2001; Aksu and Gönen, 2004). The outcome of the dynamic performance evaluation of a continuous-flow column packed with biosorbent - similar to ion-exchange columns

packed with synthetic resins – to remove heavy metals can be correlated to design and scale up of the process.



Figure 1.3. Experimental set-up used for continuous-flow bioreactor-biosorption system for removal of heavy metals: (a) bioreactor system, (b) nutrients tank for biomass production, (c) biosorption vessel, (d) pH-controller, (e) settling tanks.





Figure 1.4. Experimental set-up for removal of heavy metals by maple leaves biomass in packed-bed columns.

Generally, biomass recovery is an uneconomical method as the fresh biomass is abundant and inexpensive. Also, the number of times that the biomass can be reused could be limited. However, recycling biomass is a useful option and may increase the process economy by recovering adsorbed metals. Biomass regeneration was investigated in continuous-flow column packed with maple leaves for removal of copper ions. Recovery of the desorbed metals from the concentrated eluent solutions is another step to enhance the process economy and reduce the environmental footprint of biosorption. Electrowinning (electroextraction) is often the feasible potential metal recovery method (Volesky, 2001), which was not the focus in this research.

## 1.9. References

- [1] Aksu, Z., Gönen, F., Biosorption of phenol by immobilized activated sludge in a continuous packed bed: prediction of breakthrough curves. *Process Biochem.* 39 (2004) 599–613.
- [2] Alluri H.K., Ronda S.R., Settalluri V.S., Bondili J.S., Suryanarayana V., Venkateshwar P., Biosorption: An eco-friendly alternative for heavy metal removal, *African Journal of Biotechnology*, 6, 25 (2007) 2924-2931.
- [3] Al-Saraj M., Abdel-Latif M.S., El-Nahal I., Baraka R., Bioaccumulation of some hazardous metals by sol–gel entrapped microorganisms, *J. Non-Crystal Solid*, 248, 2–3, (1999) 137–140.
- [4] Aman T., Kzai A.A., Sabri M.U., Bano Q., Potato peels as solid waste for the removal of heavy metal Cu(II) from waste water/industrial effluent. *Colloids Surfaces B Biointerfaces* 63, 1 (2008) 116-121.
- [5] Bakkaloglu I, Butter TJ, Evison LM, Holland FS, Hancock IC., Screening of various types biomass for removal and recovery of heavy metals (Zn, Cu, Ni) by biosorption, sedimentation and desorption, *Water Sci. Technol.*, 38 (1998) 269–77.
- [6] Bashar H., Margaritis A., Berutti F., Maurice B., Kinetics and Equilibrium of Cadmium Biosorption by Yeast Cells *S. cerevisiae* and *K. fragilis*, *Int. J. Chem. Reactor. Eng.*, 1 (2003)1-16.
- [7] Bulut, Y., Tez, Z., Removal of heavy metals from aqueous solution by sawdust adsorption, *J. Environ. Sci.*, 19 (2007)160-166.

- [8] Çay S., Uyanik A., Özasik A., Single and binary component adsorption of copper(II) and cadmium(II) from aqueous solutions using tea-industry waste, *Sep. Purif. Technol.*, 38 (2004) 273.
- [9] Cojocaru C., Diaconu M., Cretescu I., Savic J., Vasic V., Biosorption of copper(II) ions from aqua solutions using dried yeast biomass, *Colloids and Surfaces A: Physicochem. Eng. Aspects*, 335 (2009) 181–188.
- [10] Das N., Vimala R., Karthika P., Biosorption of heavy metals—An overview, *Indian Journal of Biotechnology*, 7 (2008) 159-169.
- [11] Duffus J. H., Heavy metals - a meaningless term?, *IUPAC, Pure and Applied Chemistry*, 74 (2002) 793–807.
- [12] Eccles H., Removal of Heavy Metals from Effluent Streams - Why Select a Biological Process?, *Int. Biodeterior. & Biodegradation*, 35, 1-3 (1995) 5-16.
- [13] El-Ashtoukhy E.S.Z., Amin N.K., Abdelwahab O., Removal of lead(II) and copper(II) from aqueous solution using pomegranate peel as a new adsorbent. *Desalination*, 223 (2008) 162-173.
- [14] Environment Canada, Pollutant Inventories and Reporting Division (2012), National Pollutant Release Inventory (NPRI).
- [15] Farooq U., Kozinski J.A., Khan M.A., Athar M., Biosorption of heavy metal ions using wheat based biosorbents - A review of the recent literature. *Bioresour. Technol.*, 101 (2010) 5043–5053.
- [16] Farajzadeh, M.A., Monji, A.B., Adsorption characteristics of wheat bran towards heavy metal cations, *Sep. Sci. Technol.*, 38 (2004) 197–207.
- [17] Fu, F., Wang, Q., Removal of heavy metal ions from wastewaters: a review. *J. Environ. Manage.*, 92 (2011) 407–18.

- [18] Fyfe W.S., The Environmental Crisis: Quantifying Geosphere Interactions, Science, 213, 4503 (1981) 105-110.
- [19] Goldschmidt V.M., Geochemistry, Clarendon Press, Oxford, P. 730 (1954).
- [20] Gundogdu, A., Ozdes, D., Duran, C., Bulut, V.N., Soylak, M., Senturk, H.B., Biosorption of Pb(II) ions from aqueous solution by pine bark (*Pinus brutia* Ten.). Chem. Eng. J., 153 (2009) 62–69.
- [21] Health Canada, Federal-Provincial-Territorial Committee on Drinking Water of the Committee on Health and the Environment, Guidelines for Canadian Drinking Water Quality, (2014).
- [22] Ho Y.S., Wase D.A.J., Forster C.F., The adsorption of divalent copper ions from aqueous solution by sphagnum moss peat, Trans. I. Chem. E. Part B: Proc. Safety Environ. Prot., 17 (1994) 185-194.
- [23] Ho Y.S., Removal of copper ions from aqueous solution by tree fern, Water Res. 37, 10 (2003) 2323-30.
- [24] Hossain, M.A., Ngo, H.H., Guo, W.S., Setiadi, T., Adsorption and desorption of copper(II) ions onto garden grass, Bioresour. Technol., 121 (2012) 386–95.
- [25] Igwe, J. C., Abia A.A., A bioseparation process for removing heavy metals from waste water using biosorbents, African J. Biotechnol., 5, 12 (2006) 1167-1179.
- [26] Issabayeva G., Aroua M.K., Sulaiman N.M., Study on palm shell activated carbon adsorption capacity to remove copper ions from aqueous solutions, Desalination, 262 (2010) 94–98.

- [27] Issabayeva G., Aroua M.K., Nik Sulaiman N.M., Removal of lead from aqueous solutions on palm shell activated carbon, *Bioresour. Technol.*, 97 (2006) 2350–2355.
- [28] Jeffery W.G., *A World of Metals: Finding, Making and Using Metals*, 2nd Edition, a publication by the International Council on Metals and the Environment (ICME) (2001).
- [29] Joo J.H., Hassan S.H.A., Oh S.E., Comparative study of biosorption of  $Zn^{2+}$  by *Pseudomonas aeruginosa* and *Bacillus cereus*., *Int. Biodeterior. Biodegradation*, 64 (2010) 734–741.
- [30] Kazemipour M, Ansari M., Tajrobehkar S, Majdzadeh M, Reihani Kermani H., “Removal of lead, cadmium, zinc, and copper from industrial wastewater by carbon developed from walnut, hazelnut, almond, pistachio shell, and apricot stone”, *J. Hazard. Mater.*, 150 (2008) 322–327.
- [31] Kratochvil D., Volesky B., Advances in the biosorption of heavy metals, *Trends Biotechnol.*, 16, 7 (1998) 291–300.
- [32] Li, H., Lin, Y., Guan, W., Chang, J., Xu, L., Guo, J., Wei, G., Biosorption of Zn(II) by live and dead cells of *Streptomyces ciscaucasicus* strain CCNWHX 72-14, *J. Hazard. Mater.* 179 (2010) 151–159.
- [33] Lesmana S.O., Febriana N., Soetaredjo F.E., Sunarso J., Ismadji S., Studies on potential applications of biomass for the separation of heavy metals from water and wastewater, *Biochem. Eng. J.* 44 (2009) 19–41.
- [34] Lokeshwari N. and Joshi K., Biosorption of Heavy Metal (Chromium) Using Biomass, *Global J. Environ. Res.*, 3, 1, (2009) 29-35.
- [35] Machado MD, Janssens S., Soares HM, Soares EV, Removal of heavy metals using a brewer's yeast strain of *Saccharomyces cerevisiae*: advantages of using dead biomass, *J. Appl. Microbiol.*, 106, 6, (2009) 1792-804.

- [36] Ma Wei, Tobin J.M., Determination and modeling of effects of pH on peat biosorption of chromium, copper and cadmium, *Biochem. Eng. J.*, 18, (2004) 33–40
- [37] McKay G., Ho Y.S., Ng J.C.Y., Biosorption of Copper from Wastewaters: A Review, *Separ. Purif. Method*, 28, 1 (1999) 87-125.
- [38] Minamisawa M., Minamisawa H., Yoshioda S., Taki N., Adsorption Behavior of Heavy Metals on Biomaterials *J. Agric. Food Chem.*, 52 (2004) 5606–5611.
- [39] Mishra V., Balomajumder C., Agarwal V.K., Biosorption of Zn (II) onto the Surface of Non-living Biomasses: A Comparative Study of Adsorbent Particle Size and Removal Capacity of Three Different Biomasses, *Water Air Soil Pol.*, 211 (2010) 489-500
- [40] Minamisawa M., Minamisawa H., Yoshida S., Takai N., Adsorption Behavior of Heavy Metals on Biomaterials, *J. Agric. Food Chem.*, 52 (2004) 5606-5611.
- [41] Njoku V.O., Biosorption potential of cocoa pod husk for the removal of Zn(II) from aqueous phase, *J. Environ. Chem. Eng.*, [2](#), 2 (2014) 881–887
- [42] Nordberg G.F., Historical Perspectives on Cadmium Toxicology, *Toxicol. Appl. Pharm.*, 238 (2009) 192–200.
- [43] Nriagu J.O., Global Metal Pollution, Poisoning the Biosphere?, *Environment*, 32, 7 (1990) 7-33.
- [44] Nriagu J.O., Pacyna J.M., Quantitative assessment of worldwide contamination of air, water and soils by trace metals, *Nature*, 333 (1988) 134-139.

- [45] Nriagu, J.O. A history of global metal pollution, *Science*, 272 (1996) 223–224.
- [46] Paduraru, C., Tofan, L., Teodosiu, C., Bunia, I., Tudorachi, N., Toma, O., Biosorption of zinc(II) on rapeseed waste: Equilibrium studies and thermogravimetric investigations, *Process Saf. Environ. Prot.*, 94 (2015). 18–28.
- [47] Rahman M.S., Islam M.R., Effects of pH on isotherms modeling for Cu(II) ions adsorption using maple wood sawdust, *Chem. Eng. J.*, 149 (2009) 273–280.
- [48] Robson C. Oliveira, Mauricio C. Palmieri and Oswaldo Garcia Jr., “Biosorption of Metals: State of the Art, General Features, and Potential Applications for Environmental and Technological Processes”, in: Syed Shahid Shaukat, *Progress in Biomass and Bioenergy Production*, InTech, (2011) 151-176.
- [49] Sag Y., Yalcuk A., Kutsal T., Use of a mathematical model for prediction of the performance of the simultaneous biosorption of Cr VI and Fe III on *Rhizopus arrhizus* in a semi-batch reactor, *Hydrometallurgy*, 59 (2001) 77–87.
- [50] Sari, A., Tuzen, M., Kinetic and equilibrium studies of biosorption of Pb(II) and Cd(II) from aqueous solution by macrofungus (*Amanita rubescens*) biomass. *J. Hazard. Mater.*, 164 (2009) 1004–11.
- [51] Sari, A., Tuzen, M., Uluözlü, Ö.D., Soylak, M., Biosorption of Pb(II) and Ni(II) from aqueous solution by lichen (*Cladonia furcata*) biomass. *Biochem. Eng. J.*, 37 (2007) 151–158.
- [52] Srivastava S., Goyal P., *Novel Biomaterials: decontamination of toxic metals from wastewater*, Springer-Verlag Berlin (2010).

- [53] Tsezos M., Engineering aspects of metal binding by biomass, H.L. Ehrlich, C.L. Brierly (Eds.), Microbial Mineral Recovery, McGraw-Hill, USA (1990), 325–339 (Chapter 14).
- [54] Tobin J.M., White C., Gadd G.M., Metal accumulation by fungi: applications in environmental biotechnology, J. Ind. Microbiol., 13 (1994) 126-130.
- [55] Ulmanu M., Marañón E., Fernández Y., Castrillón L., Anger I., Dumitriu D., Removal of Copper and Cadmium Ions from Diluted Aqueous Solutions by Low Cost and Waste Material Adsorbents, Water, Air, and Soil Pollution, 142 (2003) 357-373.
- [56] Vieira R.H.S.F., Volesky B., Biosorption: a solution to pollution?" Int. Microbiol., 3 (2000) 17–24.
- [57] Volesky B., Naja G., Biosorption technology: starting up an enterprise, Int. J. Technol. Transf. Commer., 6 (2007) 196–211.
- [58] Volesky B., Sorption and Biosorption, BV-Sorbex, Inc., St.Lambert, Quebec, (2003).
- [59] Volesky B., "Advances in biosorption of metals: Selection of biomass types", FEMS Microbiology Reviews, 14, 291-302 (1994).
- [60] Volesky B., Biosorption and me, Water Res., 41 (2007) 4017 – 4029.
- [61] Wang J., Chen C., Biosorption of heavy metals by *Saccharomyces cerevisiae*: A review, Biotechnol. Adv. 24 (2006) 427–451.
- [62] Wan Ngah W.S., Hanafiah M.A.K.M., Removal of heavy metal ions from wastewater by chemically modified plant wastes as adsorbents: A review, Bioresour. Technol., 99, 10 (2008) 3935–3948.



- [63] Wase J., Forster C., Biosorbents for Metal Ions, Taylor & Francis, pp.1-10 (1997).
- [64] Wang L.K., Heavy Metals in the Environment, chapter2 by: Naja G.M., Volesky B., “Toxicity and Sources of Pb, Cd, Hg, Cr, As, and Radionuclides in the Environment”, Taylor & Francis (2010).
- [65] Wehrheim B., Wetterm M., Biosorption of cadmium, copper and lead by isolated mother cell walls and whole cells of *Chlorella fusca*, Appl Microbiol Biotechnol, 41 (1994) 725-728.
- [66] Yan C., Li G., Xue P., Wei Q., Li Q., Competitive effect of Cu(II) and Zn(II) on the biosorption of lead(II) by *Myriophyllum spicatum*, J. Hazard. Mater., 179 (2010) 721–8.
- [67] Yao Z.Y., Qi J.H., Wang L.H., Equilibrium, kinetic and thermodynamic studies on the biosorption of Cu(II) onto chestnut shell, J. Hazard. Mater., 174 (2010) 137–143.
- [68] Yu B., Zhang Y., Shukla A., Shukla S.S., Dorris K.L., The removal of heavy metal from aqueous solutions by sawdust adsorption — removal of copper, J Hazard Mater, 80, 1–3, (2000) 33–42.
- [69] Zouboulis A., Loukido, M., Matis K., Biosorption of toxic metals from aqueous solutions by bacteria strains isolated from metal-polluted soils. Process Biochem., 39 (2004) 909–916.

## **Chapter 2**

### **Adsorption of Toxic Metals Mixture Using Non-Viable Cells of *Saccharomyces cerevisiae***

## ABSTRACT

The use of waste biomaterial for heavy metal adsorption is an economically appealing alternative to conventional metal removal methods. In this work, biomass of *S. cerevisiae* was capable of simultaneously removing more than 98% of  $\text{Pb}^{2+}$ , 60% of  $\text{Zn}^{2+}$ , and up to 55% of  $\text{Cu}^{2+}$  ions from aqueous solutions in the concentration range of 10-50 mg/l. Model equations describing the removal efficiency of each metal were determined using Response Surface Methodology with respect to operating conditions such as pH, metal concentration, and biomass dose. Characterization of metal-biomass interactions responsible for Bio-adsorption was studied employing Zeta potential, BET, FT-IR, and EDX techniques, which indicated that the uptake of metals by non-living yeast is a surface adsorption phenomenon. The results proved the involvement of an ion exchange mechanism on the cell walls by the adsorbing metals. In the presence of all metals, yeast cells were more selective for  $\text{Pb}^{2+}$  ions.

## 2.1. Introduction

The first global inventories of metal emissions into the environment made by Nriagu and Pacyna (1988) revealed that release of heavy metals from industrial activities without proper treatment has disrupted metals' natural biogeochemical cycles causing increased levels of heavy metals in atmosphere, soils, and aquatic ecosystems. Toxic metals are non-biodegradable and persist in the environment, and through a process of bioaccumulation in plants and animals, they can enter into the food chains and pose adverse effects on human and environmental health (Srivastava and Goyal 2010).

While many methods of metal removal including ion-exchange, chemical precipitation, adsorption, etc. are available, biosorption processes based on adsorbent derived from waste and natural bio-materials exhibit significant cost and environmental benefits (Volesky 2003). Although, biosorption has long been known as

an inexpensive and promising method for heavy metal removal from wastewaters (Volesky 1990; Kotrba *et al.* 2011), industrially relevant method for removal of toxic metals has not been achieved yet (Volesky and Naja 2007; Lesmana *et al.* 2009) mainly due to perceived performance inconsistency and lack of in-depth process models. For the treatment of high volume and low concentration complex wastewaters with a mixture of toxic metals, comprehensive studies using conditions relevant to real wastewater streams are needed (Sengil and Özacar 2009).

So far, many low-cost sorbents have been investigated for single metal adsorption, but the most effective biomaterials for competitive multi-metal removal have not yet been identified. Yeasts are one of the most commonly used organisms in bioprocess engineering. Of these, *S. cerevisiae* strain is more recognized due to its high fermentation rates and easy cultivation using inexpensive media (Kordialik-Bogacka 2011). It is also readily available in large quantities as industrial fermentation waste that can be employed in biosorption processes.

Among the various heavy metals that are abundant in environment, Pb, Cu and Zn are well-recognized for their toxicity (Naja and Volesky 2009; Alluri *et al.* 2007; Igwe and Abia 2006) and their high inputs into the aquatic ecosystems from different sources such as electric power plants, metal mining and smelting, manufacturing processes, and atmospheric fallouts. The emissions of these metals are among the highest with global rates of 138, 237, and 112 thousand tons per year for Pb, Zn, and Cu, respectively (Nriagu 1990). The objective of this work was to evaluate both the single and multi-component adsorption performance of *S. cerevisiae* as adsorbent for toxic metals including  $\text{Pb}^{2+}$ ,  $\text{Cu}^{2+}$ , and  $\text{Zn}^{2+}$  ions from aqueous solutions.

The solution pH is probably the most dominant factor in biosorption of metals (Wang and Chen 2006). Marques *et al.* (2000) observed a pH shift from 4-5 to 7-8 for  $\text{Cu}^{2+}$  biosorption by brewery waste biomass of *S. cerevisiae*, which caused metal precipitation. However, most biosorption studies considered only the initial pH of metal solutions, and the change in pH during adsorption was not monitored (Ghorbani

*et al.* 2008). Thus, another objective of this work was to investigate the adsorptive performance of *S. cerevisiae* in absence of any chemical precipitation employing the chemical equilibrium data obtained from MINEQL+ database and by adjusting pH during the biosorption process to ensure that the metals are removed by biosorption only.

In this study, the optimum conditions of process parameters such as pH, initial metal concentration, and biomass dose on the multi-metal removal efficiency were determined using statistical tools such as Response Surface Methodology (RSM). Applying RSM in biosorption studies allows to reduce the number of experimental runs considering the interactions among the variables, and evaluate the individual and relative importance of parameters as well as their cumulative effects (Ghorbani *et al.* 2008; Preetha and Viruthagiri 2007; Ferreira *et al.* 2009; Cojocaru *et al.* 2009). Although the metal removal capabilities of biomaterials such as yeast cells are well established, the mechanism of metal biosorption is not yet fully known (Wang and Chen 2006). Therefore, this work also investigated the possible retention mechanisms of metal ions on yeast cell walls using different surface characterization techniques.

## **2.2. Materials and methods**

### **2.2.1. Biomass preparation**

The medium for the growth of *S. cerevisiae* (Baker's yeast from Fleischmann's Co.) was prepared using 20 g/l commercial molasses solution as hydrocarbon source, 1g/l (NH<sub>4</sub>)<sub>2</sub>SO<sub>4</sub>, and 1g/l KH<sub>2</sub>PO<sub>4</sub> (Aksu and Donmez 2003). Inoculum preparation was conducted by aseptically transferring the active dry yeast to a 500 ml flask containing the medium after being autoclaved at 121°C for 21 minutes. Then, the flask was incubated at 30°C in a shaker at 250 rpm for 16-20 hours. The bioreactor was a 15-litre vessel equipped with two series of flat blade Rushton turbine impellers. Fermentation was started by introducing the prepared inoculum to the bioreactor at an aeration rate of 1vvm and 250 rpm mixing at room temperature. After a period of 20 h (the end of

log-phase of the growth), yeast biomass was separated from the liquid medium by centrifuging at 4000 rpm for 15 minutes. Biomass was then washed several times with distilled water (Milli-Q Fisher Scientific) and then centrifuged until the supernatant was clear.

Bayrock and Ingledew (1997) reported that  $D$  value (a measure of the heat resistance of a microorganism) of *S. cerevisiae* yeasts heated at 80°C is typically in the order of seconds, which means at this temperature 90% of cells are destroyed in a matter of seconds. Since biosorption is mainly a passive process employing the dead biomass as adsorbent (Volesky 2007), yeast cells were inactivated using heat in this work. Based on the earlier heat treatment methods (Cojocaru *et al.* 2009; Padmavathy *et al.* 2003; Özer and Özer 2003; Machado *et al.* 2009), the yeast biomass were dried in a hot air oven at 65 °C for 24h.

### **2.2.2. Biosorption experiments and metal analysis**

Analytical grade  $\text{Pb}(\text{NO}_3)_2$ ,  $\text{Cu}(\text{NO}_3)_2$  and  $\text{Zn}(\text{NO}_3)_2$  were used (Alfa Aesar) for  $\text{Pb}^{2+}$ ,  $\text{Cu}^{2+}$ , and  $\text{Zn}^{2+}$  stock solutions, respectively. Nitrate was chosen as the counter ion for metal ions because of its low tendency to form metal complexes (Ma and Tobin 2004). Biomass samples of concentrations from 1–7 g/l were contacted with single and ternary metal solutions of concentration between 10–50 mg/l. The pH of the metals and biosorbent solutions was adjusted to desired values by adding 0.5N HCl/NaOH at different stages of biosorption. Although addition of NaOH for pH adjustments increases  $\text{Na}^+$  ions in the solutions, it has been shown that  $\text{Na}^+$  ions have little effect on heavy metals biosorption (Ansari *et al.* 2011).

Adsorption batch experiments were conducted in a 500 ml flask with a magnetic stirrer (200 rpm) at room temperature. The supernatant from aqueous samples was assayed for metals using an inductively coupled plasma spectrophotometer (Varian ICP-OES) with the capability to scan for all elements simultaneously with very low detection limits (10 ppb) allowing rapid and precise sample processing. Metal uptake and removal efficiency were calculated based on the mass balance in the form of:

$$q \text{ (mg metal/ g biosorbent)} = \frac{(C_i - C_e)}{m/V} \quad (1)$$

$$\text{RE (\% Removal Efficiency)} = \frac{(C_i - C_e)}{C_i} \times 100 \quad (2)$$

where  $C_i$  and  $C_e$  are the initial and equilibrium metal concentrations, respectively, in mg/l,  $m$  is the amount of dried biomass in g, and  $V$  is the solution volume in l.

### 2.2.3. Single metal solution chemistry (chemical equilibrium)

For metal treatment studies by biosorption, it is very important to know the chemical equilibrium of the ions to make sure that the biosorption is the only responsible metal removal process in absence of any chemical precipitation of metal species (Wang and Chen 2006). For this purpose, chemical equilibrium of  $\text{Pb}^{2+}$ ,  $\text{Cu}^{2+}$ , and  $\text{Zn}^{2+}$  ions in  $\text{Pb}(\text{NO}_3)_2$ ,  $\text{Cu}(\text{NO}_3)_2$ , and  $\text{Zn}(\text{NO}_3)_2$  solutions were calculated by chemical equilibria program, MINEQL+ version 3.0 (Schecher and McAvoy 1994). The general solution chemistry of these ions for concentrations 45 mg/l is shown in Figure 2.1.

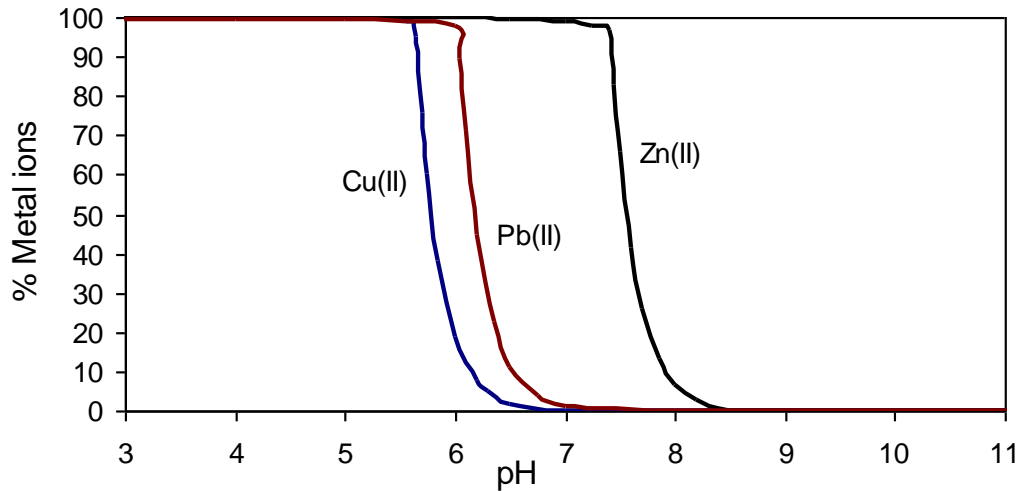


Figure 2.1.  $\text{Pb}^{2+}$ ,  $\text{Zn}^{2+}$ , and  $\text{Cu}^{2+}$  solution chemistry in single-metal solutions obtained by MINEQL+ version 3.01 (initial metal concentration= 45 mg/l).

$\text{Cu}^{2+}$ ,  $\text{Pb}^{2+}$ , and  $\text{Zn}^{2+}$  ions completely precipitated at pH around 6.5, 7, and 8.2 in the forms of tenorite ( $\text{CuO}$ ),  $\text{Pb}(\text{OH})_2$ , and zincite ( $\text{ZnO}$ ), respectively. Conversely, at pH below 5.65, 6.00, and 7.40, the metal ions  $\text{Cu}^{2+}$ ,  $\text{Pb}^{2+}$ , and  $\text{Zn}^{2+}$ , respectively, were 100% in aqueous solution (aqua ion).

#### **2.2.4. Characterization of yeast surface**

BET (Brunauer-Emmett-Teller) test was performed using Accelerated Surface Area and Porosimetry analyzer (ASAP2010 Micromeritics) to measure the surface area and porosity of yeast biomass. A surface area of  $1.59 \text{ m}^2/\text{g}$  indicates that dried yeast biomass is not a porous material in comparison to other adsorbents such as activated carbon. To identify the elements on the cell walls of yeast, Hitachi Scanning Electron Microscope SEM (S-4800) in conjunction with EDX (Energy Dispersive X-ray) analyzing system was employed. EDX spectrums of yeast biomass before and after exposure to metals were also obtained. Surface charge analysis of the yeast cells before and after biosorption was conducted by zeta potential analyzer (ZetaPlus) provided by BIC Brookhaven Instruments. Infrared spectrum of yeast biomass was obtained using a Fourier Transform Infrared Spectrometer (FTIR- Bruker) to identify the functional groups present on the yeast cells.

#### **2.2.5. Response surface methodology (RSM) for biosorption optimization**

In this study, influence of pH, initial metal concentration, and biomass dose on removal efficiency of yeast cells was characterized. The objective of using RSM was to find out an optimum operation in the design space for multi-metal biosorption. A Central Composite Design (CCD), a type of response surface design, was used (Anderson and Whitcomb 2005) which was capable of regression analysis of the experimental data and evaluating influence of each variable. A design of 20 experimental runs in five levels (coded values:  $-\alpha$ , -1, 0, +1, and  $+\alpha$ ) including 4 factorial design points ( $\pm 1$ ), and 4 star points ( $\alpha = 2$ ) representing the axial design points ( $\pm \alpha$ ) with 6 replicated center points were formulated (Table 2.1).



Table 2.1. Experimental design for multi-metal (Pb, Cu, and Zn) biosorption.

Factors	Levels				
	$-\alpha$	-1	0	1	$\alpha$
pH	4	4.5	5	5.5	6
Biomass Conc. (g/l)	1	2.5	4	5.5	7
Metal Conc. (mg/l)	10	20	30	40	50

The range of variables was selected based on the initial single metal experiments presented in the next section. Coded values of the input variables (or factors) were calculated by Design Expert program using eqn (3), and the behaviour of the system in this study for competitive metal biosorption with  $N$  input factors was estimated by an empirical quadratic model shown in eqn (4):

$$x_i = \frac{X_i - X_0}{\Delta X} \quad (3)$$

$$Y = b_0 + \sum_{i=1}^N b_i X_i + \sum_{i=1}^N b_{ii} X_i^2 + \sum_{i=1}^{N-1} \sum_{j=2}^N b_{ij} X_i X_j \quad (4)$$

Where  $X_i$  and  $X_j \dots X_k$  are the variables (or factors),  $X_0$  is the value of  $X_i$  at the center point,  $x_i$  are the coded levels of factors,  $\Delta X$  is the step change value,  $Y$  is the response,  $b_0, b_i, b_{ii}$ , and  $b_{ij}$  are the coefficients of terms of the regression equation. All the batch experiments in this work were carried out in triplicate and the mean values of three data sets are presented.

## 2.3. Results and Discussion

### 2.3.1. Multi-metal speciation modeling

Metal solution chemistry depends on the solution pH, temperature and ionic strengths. In biosorption processes, pH affects the site dissociations of biomass as well as chemical speciation of metallic ions. Different metals precipitate at different pH values, which consequently affects their removal efficiencies from aqueous solutions.

To investigate the metal removal efficiency by only biosorption without the influence of precipitation, it was very important to understand the multi-metal solution chemistry. Chemical equilibrium data obtained by speciation modeling software (MINEQL+) at pH range from 3 to 7 and metal concentrations between 5 to 100 mg/l for ternary metal system (Pb, Zn, and Cu) are presented in Figure 2.2. Using these data, the pH values were selected in a way to ensure that no precipitation of any metal in the mixture occurred. Speciation modeling data showed that no precipitation occurs in the solutions containing a mixture of  $\text{Pb}(\text{NO}_3)_2$ ,  $\text{Zn}(\text{NO}_3)_2$ , and  $\text{Cu}(\text{NO}_3)_2$  at pH 5.50 or lower when equal concentrations of each metal of 50 mg/l or lower are present in the solution. From the estimates of the chemical speciation of the studied metals present simultaneously in the solution, it was concluded that insignificant amounts of complex compounds were formed in metal-nitrate solutions (data are not shown).

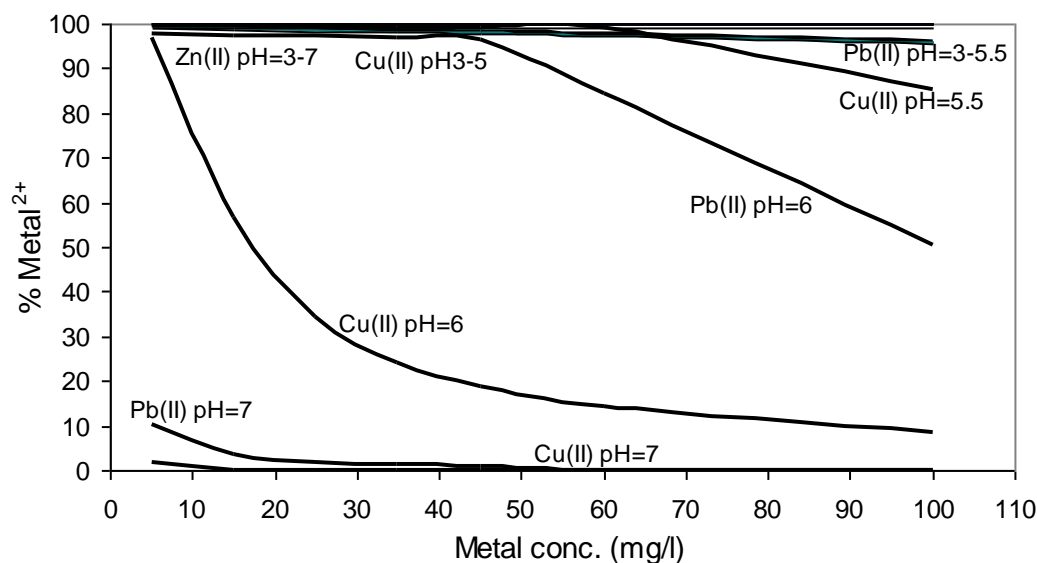


Figure 2.2. Percentage of  $\text{Pb}^{2+}$ ,  $\text{Zn}^{2+}$ , and  $\text{Cu}^{2+}$  ions in the solutions of 3-metal systems at different metal concentrations.

### 2.3.2. Single metal biosorption

Figure 2.3 presents the zeta potential curves of both metal-loaded and unloaded biomass as a function of pH. The isoelectric point, at which the cells carry zero net

charge, was found to occur at pH around 2.0, below which the cells are positively charged. The negative charge on the surface increases with increasing pH and reaches a plateau between pH 7-8. The surface charge of the untreated cells is probably due to adsorption of protons or hydrogen ions ( $H^+$ ) on the surface at  $pH < 2$  causing positive charging, and adsorption of  $OH^-$  ions at higher pH values leading to negative surface charges. Higher negative charge implies better interaction with the positively charged metallic species. The change in zeta potential profile for metal-adsorbed biomass suggested that upon cation adsorption, the surface charges were becoming less negative. The surface charge reversal occurred in presence of metal ions at pH between 2.2 to 4 instead of the sharp change that occurred in the absence of metal ions at pH 2.

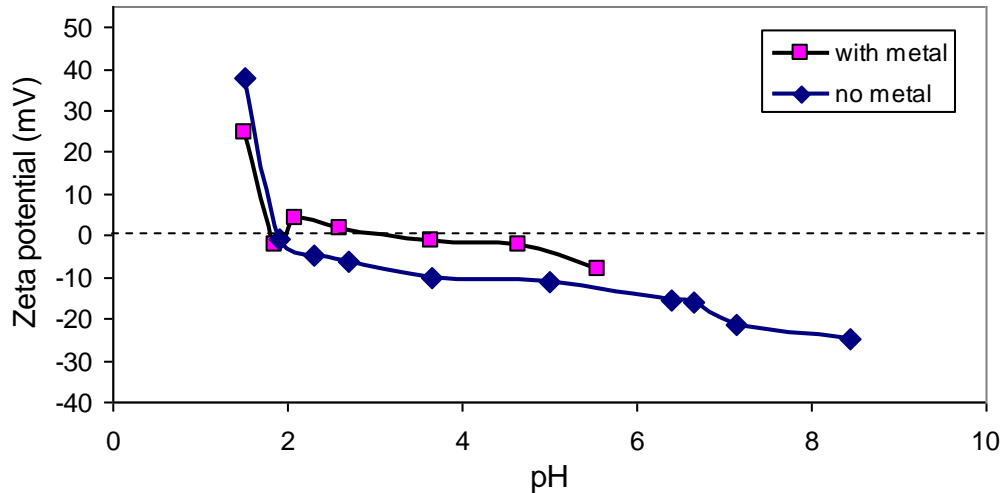


Figure 2.3. Zeta potential vs. pH for yeast cells before and after metal biosorption. 1g/l of biomass and 45 mg/l of each metal in ternary metal solution were used.

Figure 2.4 shows that the removal capacity of yeast biomass to adsorb  $Pb^{2+}$ ,  $Zn^{2+}$ , and  $Cu^{2+}$  ions depends on the solution pH. It can be observed that metal removal efficiencies increased with an increase in pH values from 3 to 5.5, 6, and 5 for  $Pb^{2+}$ ,  $Zn^{2+}$ , and  $Cu^{2+}$  ions, respectively. This increase is due to the presence of higher negative charges that are responsible for metal binding on the surface of the biomass at around pH 5 (refer to Figure 2.3). The results suggested that bio-adsorption is based on electrostatic interactions of the metal ions with the negatively charged surface of the

biomass. Metals precipitation zones are also marked in Figure 2.4 to indicate the biosorption and metal precipitation regions.

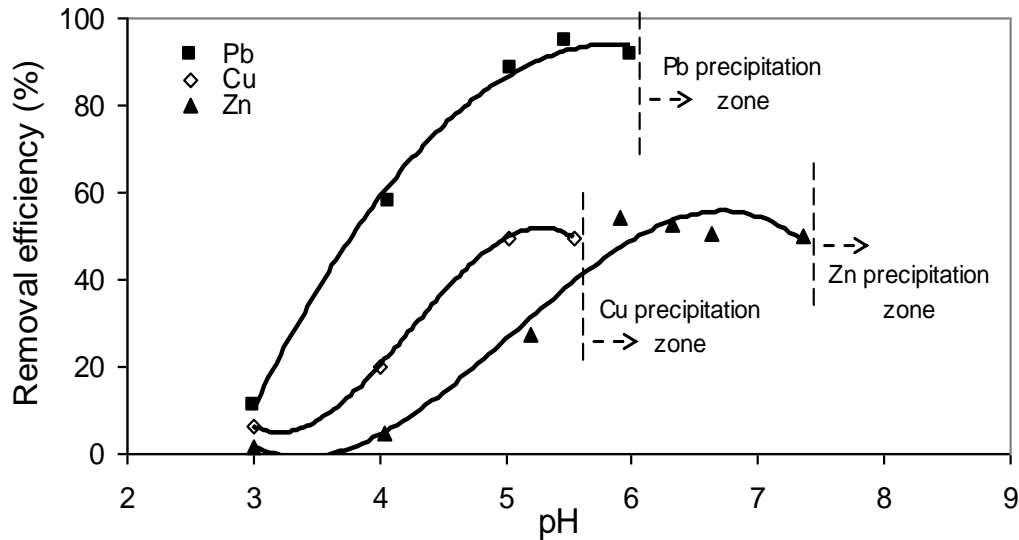


Figure 2.4. Changes in the capacity of yeast cells to retain single metal ions with solution pH (concentration of each metal: 45 mg/l).

### 2.3.3. Effect of nutrient composition on biosorption

Biosorption performances of 2 types of yeast biomass obtained from aerobic cultivation of yeast cells using two different nutrient recipes were compared for single metal (Cu) adsorption. As described before most of the biomass used in this work was obtained using molasses as hydrocarbon source. A second nutrient solution consisted of 20 g/l dextrose, 5 g/l peptone, 3 g/l yeast extract, and 3 g/l malt extract (Volesky and May-Phillips 1995; Bueno *et al.* 2008) was also used in some experiments. The results of this experiment (Figure 2.5) showed that nutrient composition for the growth of yeast cells did not affect the adsorption capacity of yeast biomass for metal adsorption, although slightly lower equilibrium concentration of  $\text{Cu}^{2+}$  occurred using molasses as the hydrocarbon source.

The effects of nutrients on uptake of metals can be as a result of different fermentation broth residues on the surface of the cells caused by different nutrients. For practical purposes, the effect of growth medium on biosorption is insignificant; however, the cost implication for using different media can be significant. The cost of the fermentation nutrient medium is an important consideration of the total biosorption process costs in real applications. The cost of dextrose is an order of magnitude more than the use of molasses for yeast growth. Thereafter, molasses was used as the growth medium for *S. cerevisiae* for all the experiments presented in this work.

#### **2.3.4. Biosorption kinetics and isotherms**

In biosorption, like any adsorption processes, binding of sorbate species from liquid to biosorbent continues until equilibrium is established between them. Kinetics study of biosorption process is necessary to determine the time required to achieve equilibrium. In this work, the first sample was taken within the few seconds of metals exposures to biomass; however, considering the centrifuge time, the first sample was actually taken within the first 3 minutes of biosorption.

Figure 2.5 indicates a rapid adsorption of metals by the biosorbent, in which, residual concentration of metal in the solution is almost constant after the first sample (3 minutes). Rapid metal biosorption is desirable for continuous operation as it determines the size of the biosorption equipment. As it is shown in Figure 2.5, the uptake rate was very fast that within less than 3 minutes more than 95% of the metal uptake was completed.

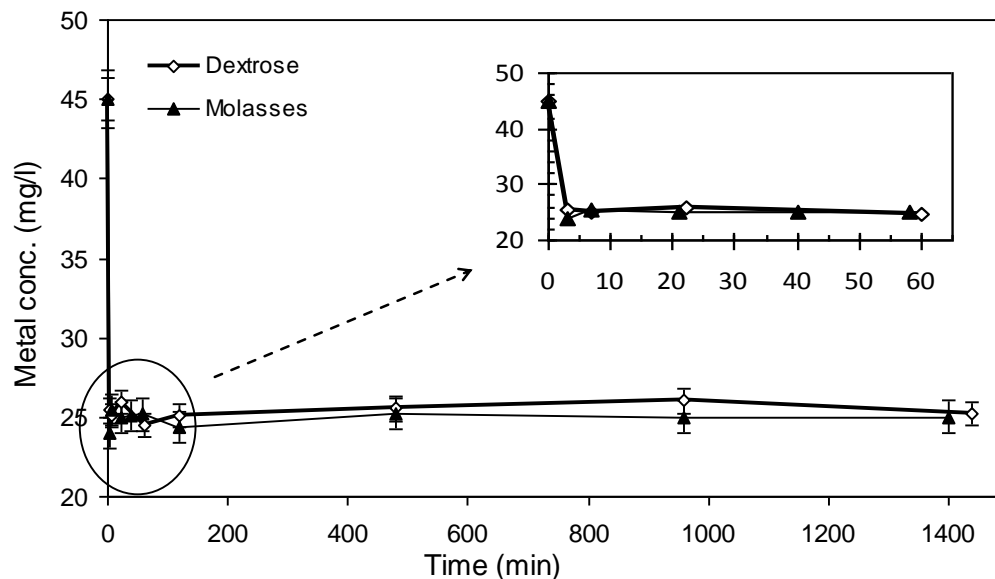


Figure 2.5.  $\text{Cu}^{2+}$  Biosorption using yeast cells cultivated in different nutrient compositions (pH=5.50, biomass conc. 4 g/l, initial  $\text{Cu}^{2+}$  concentration 45 mg/l).

To analyze the biosorption equilibrium data and biosorption performance, the linear form of Langmuir sorption model (eqn (5)) was used:

$$\frac{1}{q} = \frac{1}{q_{\max}} + \frac{1}{bq_{\max}C_f} \quad (5)$$

where  $q_{\max}$  is the maximum metal uptake in mg of metal per g of biosorbent (mg/g), and  $b$  (l/mg) is the equilibrium constant related to sorption affinity.  $q_{\max}$  is the total number of binding sites available for biosorption.

Table 2.2. Parameters of Langmuir isotherm for single metal biosorption.

Metal	$q_{\max}$ (mg/g)	$b$ (L/mg)	$R^2$
Zn	9.3	0.028	0.991
Pb	192.3	0.011	0.990
Cu	13.3	0.017	0.994

Table 2.2 shows that Langmuir isotherm exhibits a good fit to the equilibrium data. From the values of  $q_{\max}$  in Table 2.2,  $\text{Pb}^{2+}$  adsorption by *S. cerevisiae* is more favorable than  $\text{Cu}^{2+}$  and  $\text{Zn}^{2+}$ . Although, electropositivity of the tested metals follows the order:  $\text{Zn}^{2+} > \text{Cu}^{2+} > \text{Pb}^{2+}$ , adsorption of  $\text{Zn}^{2+}$  is less favorable than  $\text{Pb}^{2+}$  due to its higher hydrated radius than that of Pb (4.30 Å for Zn vs. 4.01 Å of Pb) (shown in Table 2.5).

### 2.3.5. Ternary metal biosorption system

In this study, the central composite design (CCD) was used to optimize the metal removal efficiency of yeast cells. Three independent variables, namely pH (X1), biomass dose (X2), and metal concentration (X3) were studied with six replicates at the central point and a total of 20 runs. The experimental design data are shown in Table 2.3. For each of the 3 factors, high (coded as +1) and low (coded as -1) points were selected according to the preliminary results obtained for single-metal biosorption (Figure 2.4) in absence of precipitation. The behavior of yeast biomass to adsorb metals was investigated and the significance of each variable as well as the possible interactive effects of these variables on percentage removal of metals was evaluated by variance analysis (ANOVA). A quadratic model was established on the basis of ANOVA to describe the metal capacity of biomass as a function of experimental variables for each metal in ternary metal system.

The empirical eqns (6–8) are developed based on the regression eqn (4) to generate response surface plots and contour maps for the analysis of the effects of test variables on the capacity of yeast biomass for multiple metals:

$$\text{Cu RE (\%)} = 44.05 + 1.51x_1 + 3.71x_2 - 2.74x_3 - 3.04x_1x_2 + 1.87x_1x_3 - 0.37x_2x_3 - 1.87x_1^2 - 0.72x_2^2 + 0.73x_3^2 \quad (6)$$

$$\text{Pb RE (\%)} = 92.23 + 9.22x_1 + 1.87x_2 + 3.77x_3 - 2.94x_1x_2 - 1.33x_1x_3 + 1.76x_2x_3 - 3.58x_1^2 - 0.28x_2^2 - 0.80x_3^2 \quad (7)$$

Table 2.3. Central composite design with codified ( $x_1, x_2, x_3$ ), real values ( $X_1, X_2, X_3$ ), and responses for the ternary metal biosorption system.

Run	Experimental factors						Responses		
	Orthogonal values			Real values			Cu removal	Pb removal	Zn removal
	$x_1$	$x_2$	$x_3$	$X_1$	$X_2$	$X_3$	(%)	(%)	(%)
1	0	0	0	5	4	30	44.1	92.0	16.4
2	1	1	1	5.5	5.5	40	44.0	98.1	44.9
3	0	0	$-\alpha$	5	4	10	55.3	79.7	21.4
4	1	-1	1	5.5	2.5	40	44.1	97.8	26.8
5	$\alpha$	0	0	6	4	30	*	97.9	60.4
6	$-\alpha$	0	0	4	4	30	34.0	57.0	4.6
7	0	$\alpha$	0	5	7	30	48.9	94.3	26.1
8	-1	-1	1	4.5	2.5	40	30.4	76.9	5.5
9	0	0	0	5	4	30	44.2	92.1	16.4
10	-1	-1	-1	4.5	2.5	20	36.9	72.9	6.7
11	0	0	0	5	4	30	44.0	92.0	16.5
12	0	0	0	5	4	30	44.2	92.1	16.5
13	1	-1	-1	5.5	2.5	20	41.8	96.6	29.2
14	-1	1	1	4.5	5.5	40	43.7	91.5	9.9
15	1	1	-1	5.5	5.5	20	44.5	92.3	37.6
16	-1	1	-1	4.5	5.5	20	50.5	77.9	13.6
17	0	0	0	5	4	30	44.1	92.0	16.4
18	0	$-\alpha$	0	5	1	30	33.9	87.1	3.4
19	0	0	$\alpha$	5	4	50	39.1	97.5	13.6
20	0	0	0	5	4	30	44.1	92.3	17.1

\* Cu precipitates at this solution condition, so it has been ignored in the experimental design.

$$\text{Zn RE (\%)} = 16.81 + 13.39x_1 + 5.20x_2 - 0.97x_3 + 1.89x_1x_2 + 1.22x_1x_3 + 0.88x_2x_3 + 4.12x_1^2 - 0.32x_2^2 + 0.38x_3^2 \quad (8)$$



where RE is the predicted removal efficiency (%) and  $x_1$ ,  $x_2$ , and  $x_3$  are the coded values of pH, biomass dose, and initial metal concentration, respectively, and  $x_1x_2$ ,  $x_1x_3$ , and  $x_2x_3$  represent the interactions between pH- biomass dosage, pH-initial metal concentration, and biomass dosage-metal concentration, respectively.

The 3-D graphical representations of the response surfaces and contours for removal efficiency of each metal are shown in Figure (2.6 - 2.14) based on the model eqns (6 - 8). The results for analysis of variance (ANOVA) for the response surface models are also shown in Table 2.4. The F-values (the test for comparing the variance associated with that term with the residual variance) implies that all models are significant. Values of probability (P-value) less than 0.0500 indicate model terms are significant, and values greater than 0.1000 indicate the model terms are not significant.

Table 2.4. Statistical analysis ANOVA (analysis of variance) results for the experimental design models.

<b>Response</b>	<b>Mean square</b>	<b>F-value</b>	<b>p-Value</b>	<b>R<sup>2</sup></b>	<b>Adj-R<sup>2</sup></b>
Cu Removal Efficiency	66.60	20.79	< 0.0001	0.954	0.908
Pb Removal Efficiency	231.06	78.62	< 0.0001	0.986	0.974
Zn Removal Efficiency	425.49	81.67	< 0.0001	0.987	0.974

ANOVA results indicated that for removal of all metals,  $X_1$ ,  $X_2$ ,  $X_1X_2$ , and  $X_1^2$  are significant model terms, which means that pH ( $X_1$ ) and biomass dose ( $X_2$ ) as well as their combination are dominant factors affecting the removal efficiency of all three metals by yeast biomass. As shown in the contour plots in Figures 2.7 and 2.9, initial metal concentration-pH and biomass-pH interactions were found to have significant model terms for  $\text{Cu}^{2+}$  and  $\text{Pb}^{2+}$ , respectively.

As can be seen in Figures 2.6 and 2.9, an increase in pH (from 4 to 6) and biomass dose (from 1 to 7 g/l) led to an increase followed by a slight decrease in removal of  $\text{Cu}^{2+}$  and  $\text{Pb}^{2+}$  from aqueous solutions. But,  $\text{Zn}^{2+}$  adsorption had an increasing trend in the studied pH and yeast cell concentration ranges (Figure 2.12).

With increasing biomass dose, higher binding sites or greater surface area for metal adsorption are available. As mentioned earlier, changes in solution pH affects solution chemistry, available functional groups for biosorption, and surface charges. A combination of these factors determines the overall effect of pH on biosorption of metals. As the pH lowers, the hydrogen ions compete with the metal ions for the sorption sites and restrict the metal cations' approach to the wall ligands (Volesky 2003; Özer and Özer 2003).

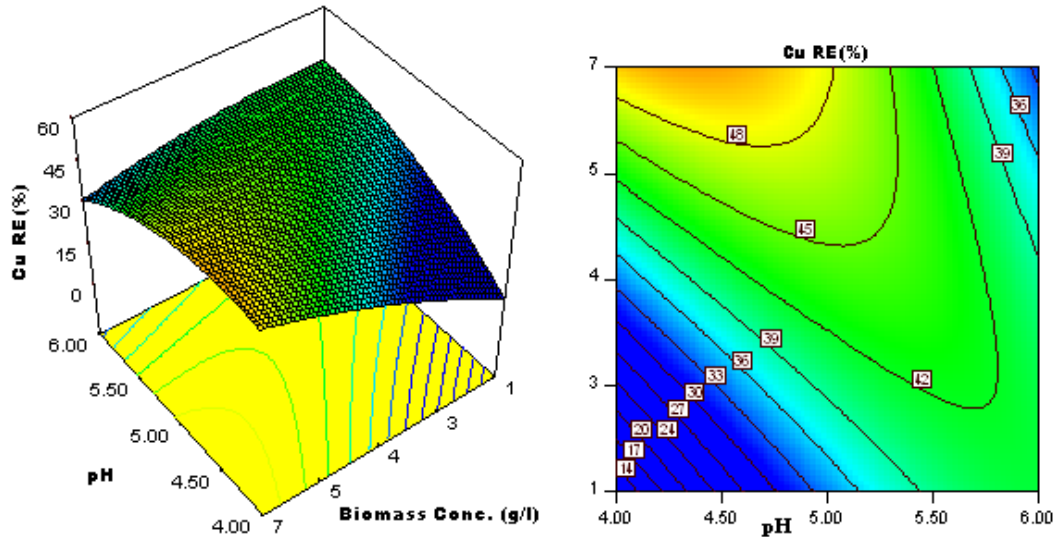
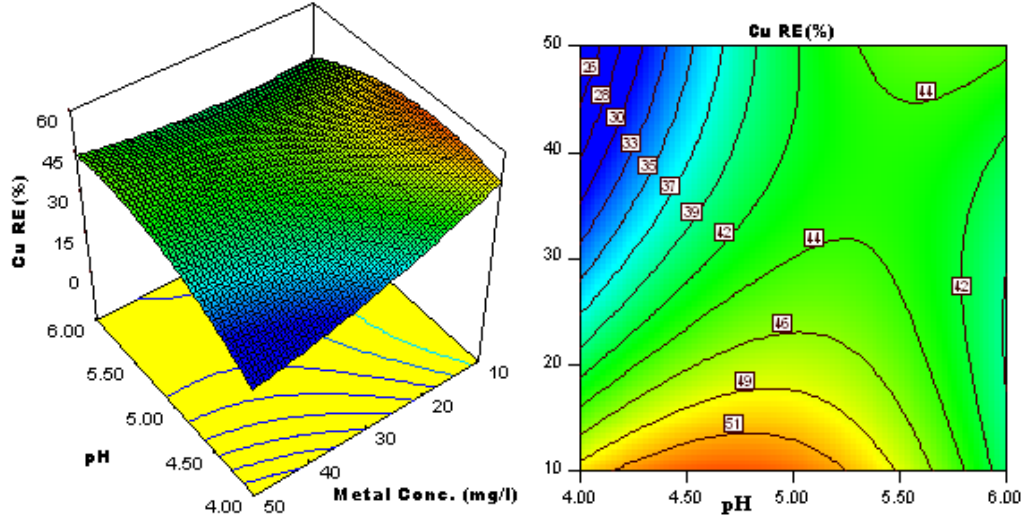


Figure 2.6. Response surface and contour curves showing the interactive effect of pH and biomass dose on percentage removal (RE) of  $\text{Cu}^{2+}$ , keeping initial metal concentration at its centre level (30 mg/l).

The variations of removal efficiencies of  $\text{Cu}^{2+}$  and  $\text{Pb}^{2+}$  ions with initial metal concentration in terms of pH and biomass dose are shown in Figures 2.7, 2.8 and Figures 2.10, 2.11 for each metal, respectively.  $\text{Cu}^{2+}$  removal slightly decreased with

increase in initial metal concentration in the solution for any combinations of pH and biomass dose.



For  $\text{Pb}^{2+}$  ions, it was found that initial metal concentration has a direct effect on  $\text{Pb}^{2+}$  removal. However, metal concentration from 10 to 50 mg/l has no significant effect on  $\text{Zn}^{2+}$  removal efficiency having vertical lines in counter plots of both biomass vs. metal concentration and pH vs. metal concentration as shown in Figures 2.13 and 2.14.

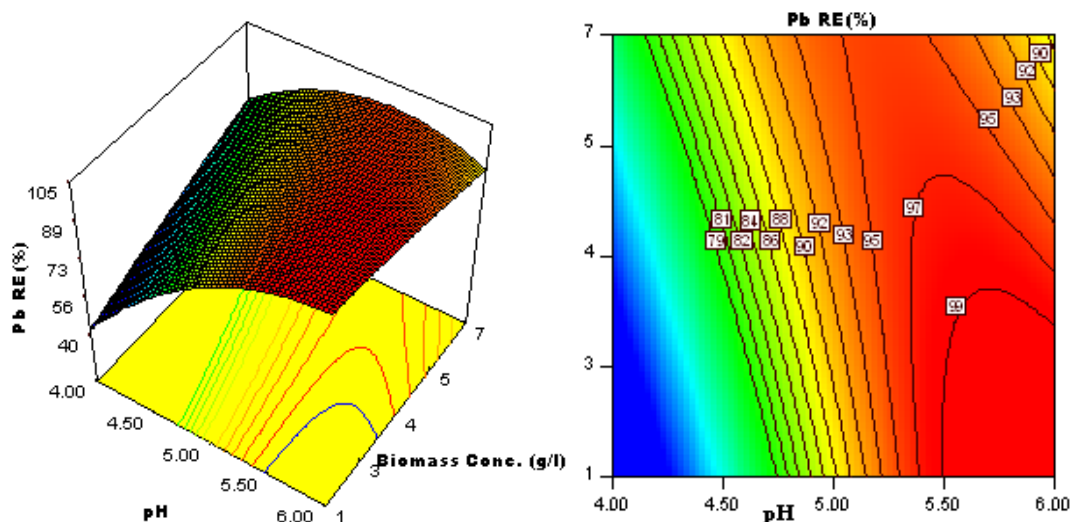


Figure 2.9. Response surface and contour curves showing the interactive effect of pH and biomass dose on percentage removal (RE) of  $\text{Pb}^{2+}$ , keeping initial metal concentration at its centre level (30 mg/l).

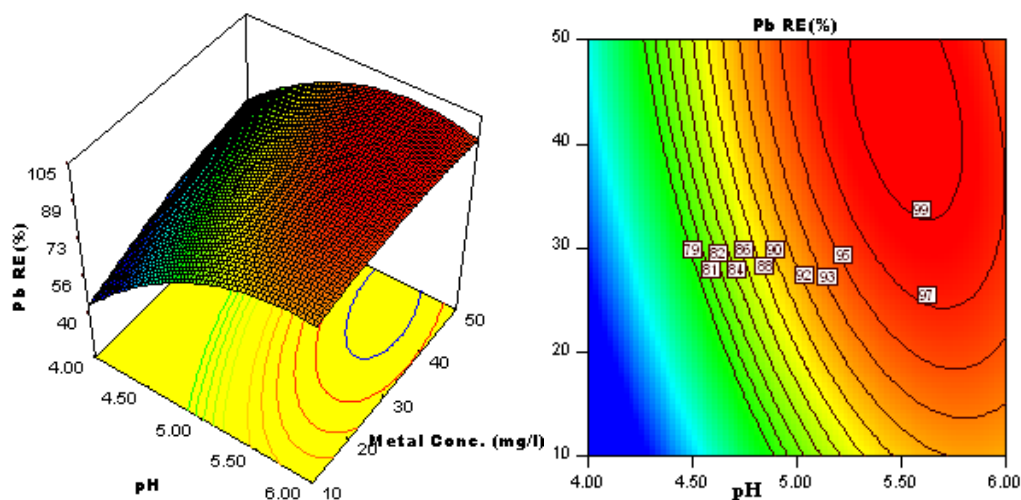


Figure 2.10. Response surface and contour plots showing the interactive effect of pH and initial metal concentration on removal efficiency (RE) of  $\text{Pb}^{2+}$ , keeping biomass dose at its centre level (4 g/l).

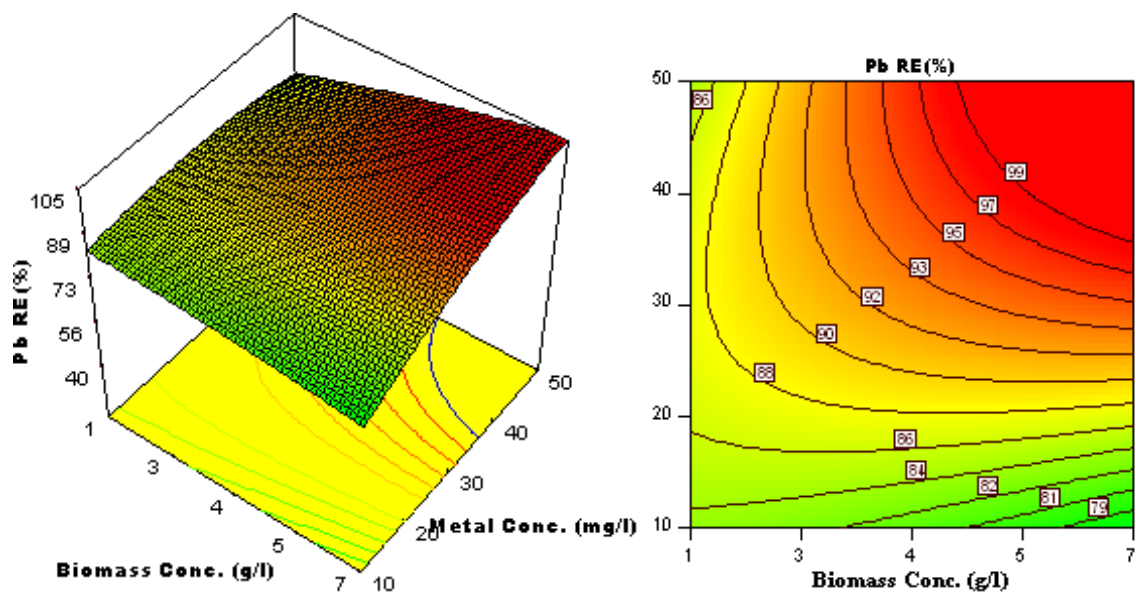


Figure 2.11. Response surface and contour plots showing the interactive effect of biomass dose and initial metal concentration on percentage removal (RE) of  $\text{Pb}^{2+}$ , keeping pH at its centre level (pH=5.0).

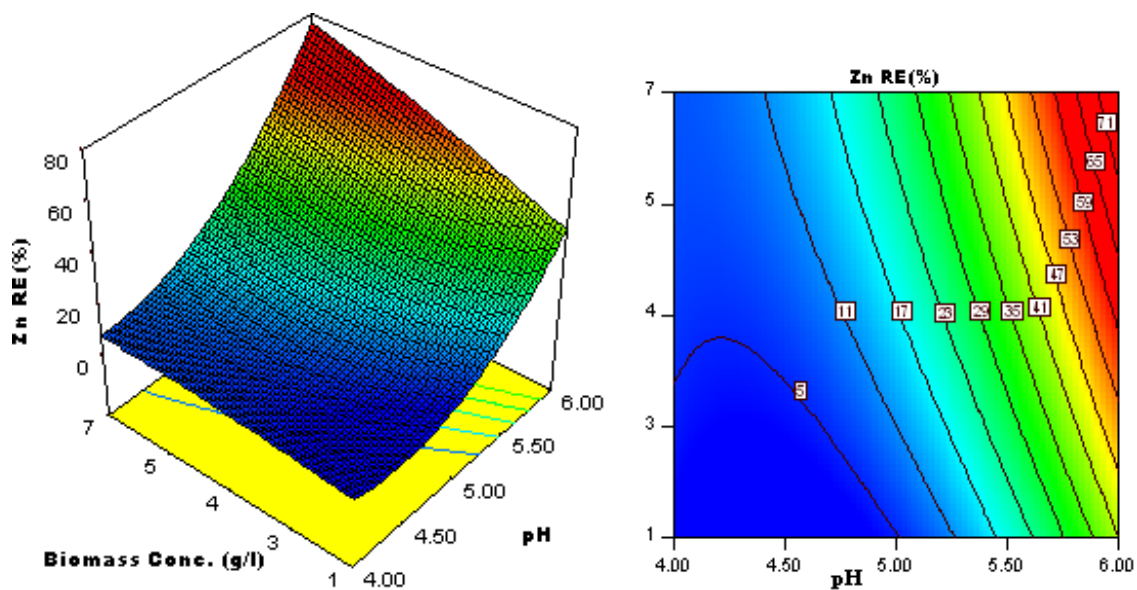


Figure 2.12. Response surface and contour plots showing the interactive effect of pH and biomass dose on percentage removal (RE) of  $\text{Zn}^{2+}$ , holding initial metal concentration at its centre level (30 mg/l).

For  $\text{Zn}^{2+}$  ions,  $X_1$ ,  $X_2$ ,  $X_1X_2$ , and  $X_1^2$  are the only significant model terms with F values less than 0.05 without any significant interactive terms between initial  $\text{Zn}^{2+}$  concentration and other variables.

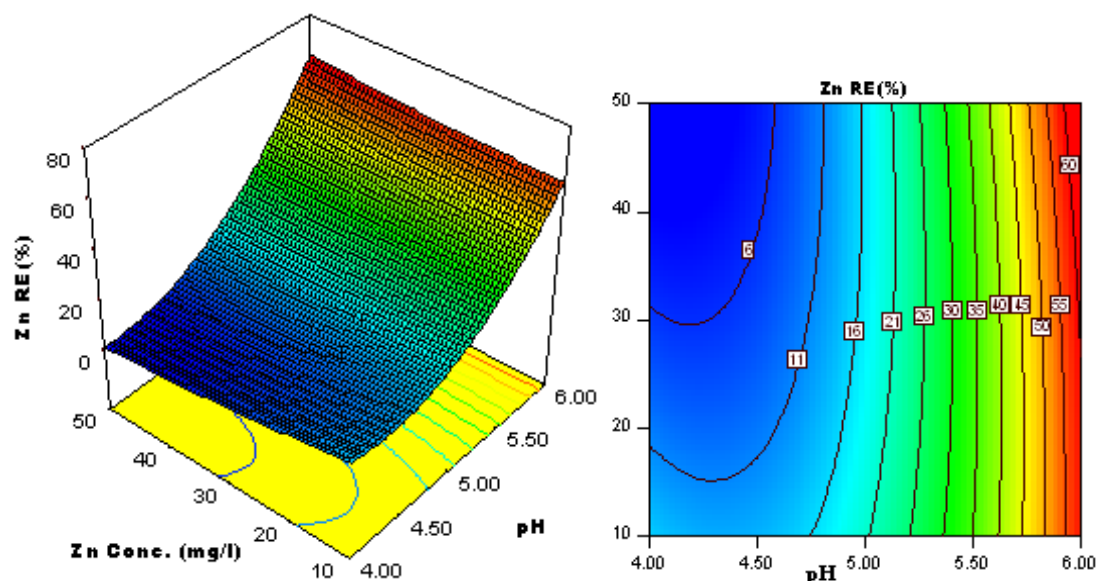


Figure 2.13. Response surface and contour plots showing the interactive effect of pH and initial metal concentration on removal efficiency (RE) of  $\text{Zn}^{2+}$ , holding biomass dose at its centre level (4 g/l).

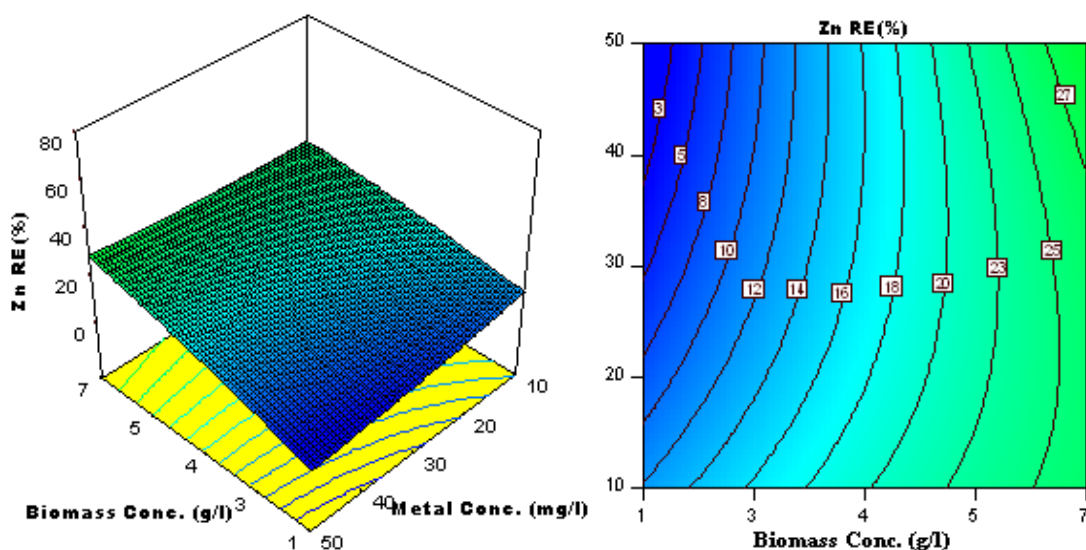


Figure 2.14. Response surface and contour plots showing the interactive effect of biomass dose and initial metal concentration on removal efficiency (RE) of  $\text{Zn}^{2+}$ , holding pH at its centre level (pH=5.0).

The fit of the models to experimental data are evaluated by  $R$ -squared and adjusted  $R$ -squared coefficients. As shown in Table 2.4,  $R^2$  of 0.954 – 0.987 and Adj- $R^2$  of 0.908 – 0.974 were obtained for model eqns. (6 - 8) predicting removal efficiency of  $Pb^{2+}$ ,  $Cu^{2+}$ , and  $Zn^{2+}$  in multi-metal system.

The experimental and predicted responses for biosorption of  $Pb^{2+}$ ,  $Zn^{2+}$  and  $Cu^{2+}$  in multi-metal system are compared in Figure 2.15 showing a good fit between them. Overall, it was found that  $Pb^{2+}$  removal can reach up to a maximum of 98% (RE) at pH 5, biomass dose 5.5 g/l, and initial metal concentration of 40 mg/l.  $Cu^{2+}$  maximum removal efficiency was 55% at pH 5, biomass concentration 4g/l, and  $Cu^{2+}$  concentration of 10 mg/l. For  $Zn^{2+}$  ions, maximum removal capacity of yeast cells was 60% at pH 6, biomass dose 4 g/l, and 30 mg/l of metal. The results indicate that  $Pb^{2+}$  ions have the greatest affinity to the binding sites on the walls of *S. cerevisiae* in both single-metal and ternary metal systems. In the following sections simultaneous effects of environmental factors on removal capacity of yeast cells for ternary metal system will be reported using response surface optimization and solving the model equations for removal efficiency of metals.

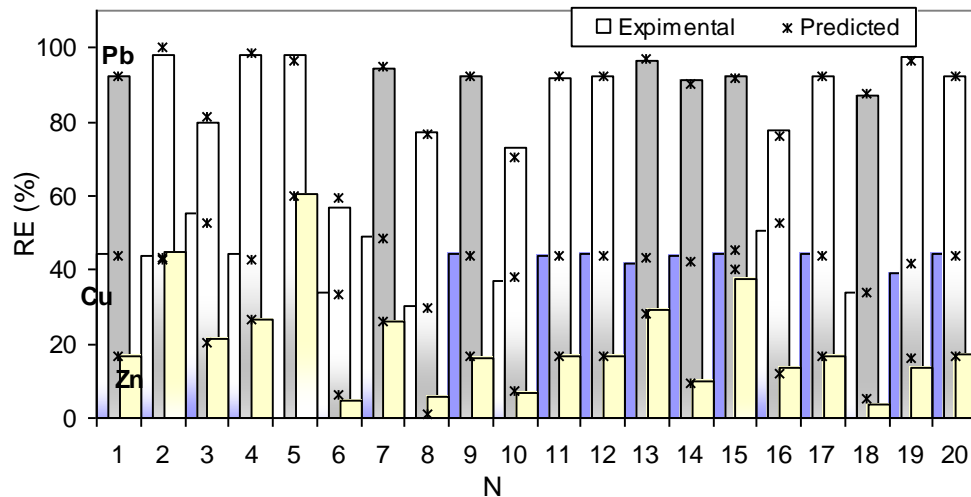


Figure 2.15. Experimental vs. predicted data for removal efficiency (RE) of  $Pb^{2+}$ ,  $Zn^{2+}$ , and  $Cu^{2+}$  in ternary metal system.

### 2.3.6. Competitive metal uptake (ternary metal system of Pb, Cu, and Zn)

Most of the reported results for competitive biosorption of metals show that the uptake of metal ions from a multi-metal system reduces compared to those obtained from single metal solutions (Ansari *et al.* 2011). To evaluate this, the extent of competition among  $\text{Pb}^{2+}$ ,  $\text{Cu}^{2+}$ , and  $\text{Zn}^{2+}$  ions for binding sites of yeast cells in a mixed metal solution was tested and the results are demonstrated in Figure 2.16, which shows a minor increase in uptake of  $\text{Pb}^{2+}$  ions (from 13.4 to 14.9 mg/g) in presence of equal concentrations of  $\text{Cu}^{2+}$  and  $\text{Zn}^{2+}$  ions.

In ternary metals mixtures, uptake capacity of  $\text{Cu}^{2+}$  and  $\text{Zn}^{2+}$  slightly decreased; but, the sum of accumulated metals on the metal affinity sites of yeast cells did not change for each system (single-metal vs. 3-metal systems). Therefore, though the yeast cells of *S. cerevisiae* were found to be more selective for  $\text{Pb}^{2+}$  ions in multi-metal biosorption, presence of a mixture of three metal ions (Pb, Zn, and Cu) in biosorption solution did not affect the overall biosorptive capacity of yeast biomass.

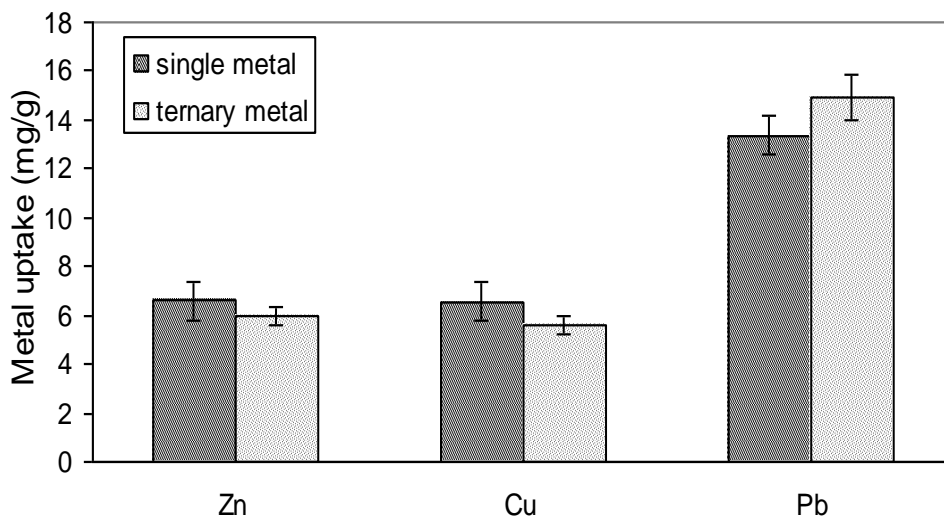


Figure 2.16. Comparison of uptake of single metals (metal concentration: 50 mg/l; pH 5.50; biomass dose: 4g/l) with uptake of metals in a ternary metal system ( $\text{Pb}^{2+}$ : 50mg/l,  $\text{Cu}^{2+}$ : 50mg/l,  $\text{Zn}^{2+}$ : 50mg/l; pH 5.50, biomass load: 4g/l).



This finding is consistent with the observations of Ferraz and Teixeira (1999) for co-ion effects on the metal uptake by the use of brewer's yeast. Sengil and Özacar (2009) observed a decrease in the biosorption of  $\text{Pb}^{2+}$  ions in presence of  $\text{Cu}^{2+}$  and  $\text{Zn}^{2+}$  ions. However, in binary metal system of Pb-Zn, presence of  $\text{Zn}^{2+}$  ions in different concentrations did not have any effects on  $\text{Pb}^{2+}$  ions uptake.

Considering a finite number of binding sites on yeast biomass and the competition between metal ions for occupying the available sites in the multi-element biosorption system, it can be concluded that adsorptive behaviour of yeast cells may vary with sequence of introducing the metals to the system. When metals are dissolved in water to form diluted solutions, metal ions are surrounded by water molecules and create hydrated species:



where  $\text{M}^{i+}(\text{aq.})$  represents hydrated metal ion, and (i) is the charge of the cation. As shown in Table 2.5, all three studied metal ions have the same covalent charges. Ionic radii of Cu and Zn are very close as they have atomic numbers of 29 and 30, respectively. But, Pb has a larger ionic radius and hence lower hydrated radius compared to Cu and Zn. Consequently, Pb has lower enthalpy of hydration and higher electronegativity than other two metals.

It has been reported that ions with higher hydrated radius possess stronger hydration enthalpy, which means the energy required to detach water molecules from those cations to make them available for binding sites on adsorbents is comparatively higher than ions with lower hydrated radius (Sengil and Özacar 2009; Motsi *et al.* 2009). Özer and Özer (2003) also observed different affinities of Pb, Ni, and Cd onto yeast cells in the order of metals atomic radius as well as electronegativity of the atoms.

Table 2.5. Ionic properties of tested metals in biosorption by yeast cells.

Cation	Charge	Ionic radius (Å)	Hydrated radius (nm)	Electronegativity	Enthalpy of hydration (kJ/mol)
Pb	2+	1.19	0.401	2.33	-1481
Cu	2+	0.73	0.419	1.90	-2100
Zn	2+	0.74	0.430	1.65	-2046

Sources: Sengil and Özacar (2009), Motsi et al.(2009), Amarasinghe and Williams (2007).

According to the hydration radii and electronegativity, the magnitude of adsorption should be  $\text{Pb}^{2+} > \text{Cu}^{2+} > \text{Zn}^{2+}$  and also according to the hydration enthalpies the sequence of biosorption should be  $\text{Pb}^{2+} > \text{Zn}^{2+} > \text{Cu}^{2+}$ . These orders of metal adsorptions are consistent with the experimental results of the present work for biosorption of metals by yeast cells for different environmental conditions. For instance, as shown in Figure 2.4 for single metal biosorption and Table 2.3 for tri-metallic combinations, metal removal capacity of yeast biomass follows the opposite order of changes in the hydration radius of the metals ( $\text{Pb}^{2+} > \text{Cu}^{2+} > \text{Zn}^{2+}$ ), whereas for pH around 6, which is more favorable for  $\text{Zn}^{2+}$  ions, the order changes to the sequence of enthalpy of hydration ( $\text{Pb}^{2+} > \text{Zn}^{2+} > \text{Cu}^{2+}$ ) assuming that no metal precipitation occurs.

### 2.3.7. Characterization of yeast-metal interactions (mechanism of biosorption)

As mentioned earlier, the BET results revealed that yeast cells are not porous. Therefore, most of the metal interaction occurs only on the surface of the non-living biomass. FTIR spectroscopy was used to determine the functional groups on the yeast cells involved in the metal binding process. Elemental analysis of the cells by EDX spectroscopy was used as a surface characterization technique to provide qualitative

and quantitative information of the elements presented on the surface of the cells (Michalak *et al.* 2010).

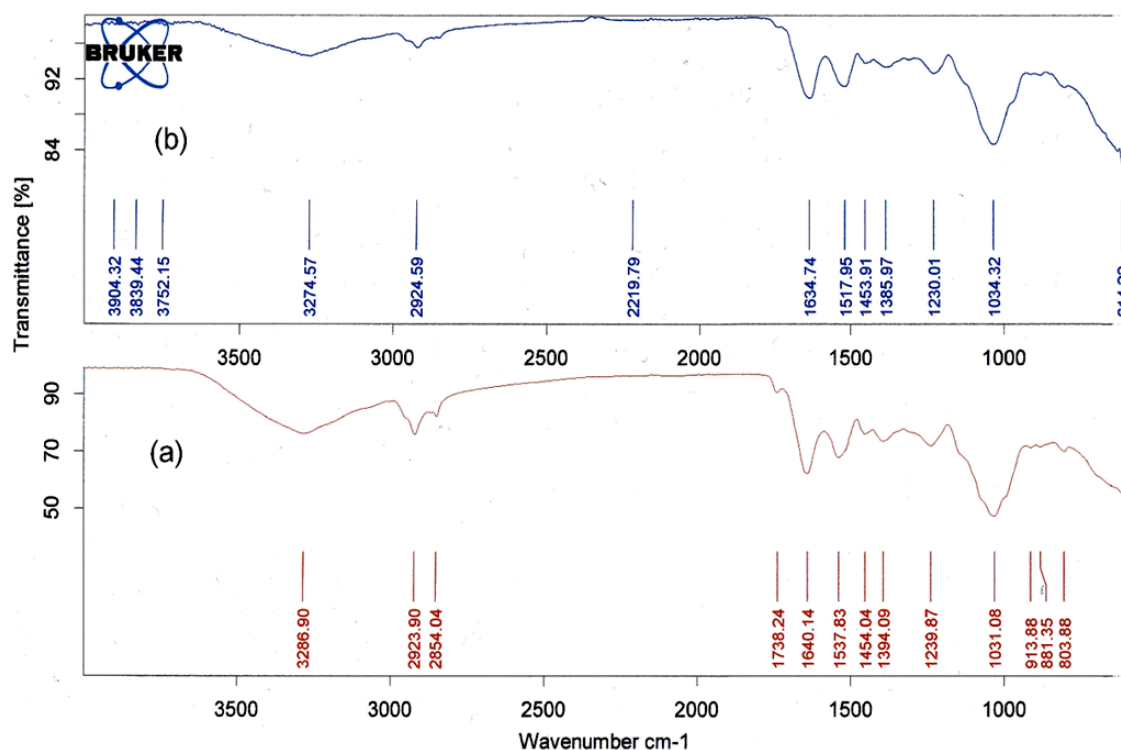


Figure 2.17. FTIR spectra of dried yeast cells (a) before and (b) after metal adsorption.

Figure 2.17 depicts the FT-IR spectrum of unloaded yeast cells in the range of 600–4000  $\text{cm}^{-1}$ . The spectrum shows a distinct peak at 3286  $\text{cm}^{-1}$  indicating the existence of hydroxyl (–OH) and (–NH) groups. The doublet peaks at 2923  $\text{cm}^{-1}$  and 2854  $\text{cm}^{-1}$  may represent C–H stretching vibrations, while peak at 1640  $\text{cm}^{-1}$  can be considered as C=O stretching vibration of a carboxylic acid, peak at 1537  $\text{cm}^{-1}$  represents amide II bond, 1239  $\text{cm}^{-1}$  can be assigned to P=O bond, and the absorption band at 1076  $\text{cm}^{-1}$  can be due to –CN or –C–O stretching vibrations (Bueno *et al.* 2008; Choi and Yun 2006; Minamisawa *et al.* 2004).

The observed changes in the spectrum of the metal-loaded cells with respect to unloaded cells are the shifts in wavenumbers, which are mainly pertaining to –COOH, –OH, and –NH bonds on the cell walls (Table 2.6). Similar changes have been observed for cadmium loaded sewage sludge by Choi and Yun (2006); and by Akar *et al.* (2005) for fungal biomass of *Botrytis cinerea*.

Table 2.6. FT-IR adsorption bands and suggested corresponding groups of control and Cu-loaded yeast cells.

Functional group (possible)	Wavenumber (cm <sup>-1</sup> )	
	Unloaded biomass	Metal-loaded biomass
(-OH and -NH groups)	3286	3274
C-H stretching	2932	2924
C-H stretching	2854	2855
C=O stretching (COOH)	1640	1634
Amide II band	1537	1517
C=O stretching	1454	1453
CH <sub>2</sub> bending vibrations, carboxylate stretching	1397	1385
P=O, C–N stretching	1239	1230
CN stretching	1031	1034
Sources: Bueno <i>et al.</i> (2008), Choi and Yun (2006), Minamisawa <i>et al.</i> (2004), Akar <i>et al.</i> (2009).		

EDX spectrum of in situ chemical composition of yeast cells before and after metal uptake is shown in Figures 2.18(a),(b). Comparing the peaks for untreated and metal-adsorbed biomass that has appeared at 2.3426, 1.0118, and 0.9297 kev (kilo electron volt) for Pb<sup>2+</sup>, Zn<sup>2+</sup>, and Cu<sup>2+</sup> ions, respectively, confirms that biosorption is mainly a surface adsorption that occurs onto the cell walls of yeast cells. The EDX spectra also show the peaks of potassium (K) at 3.3129 kev have disappeared after biosorption. This observation suggests the possibility of replacement of metal ions with K<sup>+</sup> ions on

the cell walls of yeast, which implies that an ion exchange mechanism is also involved between metal ions in the solution and the ions on the yeast cell surface.

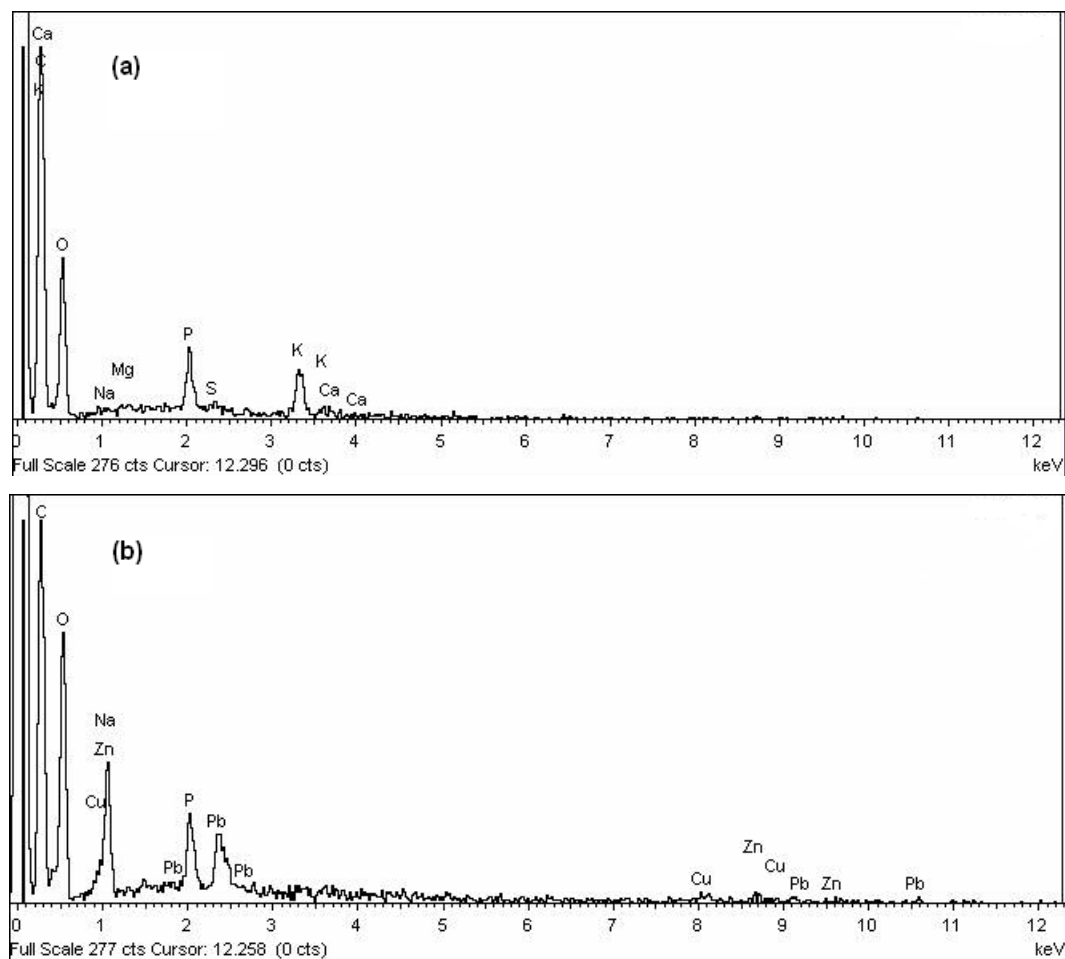


Figure 2.18. Elemental analyses for (a) untreated yeast cells; and (b) metal-treated yeast cells in simultaneous adsorption of  $\text{Pb}^{2+}$ ,  $\text{Cu}^{2+}$ , and  $\text{Zn}^{2+}$ .

ICP metal analysis results for the supernatants of dissolved biomass solutions before and after metal biosorption showed increased levels of  $\text{K}^+$ ,  $\text{Mg}^{2+}$ , and  $\text{Na}^+$  concentrations after biosorption (data are not shown). Increase in  $\text{Na}^+$  concentration was mainly because of NaOH additions for pH control; but, the substantial increase in the concentration of  $\text{K}^+$  ions confirmed the EDX results for ion exchange mechanism.

### 2.3.8. Biosorption process optimization

In previous sections, individual maximum removal efficiencies of yeast for  $\text{Pb}^{2+}$ ,  $\text{Zn}^{2+}$ , and  $\text{Cu}^{2+}$  were obtained based on design experiment results. For real applications, any changes in the environmental conditions for metal removal, such as pH of the biosorption column, would lead to different percentage removals of each metal in the mixture. The second degree polynomial regression eqns (6-8) were solved by Design Expert7 to obtain the optimum conditions in the experimental design space that ensures a combined maximum percentage removal in biosorption process involving three metals in absence of any chemical precipitation.

Table 2.7. Optimal conditions for removal of a mixture of  $\text{Pb}^{2+}$ ,  $\text{Zn}^{2+}$ , and  $\text{Cu}^{2+}$  ions by biosorption using *S. cerevisiae* to reach the target of 90%  $\text{Pb}^{2+}$  removal in a ternary metal wastewater stream.

Input parameters		Model outputs (optimum values)	
Pb Removal Efficiency (%)	90	pH	5.52
Initial metal load (mg/l)	20	Biomass dose (g/l)	6.15
		Cu percentage removal (%)	45
		Zn percentage removal (%)	44

The optimum values of the biosorption variables in this study to reach a maximum removal of 90% of  $\text{Pb}^{2+}$  ions of an industrial waste stream containing 20 mg/l of  $\text{Pb}^{2+}$ ,  $\text{Zn}^{2+}$ , and  $\text{Cu}^{2+}$  ions (as an example) are summarized in Table 2.7. Depending on the concentration of heavy metals in an industrial effluent, and the target removal for each metal, the model equations can be solved and the optimum conditions corresponding to the desired metal removal by biosorption can be obtained.

## 2.4. Conclusions

Biosorption studies were carried out with both single metal and ternary metal solutions of  $\text{Pb}^{2+}$ ,  $\text{Zn}^{2+}$ , and  $\text{Cu}^{2+}$ . The non-living cells of *S. cerevisiae* adsorb  $\text{Pb}^{2+}$  ions more

than copper and zinc ions both in single and multi-metal solutions. In ternary metal system, yeast cells retained its overall metal uptake capacity, although, a slight increase in  $\text{Pb}^{2+}$  ions uptake and a slight reduction in  $\text{Zn}^{2+}$  and  $\text{Cu}^{2+}$  ions uptake occurred.

The FTIR analysis on the spectra of untreated and metal-treated biomass revealed their chemical environment responsible for biomass-metal interactions. Comparing the EDX spectra of the dried biomass before and after metal exposure, and the ICP results of their supernatant solutions (mainly for  $\text{K}^+$  ions) suggested the involvement of an ion exchange mechanism in adsorption of metals by yeast cells. Additionally, changes in the electrokinetic (Zeta potential) properties of *S. cerevisiae* in presence of metals suggested that the mechanism of bio-adsorption can be based on electrostatic interactions of the metal ions with the negatively charged functional groups of the biomass surface.

The regression analysis by RSM was used to predict the performance of simultaneous adsorption of  $\text{Pb}^{2+}$ ,  $\text{Cu}^{2+}$ , and  $\text{Zn}^{2+}$  on the yeast cells. The resulted model equations for metal removal efficiency fitted well with quadratic equations with statistically significant model F ratios ( $<0.0500$ ) and the Adj- $R^2$  values of greater than 0.91. Process optimization helped to evaluate the simultaneous effects of pH, initial metal concentration, and biomass dose on competitive biosorption of metals by yeast cells. Since biosorption of heavy metals is a highly pH-dependent process, pH control was imperative during the adsorption process to ensure that biosorption was the only mechanism responsible for metal removal. Nevertheless, a combination of biosorption and chemical precipitation might be useful for practical applications in commercial scale. The results obtained in this work provide the framework for further study on biosorption of metals in continuous systems.

## 2.5. Acknowledgement

This work was supported by NSERC Discovery Grants awarded to Drs. A. Margaritis and M.B. Ray.

## 2.6. References

- [1] Akar S.T., Gorgulu A., Anilan B., Kaynak Z., Akar T., Investigation of the biosorption characteristics of lead(II) ions onto *Symphoricarpus albus*: batch and dynamic flow studies, J. Hazard. Mater., (2009) 165, 126–133.
- [2] Akar T., Tunali S., Kiran I., *Botrytis cinerea* as a new fungal biosorbent for removal of Pb(II) from aqueous solutions, Biochem. Eng. J., (2005) 25, 227–235.
- [3] Aksu Z., Donmez G., A comparative study on the biosorption characteristics of some yeasts for Remazol Blue reactive dye, Chemosphere, (2003) 50, 1075–1083.
- [4] Alluri H.K., Ronda S.R., Settalluri V.S., Bondili J.S., Suryanarayana, V., Venkateshwar P., Biosorption: an eco-friendly alternative for heavy metal removal, Afr. J. Biotechnol., (2007) 6, 2924–2931.
- [5] Amarasinghe B.M.W.P.K., Williams R.A., Tea waste as a low cost adsorbent for the removal of Cu and Pb from wastewater, Chem. Eng. J., (2007) 132, 299–309.
- [6] Anderson M.J., Whitcomb P.J., RSM simplified: optimizing processes using response surface methods for design of experiments, Boca Raton, FL: CRC Press, (2005).
- [7] Ansari M.I., Masood F., Malik A., Bacterial Biosorption: A Technique for Remediation of Heavy Metals, in: Ahmad, I., Ahmad, F. and Pichtel, J., eds., Microbes and Microbial Technology Agricultural and Environmental Applications, Springer, (2011) 283–319.
- [8] Bayrock D., Ingledew W.M., Fluidized bed drying of baker's yeast: moisture levels, drying rates, and viability changes during drying, Food Res. Int., (1997) 30, 6, 407–415.
- [9] Bueno B.Y.M., Torem M.L., Molina F., de Mesquita L.M.S., Biosorption of lead(II), chromium(III) and copper(II) by *R. opacus*: Equilibrium and kinetic studies, Miner. Eng., (2008) 21, 65–75.



- [10] Choi S.B., Yun Y.S., Biosorption of cadmium by various types of dried sludge: an equilibrium study and investigation of mechanisms, *J. Hazard. Mater.*, (2006) B138, 378–383.
- [11] Cojocaru C., Diaconu M., Cretescu I., Savic J., Vasic V., Biosorption of copper(II) ions from aqua solutions using dried yeast biomass, *Colloid Surface A.*, (2009) 335, 181–188.
- [12] Ferraz A.I., Teixeira J.A., The use of flocculating brewer's yeast for Cr (III) and Pb(II) removal from residual wastewaters, *Bioprocess Eng.*, (1999) 21, 431–7.
- [13] Ferreira S., Duarte A.P., Ribeiro M.H.L., Queiroz J.A., Domingues F.C., Response surface optimization of enzymatic hydrolysis of *Cistus ladanifer* and *Cytisus striatus* for bioethanol production, *Biochem. Eng. J.*, (2009) 45, 192–200.
- [14] Ghorbani F., Younesi H., Ghasempouri S.M., Zinatizadeh A.A., Amini M., Daneshi A., Application of response surface methodology for optimization of cadmium biosorption in an aqueous solution by *Saccharomyces cerevisiae*, *Chem. Eng. J.*, (2008) 145, 267–275.
- [15] Igwe J.C., Abia A.A., A bioseparation process for removing heavy metals from waste water using biosorbents, *Afr. J. Biotechnol.*, (2006) 5, 1167–1179.
- [16] Kordialik-Bogacka E., Surface properties of yeast cells during heavy metal biosorption, *Cent. Eur. J. Chem.*, (2011) 9, 348–351.
- [17] Kotrba P., Mackova M., Macek T., *Microbial biosorption of metals*, Springer, (2011).
- [18] Lesmana S.O., Febriana N., Soetaredjo F.E., Sunarso J., Ismadji S., Studies on potential applications of biomass for the separation of heavy metals from water and wastewater, *Biochem. Eng. J.*, (2009) 44, 19–41.
- [19] Ma W., Tobin J.M., Determination and modeling of effects of pH on peat biosorption of chromium, copper and cadmium, *Biochem. Eng. J.*, (2004) 18, 33–40.
- [20] Machado M.D., Janssens S., Soares H.M.V.M., Soares E.V., Removal of heavy metals using a brewer's yeast strain of *Saccharomyces cerevisiae*:

- advantages of using dead biomass, *J. Appl. Microbiol.*, (2009) 106, 1792–1804.
- [21] Marques P.A.S.S., Rosa M.F., Pinheiro H.M., pH effects on the removal of  $\text{Cu}^{2+}$ ,  $\text{Cd}^{2+}$  and  $\text{Pb}^{2+}$  from aqueous solution by waste brewery biomass, *Bioprocess Eng.*, (2000) 23, 135–141.
- [22] Michalak I., Chojnacka K., Marycz K., Using ICP-OES and SEM-EDX in biosorption studies, *Mikrochim. Acta*, (2010) 172, 65–74.
- [23] Minamisawa M., Minamisawa H., Yoshida S., Takai N., Adsorption behavior of heavy metals on biomaterials, *J. Agric. Food Chem.*, (2004) 52, 5606–5611.
- [24] Motsi T., Rowson N.A., Simmons M.J.H., Adsorption of heavy metals from acid mine drainage by natural zeolite, *Int. J. Miner. Process*, (2009) 92, 42–48.
- [25] Naja G.M., Volesky B., Toxicity and sources of Pb, Cd, Hg, Cr, As, and radionuclides in the environment, in: Wang, L.K., Chen, J.P., Hung, Y.T. and Shammass, N.K., eds., *Heavy metals in the environment*, Boca Raton CRC Press, (2009) Chapter 2.
- [26] Nriagu J.O., Global metal pollution, poisoning the biosphere? , *Environment*, (1990) 32, 7: 7–11; 28–33.
- [27] Nriagu J.O., Pacyna J.M., Quantitative assessment of worldwide contamination of air water and soils by trace metals, *Nature*, (1988) 333, 134–139.
- [28] Özer A., Özer D., Comparative study of the biosorption of Pb(II), Ni(II) and Cr(VI) ions onto *S. cerevisiae*: determination of biosorption heats, *J. Hazard. Mater.*, (2003) B100, 219–229.
- [29] Padmavathy V., Vasudevan P., Dhingra, S.C., Biosorption of nickel(II) ions on Baker's yeast, *Process Biochem.*, (2003) 38, 1389–1395.
- [30] Preetha B., Viruthagiri T., Application of response surface methodology for the biosorption of copper using *Rhizopus arrhizus*, *J. Hazard. Mater.*, (2007) 143, 506–510.

- [31] Schecher W.D., McAvoy D.C., MINEQL+: A Chemical Equilibrium Program for Personal Computers, Version 3.0, Environmental Research Software, (1994) Hallowell, Maine.
- [32] Sengil I.A., Özacar M., Competitive biosorption of  $Pb^{2+}$ ,  $Cu^{2+}$  and  $Zn^{2+}$  ions from aqueous solutions onto valonia tannin resin, J. Hazard. Mater., (2009) 166, 1488–1494.
- [33] Srivastava S., Goyal P., Novel Biomaterials: decontamination of toxic metals from wastewater, Springer-Verlag Berlin, (2010).
- [34] Volesky B., Sorption and biosorption, BV-Sorbex Inc., St. Lambert, Quebec, (2003).
- [35] Volesky B., Biosorption of heavy metals, CRC Press, Boca Raton, FL, (1990).
- [36] Volesky B., Biosorption and me, Water Res., (2007) 41, 4017–4029.
- [37] Volesky B., May-Phillips H.A., Biosorption of heavy metals by *Saccharomyces cerevisiae*, Appl. Microbiol. Biotechnol., (1995) 42, 797–806.
- [38] Volesky B., Naja G., Biosorption technology: starting up an enterprise, Int. J. Technol. Transf. Commer., (2007) 6, 196–211.
- [39] Wang J., Chen C., Biosorption of heavy metals by *Saccharomyces cerevisiae*: A review, Biotechnol. Adv., (2006) 24, 427–451.

## **Chapter 3**

# **Removal of Heavy Metals from Aqueous Solutions Using *Saccharomyces cerevisiae* in a Continuous Bioreactor- Biosorption System**

## Abstract

The adsorption behaviour of unmodified yeast cells of *Saccharomyces cerevisiae* to remove  $\text{Pb}^{2+}$  and  $\text{Cu}^{2+}$  ions from aqueous solutions in continuous mode was studied. Yeast biomass showed mediocre capacity for  $\text{Cu}^{2+}$  ions compared to that of  $\text{Pb}^{2+}$  ions in the metals concentrations range of 10 – 180 mg/l. Metal-binding capacity of yeast cells reached to a maximum of 29.9 mg/g and 72.5 mg/g for  $\text{Cu}^{2+}$  and  $\text{Pb}^{2+}$  ions, respectively, under similar experimental conditions. The rate of biosorbent production in the continuous bioreactor, governed by dilution rate equal to maximum specific growth rate of the cells, was the limiting factor of the biosorption system. At low metal concentration,  $\text{Cu}^{2+}$  removal by yeast cells was higher than previously studied heat-deactivated yeast biomass suggesting involvement of both intracellular and surface-based sequestrations. The removal efficiencies of the test metals decreased as the initial metal concentrations increased. Equilibrium adsorption of the metals by yeast cells was well described by the Langmuir isotherm model. The adsorption kinetics data fitted to diffusion-based and chemical reaction-based models showed intracellular diffusion as the rate controlling step at low metal loads. The results obtained suggest that the use of live yeast cells in a self-contained continuous adsorption system is an effective method for removal of heavy metals from industrial effluents reducing biomass pretreatment and preparation steps as well as achieving on-line adsorbent production, biosorption, and effluent treatment.

## 3.1. Introduction

Biosorption is an attractive method for heavy metal removal from metal-laden effluents due to low cost and high efficiency of the process. Despite increased understanding of biosorption phenomenon and abundance of research in this field, an industrially relevant method for biosorption technology has not been fully realized yet

(Wang and Chen, 2006; Volesky and Naja, 2007; Lesmana et al., 2009; Wang and Chen, 2009; Fomina and Gadd, 2014). Most of the studies in the field deal with batch equilibrium studies relating adsorbate, adsorbent, and operating conditions.

Although biosorption is defined as the property of certain non-living biomaterials to bind and concentrate selected ions or other molecules from aqueous solutions (Volesky, 2007), it can occur in both living and dead microorganisms (Tobin et al., 1994; Fomina & Gadd, 2014). Metal uptake is a combination of a metabolism independent physical process, followed by a metabolic step known as bioaccumulation (Wehrheim and Wettern, 1994). To the best of our knowledge, no studies have been reported on the use of yeast cells in a combined continuous bioreactor-biosorption system for the removal of heavy metals from aqueous solutions.

Removal of heavy metals in continuous mode was earlier reported as a preferred choice in some metal adsorption studies. For instance, Kapoor and Viraraghavan (1998) used immobilized cells of *A. niger* in a continuous operation for the removal of metal solutions containing cadmium, copper lead, and nickel. Marques et al. (2007) used a fixed-bed reactor for Cd removal using immobilized cells of an industrial strain of *Saccharomyces cerevisiae*. There are certain potential limitations of continuous fixed bed adsorption: low density of fungal biomass reported to be problematic in fixed-bed operation due to clogging and subsequent release of biomass in the treated wastewater.

Immobilization of biomass also causes mass transfer limitations by hindering the access of the metals to the biosorbent sites compared to suspended biosorbents (Tsezos, 1990; Cassidy et al., 1996). Moreover, since the regeneration capacity of immobilized cells is limited, biomass needs to be frequently replaced, which is a costly process. However, continuous operation is the only viable way of treating large volume of wastewater in a reasonable time, and this is where most of the bench scale batch biosorption studies are limited in their scope. Biosorbents with different degrees of metal adsorption capacities, availability, and selectivity have been shown to be

promising for metal removal from aqueous solutions in batch laboratory scale, but it is their applicability in continuous mode that makes this treatment method attractive for industrial application.

Based on our earlier work (Amirnia et al., 2012) on the removal of  $\text{Cu}^{2+}$ ,  $\text{Pb}^{2+}$  and  $\text{Zn}^{2+}$  by *S. cerevisiae* in a batch system, continuous metal adsorption using *S. cerevisiae* in an air-lift vessel was attempted in this work. Very little information is available in literature on the use of unmodified live and resting cells for biosorption (Gonen and Aksu, 2008).

The main objective of this work was to examine the ability of yeast cells to be produced and utilized in a continuous fashion for removing metal ions in water. This is regarded as one of the desirable characteristics for a good and useful biosorbent (Lokeshwari and Joshi, 2009). The yeast cells produced in the continuous bioreactor system provided continuously fresh surface for adsorption of the metals without the need for costly pretreatment steps, such as harvesting, separating, heat-killing, drying, and storage of biomass. Copper and lead ions were chosen as the model metals for biosorption due to their widespread use in metal industry and their toxicity for humans and environmental health (Health Canada, 2013; Reisman et al., 1987).

## **3.2. Material and Methods**

A schematic of the continuous biosorption system is shown in Figure 3.1. A 1.2 liter plexiglass double draft fluidized vessel was used as the adsorption column whereas yeast biomass as biosorbent was produced in a 1.5 liter stirred tank bioreactor. The sampling points, biosorbent and metal solution flow lines, adsorption and biomass separation sections are illustrated in Figure 3.1.

### **3.2.1. Biomass Preparation**

Yeast inoculum was prepared by aseptically transferring the active dry yeast (Fleischmann's Co) to a 500 ml flask containing the sterile medium. The flask was

incubated at 25 °C in a shaker at 200 rpm and the bioreactor was inoculated with the yeast suspension harvested at its late exponential phase of batch growth (~16-20 hours of incubation).

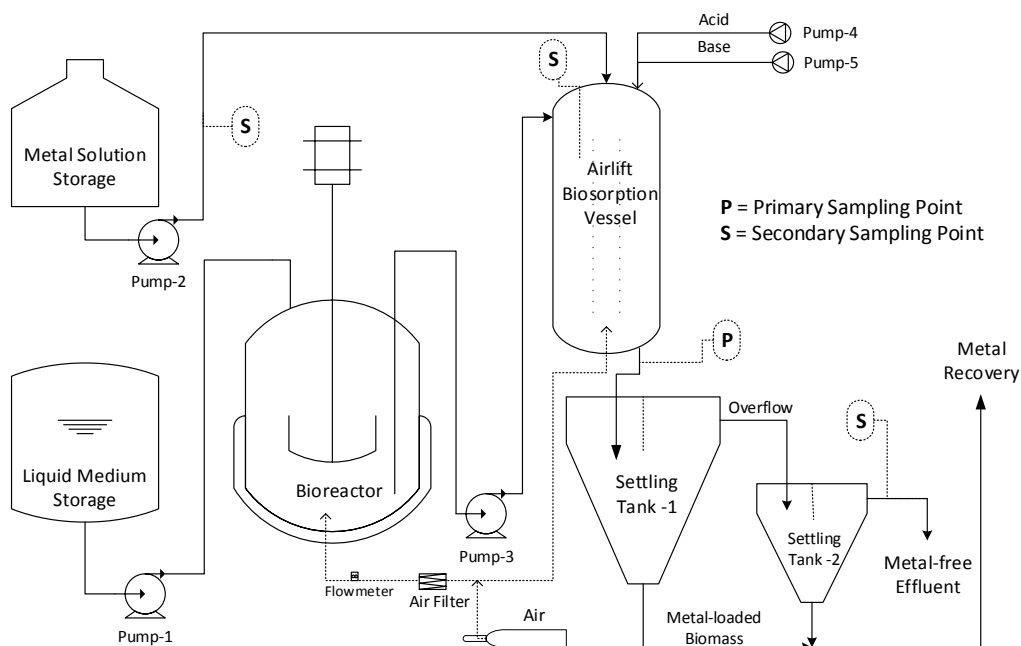


Figure 3.1. Schematic process flow diagram of the continuous biosorption system (sampling points are shown on the diagram).

The bioreactor was agitated at 200 rpm and aerated with an air flow of 1vvm (1.5 liter/min) at room temperature. The liquid medium was comprised of 20 g/l dextrose, 5 g/l peptone, 3 g/l yeast extract, and 3 g/l malt extract, similar to the nutrients used by Volesky and May-Phillips (1995). A steady exponential growth phase was maintained in the bioreactor by altering the liquid medium volumetric flow rate into the reactor and the outflow of biomass from the reactor.



### 3.2.2. Analytical method

Copper and lead were used as model metals for biosorption. Stock solutions of  $\text{Cu}^{2+}$  and  $\text{Pb}^{2+}$  ions were prepared using copper (II) sulfate pentahydrate ( $\text{CuSO}_4 \cdot 5\text{H}_2\text{O}$ ) and  $\text{Pb}(\text{NO}_3)_2$ , respectively. Samples were regularly collected from the feed tank, airlift vessel's sampling port (C), liquid outlet from the airlift column (F), and the overflow of the 2<sup>nd</sup> settling tank (details illustrated in Figures 3.1 and 3.2). Metal concentrations of the samples were analyzed using inductively Coupled Plasma Optical Emission Spectrometry (ICP-OES, Varian Varian, Inc., Vista-Pro Axial) after centrifugation and removal of biomass.

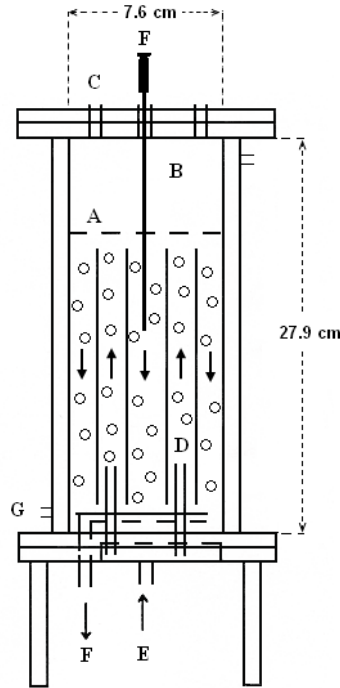


Figure 3.2. Schematic diagram of the 2-L double draft airlift adsorption column: (A) liquid level, (B) head space, (C) sampling ports, (D) air jet orifices, (E) air inlet, (F) liquid outlet, (G) jacket (adapted from Bashar et al., 2003).

Metal uptake capacity,  $q_t$  (mg / g) and removal efficiency, RE (%) of biomass were obtained based on mass balance in the following forms:

$$q_t = \frac{(C_0 - C_t)}{C_{Biomass}} \quad (1)$$

$$\text{RE (\% Removal Efficiency)} = \frac{(C_0 - C_t)}{C_0} \times 100 \quad (2)$$

where  $C_0$  (mg / l) was the initial metal concentration at the bulk solution,  $C_t$  (mg / l) outlet metal concentration at time  $t$ , and  $C_{Biomass}$  the concentration of biomass (g / l) at time  $t$ . At equilibrium,  $C_t = C_e$ .

### 3.2.3. Maximum specific growth rate of yeast cells

The growth curve of *S. cerevisiae* (Figure 3.3) was determined by taking samples from the bioreactor and measuring the optical density and dry weight of *S. cerevisiae* cells. The exponential phase represented the cells maximum specific growth rate ( $\mu_{\max}$ ). The value of  $\mu_{\max}$  was obtained from the slope of the plot of  $\ln x$  vs. time.

The rate of biomass production in batch system during the exponential phase is expressed as (Walker, 1998);

$$\frac{dx}{dt} = \mu \cdot x \quad (3)$$

$$\ln\left(\frac{x}{x_0}\right) = \mu \cdot t \quad \text{or, } x = x_0 e^{\mu \cdot t} \quad (4)$$

In continuous system, fresh medium for yeast growth was supplied in a steady rate into the bioreactor; therefore, there was no depletion of nutrients, and yeast cells experienced prolonged period of exponential growth without entering into deceleration and stationary phases (Walker, 1998). The change in biomass concentration in continuous culture system is described as:

$$\frac{dx}{dt} = \mu x - Dx \quad (5)$$

where  $D$  is the dilution rate ( $h^{-1}$ ). At steady state, the yeast growth rate remained constant ( $dx/dt = 0$ ) and the growth rate of the cells ( $D = \mu$ ) was dictated by dilution rate. According to Eq. (5), for dilution rates more than  $\mu_{\max}$ , the biomass concentration in the bioreactor will decrease with time as the cells will be washed out from the bioreactor.

Optimized biomass productivity required for biosorption with maximum surface area possible necessitates that the specific growth rate in the bioreactor be as high as possible. As shown in Figure 3.3, yeast cells attained a specific growth rate of  $0.0994 h^{-1}$ , so the biomass discharge flowrate from bioreactor for an operating volume of 1.5 liter was adjusted to be  $2.49 ml/min$ . The biomass concentration in the bioreactor was examined by taking periodic samples from the bioreactor and measuring the optical density.

### **3.2.4. Continuous biosorption operation**

As illustrated in Figure 3.1, the bioreactor-biosorption system was operated in a continuous mode. A constant cell population size and a constant level of liquid culture in the bioreactor were maintained by keeping  $D = \mu$ . A one-time batch incubation was required before cells inoculation in the bioreactor containing liquid medium reached steady state.

When biomass concentration reached around  $3 g/l$  in the bioreactor, feed and liquid culture pumps (pump 1, and 3 in Figure 3.1) were started simultaneously to deliver the nutrients to bioreactor and the biomass solution to the airlift adsorption column, respectively. Metal solution was fed into the adsorption column by pump 2 co-current to the biomass flow. When the liquid level reached to a point that air bubbles circulation was complete in the adsorption column (Level A in Figure 3.2), the discharge valve was opened to keep the liquid level constant in the adsorption column.

Gravity flow was used to transfer the metal-loaded biomass from adsorption column to settling tanks. Biomass was separated from liquid using two settling tanks in series. Separated biomass was periodically discharged from the settling tanks to be used in batch desorption process, which was not used in the present work. The stable and steady state operation of the continuous system ran for 8 weeks in a row until all the required data were collected.

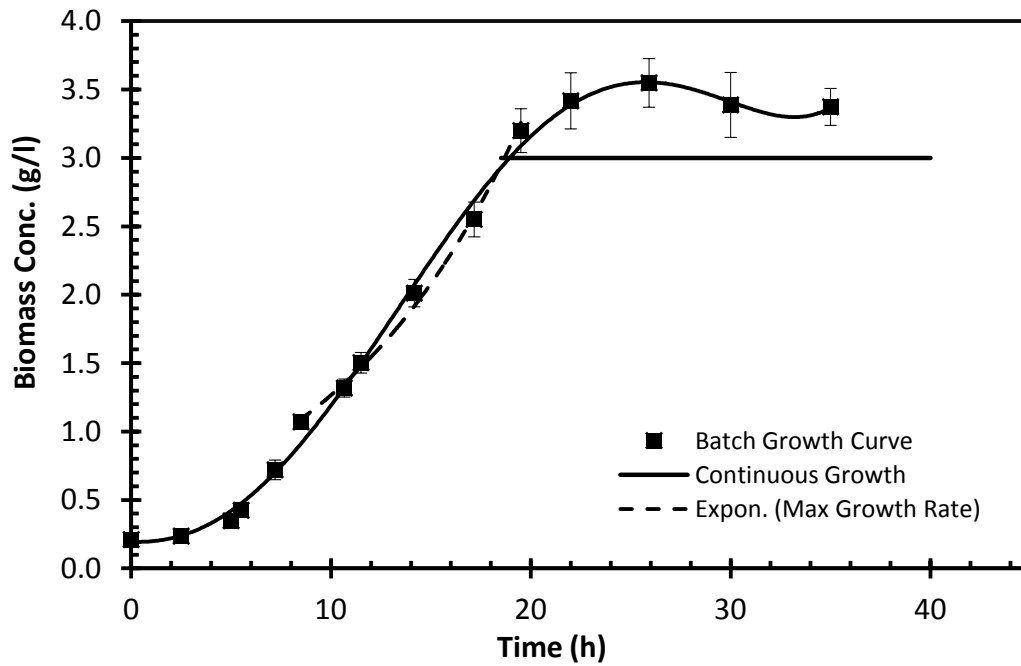


Figure 3.3. Yeast growth curves in batch and continuous culture. In the continuous system, the growth curve became constant at the biomass concentration of 3 g/l at the end of exponential growth phase.

### 3.2.5. Adsorption column

A double-draft airlift column was used for biosorption experiments, in which, air bubbles through the draft tubes concentrically located inside the column mix the contents of the column. Figure 3.2 shows the column dimensions and air bubbles circulation pattern which created a good mixing and suspension of biosorbents in the system. The air orifices were located in the annular region between the outer and inner

draft tubes. This type of contactor was used to create a low shear mixing without the use of an agitator to allow settling of the agglomerated bioparticles in the adsorption column. Scaled up airlift system would also be less energy intensive compared to a stirred tank.

White and Gadd (1990) showed that an airlift bioreactor can remove thorium by fungal biomass more effectively than a stirred tank. Pilkington et al. (1998) also found that gas lift draft tube systems are attractive for large scale industrial applications as these systems provide good mixing, consume low power, and are of simple construction.

### 3.2.6. Adsorption surface area

Total yeast cell count in the column was measured using a Neubauer hemocytometer. The diluted cell suspension was placed in the counting chambers including 25 squares (each square has an area  $0.025 \text{ mm}^2$  and depth of  $0.1 \text{ mm}$ ) and the number of cells was counted using an optical microscope with a 40X objective. The total cells per unit volume or the concentration of the cells were  $57.6 \times 10^9 (\pm 15\%)$  cells/ml, and the number of cells per unit mass of biomass was calculated to be  $19.2 \times 10^9 (\pm 15\%)$  cells/mg dry wt.

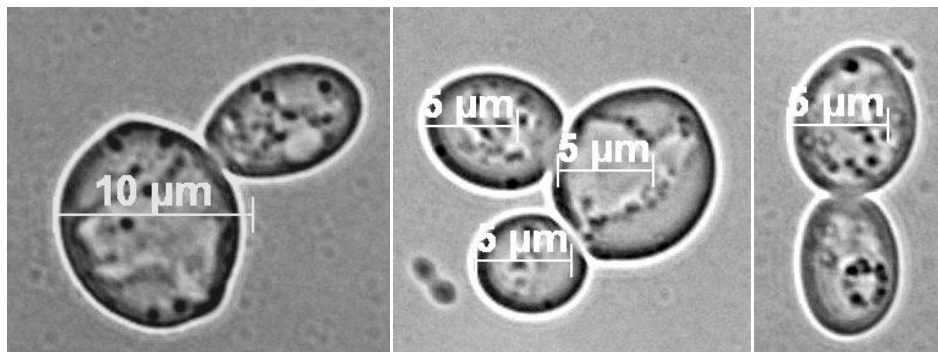


Figure 3.4. Size of yeast cells observed under optical microscope with 100X magnification

The size of yeast cells in the bioreactor varied from 5 – 9  $\mu\text{m}$  (Figure 3.4). Considering a prolate spheroid shape for yeast cells with polar diameter of 7.5  $\mu\text{m}$  and equatorial diameter of 6  $\mu\text{m}$ , the surface area of cells,  $S$ , available for adsorption of metals can be calculated as (Selby, 1969);

$$S = 2\pi a^2 \left( 1 + \frac{b}{a.e} \sin^{-1} e \right) \quad (6)$$

Where  $a$  is the equatorial radius,  $l$  the polar radius,  $e^2 = (1 - a^2/b^2)$ , and arcsine value is in radians. Using Eq. (6), the external surface area of each cell is 132.4  $\mu\text{m}^2$ . Therefore, considering the above calculated cell population, the estimated total area available for mass transfer was ~2500 ( $\pm 15\%$ )  $\text{m}^2/\text{g}$  dry wt. cells.

### 3.3. Results and Discussion

#### 3.3.1. Optimal physicochemical conditions

Environmental conditions such as solution pH, biomass concentration, and metal concentration are important factors affecting the biosorption of metals. Among them, solution pH is of paramount importance as it affects metal ion speciation in solution, surface charge of the biomass, and chemistry of biomass binding sites (Amirnia et al., 2012).

In the continuous biosorption system used in this study, the biomass concentration in the bioreactor was constant (3 g/l). However, biomass and metal concentrations varied in the adsorption column based on the feed concentration and the metal/biomass flowrate ratio. The mass balance results in the biosorption column for metals are summarized in Table 3.1.

All experiments were conducted at the ambient temperature of 22 °C. Solution pH was automatically controlled with a pH-controller connected to acid and base pumps with variable speeds (Figure 3.1). The optimal biosorption pH for each metal (namely, pH= 5.5 for Cu and pH=5.0 for Pb) was used based on our earlier results obtained from

batch adsorption experiments (Amirnia et al., 2012). At steady state, the sugar content in the bioreactor's discharge was monitored using DNS method and was approximately 0.1 g/l.

Table 3.1. Metal and biomass concentration fluctuations in the inlet of biosorption tank affected by the flowrate ratio of metal over biomass.

<b>Metal Feed Concentration</b> (mg/l)	<b>Biomass Conc. (g/l)</b>		
	2.5	1.5	0.75
	<b>Flowrate Ratio</b> (Metal/Biomass)		
	0.2	1	3
	<b>C<sub>0</sub>, Initial Metal Concentration</b> in Adsorption Column (mg/l)		
10	-	-	8
20	-	10	15
30	-	15	22.5
60	10	30	45
100	16.7	50	75
120	20	60	90
140	23.3	70	105
180	30	90	135
240	40	120	180
360	60	180	-
720	120	-	-
1080	180	-	-

### 3.3.2. Mixing time

Mixing times of the airlift fluidized column and a same size stirred tank equipped with one set of 45° pitched turbine 6-blade impeller were evaluated in different airflow rates and RPM, respectively.

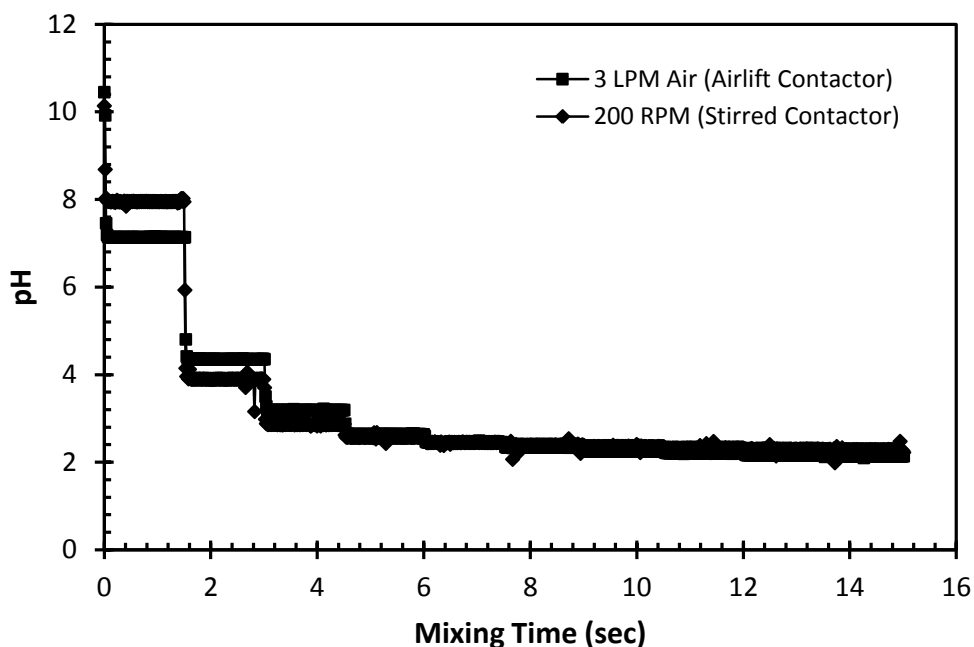


Figure 3.5. Mixing time comparisons for the airlift and stirred contactors of same volume.

Mixing time was measured by adding 5 ml of 2M HCl and 2M of NaOH to each system and monitoring the rate of change of pH by a pH-meter connected to LabTech software, which had the ability of recording 60 pH values per second. Airflow of 2 to 8 LPM (Std L.min<sup>-1</sup>), and mixing rates of 150 to 350 rpm were used and the mixing times were compared. This experiment confirmed that mixing time does not improve beyond 3 LPM and 200 rpm for the same volume airlift column and stirred tank, respectively (results not shown). Test results also showed that mixing times for the



airlift fluidized contactor at 3LPM airflow is equivalent to a 200 rpm stirred tank (Figure 3.5).

### **3.3.3. Continuous adsorption studies**

Figure 3.6 shows the adsorption test results for  $\text{Cu}^{2+}$  and  $\text{Pb}^{2+}$  ions with yeast cells in the continuous system at steady state. The amount of metal ions adsorbed per unit mass of biomass at equilibrium increased with increase in initial metal concentrations. Yeast cells had good adsorption capacity for  $\text{Pb}^{2+}$  ions, exceeding 20 and 74 mg of Pb per g of biomass for the 5 and 40 mg/l equilibrium concentrations of  $\text{Pb}^{2+}$ , respectively. For  $\text{Cu}^{2+}$  ions, the uptake of metals by cells at the same biomass and metal equilibrium concentrations reached to about 4 and 16 mg  $\text{Cu}^{2+}$ /g, respectively.

The increase in adsorption capacity for metals by the increase in initial metal concentration from 10 to 180 mg/l can be attributed to increase in concentration difference as driving force for mass transfer of metals between the liquid phase and the adsorbent yeast biomass. Metals removal efficiencies were also influenced by the initial concentration of the metals in the liquid phase (Figure 3.6). Steady state removal of metals decreased with the initial metal concentration due to fixed amount of biosorbent available for biosorption. On the other hand, equilibrium adsorption increased with the increased concentration due to higher values of the numerator in Eq. (1).

### **3.3.4. Continuous vs. batch sorption**

Batch studies for metal biosorption by yeast cells are widely reported. The studies by Volesky (1994) and Wang and Chen (2006) indicated that yeast biomass is a mediocre biosorbent due to fermentation broth residues adhered to the surface of the cells that affects metal uptakes. Other studies such as Bashar et al. (2003) and Volesky (2003) reported high affinity of yeast cells for some cations such as Cd and Pb up to 10% of the mass of biomass. On the other hand, Volesky and May-Phillips (1995) observed a 3-fold increase in copper uptake by live cells of Baker's yeast compared to dead yeast

*S. cerevisiae*. However, the study by Machado et al. (2009) indicated that for  $\text{Cu}^{2+}$  ions, live and dead brewer's yeast cells have similar accumulations.

In this work, as depicted in Figure 3.7, live yeast cells showed 25.2%, 21.3%, and 11.3% higher adsorption capacities for  $\text{Cu}^{2+}$  ions than previously reported for non-living cells (Amirnia et al., 2012) at initial metal concentration of 10 mg/l, 15 mg/l, and 30 mg/l, respectively, and at a biomass dose of 1.5 g/l. However, metal removal percentage for living cells was almost the same as non-living cells at metal concentration of 50 mg/l, and 14.3% lower at metal concentration of 60 mg/l. Biosorption of metals on non-living cells is known to be a passive phenomenon (Wang and Chen, 2006; Volesky, 2007).

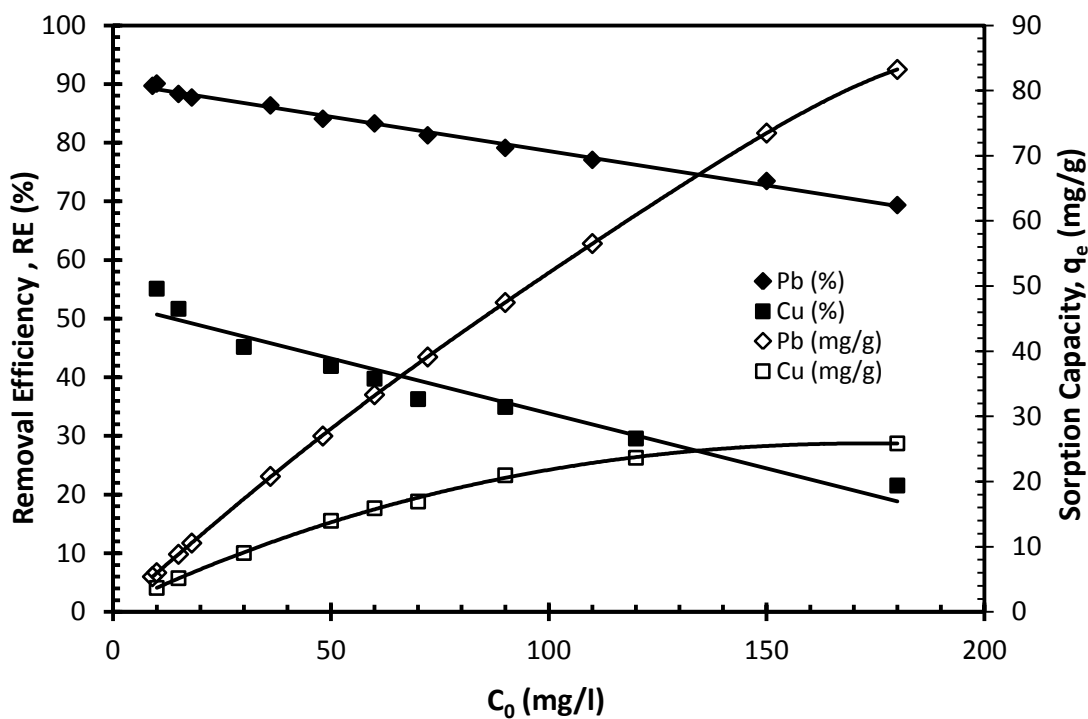


Figure 3.6. Metal uptake (mg/g) and percentage removal (%) plots for biosorption of test metals at different initial concentrations and biomass dose of 1.5 g dry wt./l in continuous biosorption system (data represents an average of three independent experiments).

The higher binding capacity of living yeast cells for copper implies an involvement of an active and dynamic copper-binding mechanism. On the other hand, an average decrease of 9.5% was observed for the percentage removal of  $\text{Pb}^{2+}$  ions at the same range of metal concentrations. The lower Pb binding capacity of live yeast cells than that of non-living cells could be explained by live cells' toxicity and metal tolerance mechanisms impeding the excessive  $\text{Pb}^{2+}$  bindings on the cells. Suh et al. (1998) observed that  $\text{Pb}^{2+}$  ions penetrate into the inner cellular parts of live *S. cerevisiae* after 24 h exposure to the metal, which may result in a higher accumulation of  $\text{Pb}^{2+}$  ions by live cells than that of non-living cells. However, they showed a lower initial  $\text{Pb}^{2+}$  accumulation rates (< 24 h) for live cells in comparison to dead cells, which is in agreement with our findings in this work having a limited contact time in the biosorption column.

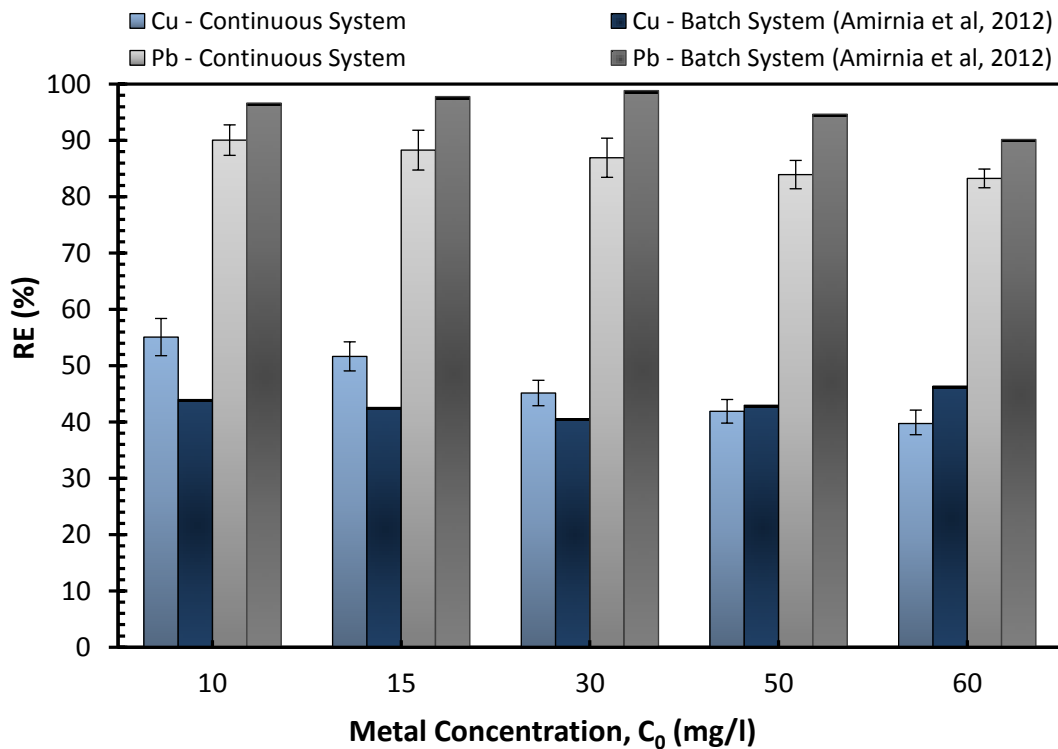


Figure 3.7. Batch vs. continuous adsorption performance comparisons for  $\text{Cu}^{2+}$  and  $\text{Pb}^{2+}$  ions under similar environmental conditions (e.g. biomass dose; 1.5 g/l, pH 5.5 for  $\text{Cu}^{2+}$ , and 5.0 for  $\text{Pb}^{2+}$  adsorption). Heat-dried non-living cells used in previously studied batch experiments (Amirnia et al., 2012).

The results for adsorption of  $\text{Cu}^{2+}$  and  $\text{Pb}^{2+}$  ions shown in Figure 3.7 indicated that live yeast cells may control the intracellular and surface uptake of the metals based on the possible level of toxicity of the aqueous phase surrounding the cells. The degree of toxicity in this work was related to the type of the essential metal  $\text{Cu}^{2+}$  vs. non-essential  $\text{Pb}^{2+}$  and their concentration level in the liquid.

### 3.3.5. Retention of metal-loaded biomass

For continuous adsorption, it is important to separate the spent biomass followed by regeneration, a practice seldom is followed in biosorption due to low cost of biosorbents. In this work, the potential of regeneration of the exhausted yeast was evaluated. As shown in Figure 3.1, two overflow settling tanks in series are used for biomass separation after biosorption.

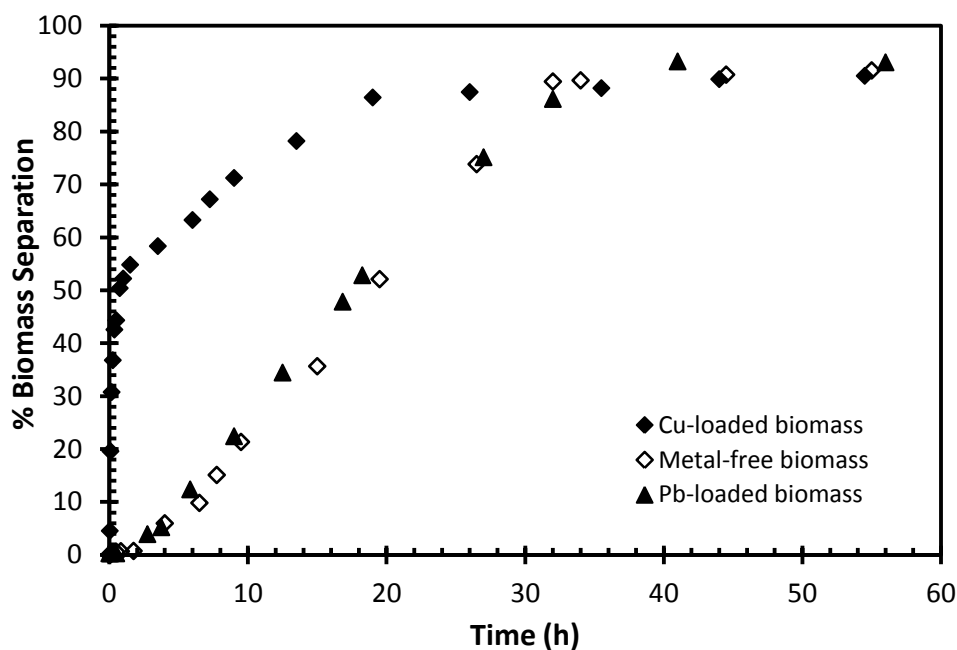


Figure 3.8. Comparison of biomass separation efficiency for metal-free biomass and metal-loaded biomass.

The good flocculation capability of brewing yeast cells is one of the major factors when brewers select strains for beer production. Yeast flocculation is facilitated in presence of heavy metals, for example, cells usually settled in presence of  $\text{Ca}^{2+}$  ions, which allows binding of specific cell wall proteins of neighboring cells, called as 'lectins' (Machado et al., 2008; Soares and Mota, 1997). Machado et al. (2008) showed that more than 95% of the brewer's yeast biomass was settled after 5 minutes at the presence of heavy metals acting as flocculants similar to  $\text{Ca}^{2+}$  ions.

In this work, settling time for copper-loaded biomass was faster than lead-loaded biomass. About 50% of biomass was settled naturally in 30 minutes after copper adsorption; however, Pb ions did not accelerate the settling time of the biomass after biosorption (Figure 3.8). Similarly, Gouveia and Soares (2004) showed that flocculent cells of *S. cerevisiae* remained dispersed in the presence of  $\text{Pb}^{2+}$  ions, while they were able to flocculate in the presence  $\text{Cu}^{2+}$ ,  $\text{Ni}^{2+}$ ,  $\text{Zn}^{2+}$  and  $\text{Cd}^{2+}$  ions. Allowing higher cell-to-cell contact by decreasing the negative electrostatic charges in the yeast cell walls, such as lowering the pH, can cause cells flocculation (Stratford, 1992).

Metal binding on the cell surface can also lower the negative cell surface charge and therefore enhance the potential for cells' flocculation. Since we were using baker's yeast strains of *S. cerevisiae*, the cells agglomeration was more likely to be the responsible mechanism for facilitating the separation of Cu-loaded biomass. The adsorption capacity for  $\text{Pb}^{2+}$  was much higher than the  $\text{Cu}^{2+}$  for *S. cerevisiae*; therefore, it was possible to have a charge reversal of the yeast biomass in presence of surface adsorbed  $\text{Pb}^{2+}$  causing lower agglomeration of the yeast cells.

### **3.3.6. Effect of mass flowrate**

The continuous system's response to changes in metal mass flowrates is shown in Figure 3.9. Increase in metal mass flowrates resulted in a decrease in the uptake of metals and percentage removal due to decrease in biomass dose and contact time in the airlift biosorption column. As shown in Table 3.1, with the change of metal/biomass

flowrate ratio from 0.2 to 3, biomass concentration in the adsorption column decreased from 2.5 g/l to 0.75 g/l.

Figure 3.9 shows the equilibrium isotherm sorption plots ( $C_e$  vs.  $q_e$ ) for different biomass concentrations in the continuous system. It was observed that, with the increase in the concentration of adsorbent, the amount of uptake of metals also increased, which can be attributed to greater surface area and the availability of greater adsorption sites at higher amounts of biomass. Metal uptake values gradually achieved a plateau at higher metal equilibrium concentrations.

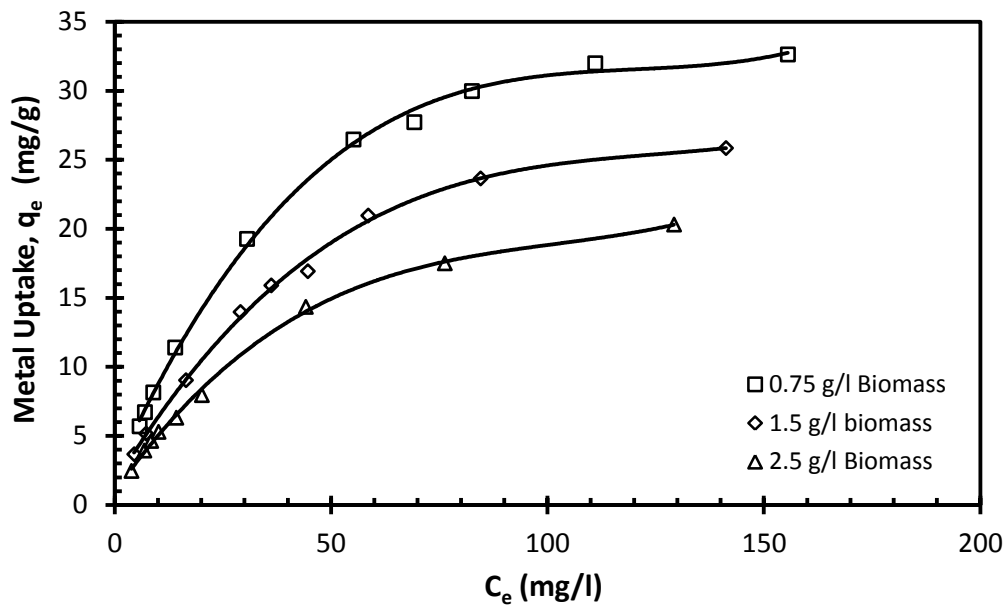


Figure 3.9. Comparison of sorption performance of yeast cells for Cu (II) at different biomass concentrations obtained at different metal inlet flowrates into the biosorption vessel.

The influence of metal inlet concentration on percentage removal of ions by yeast cells at initial metal concentrations between 10 – 180 mg/l is presented in Figure 3.10. Increase in metal inlet concentration and also a decrease in biomass concentration led to a decrease in metal percentage removal of ions by yeast cells.

### 3.3.7. Adsorption isotherms

The effectiveness of metal-biomass interactions can be evaluated by sorption isotherm models, which can be utilized for optimization of adsorbent use (Malamis and Katsou, 2013). The Langmuir model (Langmuir, 1918) is the well-known monolayer sorption isotherm that relates the sorbate's equilibrium concentration to sorbent's capacity. The Langmuir equation may be rearranged as,

$$q = q_{\max} \frac{bC_e}{1 + bC_e} \quad (7)$$

where  $q_{\max}$  (mg/g) represents the maximum capacity of adsorbent for metals and  $b$  (l/mg) is the Langmuir equation coefficient, and  $C_e$  is the equilibrium metal concentration. The data shown in Figure 3.11 indicate that the Langmuir isotherm suited well for  $\text{Cu}^{2+}$  and  $\text{Pb}^{2+}$  adsorption by yeast cells.

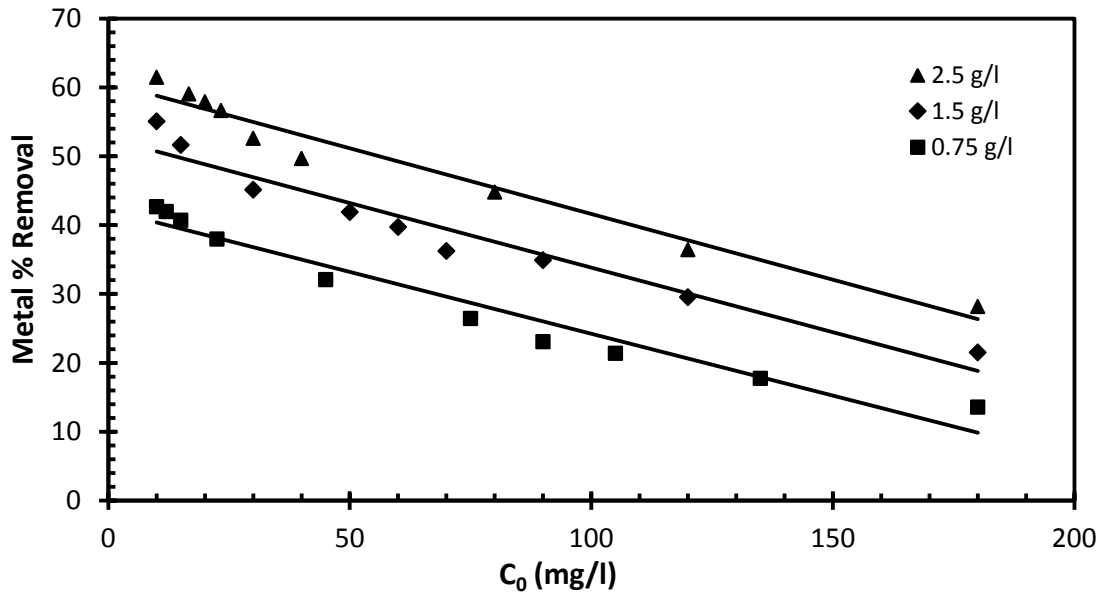


Figure 3.10. Effect of biomass dose, controlled by metal-biomass flowrates ratios, on percentage removal of  $\text{Cu}^{2+}$  by yeast biomass in continuous system.

The Langmuir model values ( $q_{\max}$ ,  $b$ ) calculated by fitting the model to the equilibrium adsorption data and the model correlation coefficients are shown in Table 3.2. The

maximum sorption capacity of yeast biomass for  $\text{Cu}^{2+}$  ions decreased from 42.5 mg/g to 21.9 mg/g as the metal-biomass flowrate ratio decreased from 3 to 0.2 (Tables 3.1, 3.2) in the continuous system. At the same biomass doses, yeast cells showed a higher biosorption capacity for  $\text{Pb}^{2+}$  ions than of that for  $\text{Cu}^{2+}$  ions from the values of  $q_{\max}$  presented in Table 3.2.

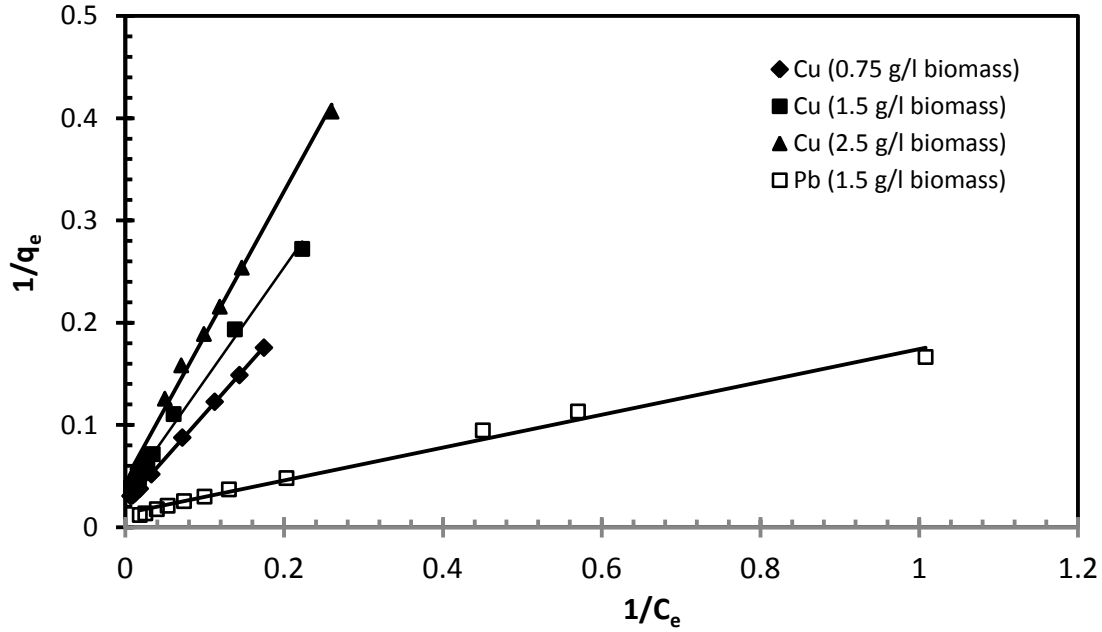


Figure 3.11. The linearized Langmuir isotherm plots for the adsorption of  $\text{Cu}^{2+}$  and  $\text{Pb}^{2+}$  ions onto yeast cells in continuous mode.

To identify the favorable adsorbents and adsorption process, Hall et al. (1966) introduced the following dimensionless equilibrium parameter  $R_L$  based on the Langmuir isotherm coefficient  $b$  ;

$$R_L = \frac{1}{1 + bC_0} \quad (8)$$

Eq. (8) was used by Ho et al. (2005) and Chen and Wang (2010) to predict whether a sorption process is favorable ( $0 < R_L < 1$ ), or unfavorable ( $R_L > 1$ ). The lower the value of  $R_L$  is, the higher the affinity of adsorbent to the adsorbed species. From Table 3.2,



Pb<sup>2+</sup> ions have lower  $R_L$  values (0.061 - 0.537) than Cu<sup>2+</sup> ions (0.155 - 0.768) at similar environmental conditions; thus, yeast biomass has higher affinity for Pb<sup>2+</sup> ions. By increasing biomass dose in the biosorption tank from 0.75 g/l to 2.5 g/l,  $R_L$  values of Cu<sup>2+</sup> ions slightly decreased suggesting more favorable adsorption of metals at higher biomass concentrations. However, for all studied test conditions in Table 3.2, the values of  $R_L$  was less than one ( $0 < R_L < 1$ ) indicating favorable adsorption processes for both metals.

Table 3.2. Langmuir isotherm model parameters for biosorption of metals in continuous system

<b>Metal</b>	<b>Conc. (mg/l)</b>	<b>Biomass</b>	<b><math>q_{\max}</math></b>	<b><math>b</math></b>	<b><math>R_L</math></b>	<b><math>R^2</math></b>
		<b>Conc. (g/l)</b>	<b>(mg/l)</b>	<b>(l/mg)</b>		
Cu <sup>2+</sup>	10 - 180	0.75	42.6	0.0269	0.171 - 0.788	0.997
Cu <sup>2+</sup>	10 - 180	1.5	29.9	0.0303	0.155 - 0.768	0.995
Cu <sup>2+</sup>	10 - 180	2.5	21.9	0.0322	0.147 - 0.756	0.995
Pb <sup>2+</sup>	10 - 180	1.5	72.5	0.0861	0.061 - 0.537	0.995

### 3.3.8. Adsorption kinetics

Figure 3.12 shows the time profile of Cu<sup>2+</sup> adsorption by yeast biomass at four different metal concentrations. Metal biosorption process took place in two steps: 1) rapid stage which represented a surface adsorption mechanism; 2) slow stage until the biomass saturation was achieved, which was controlled by an intracellular diffusion process. Kinetics of adsorption of Cu<sup>2+</sup> on yeast cells was tested by the first-order and second-order kinetic models. First-order kinetic equation presented by Lagergren (1898) based on the capacity of solid is in the following form;

$$\frac{dq_t}{dt} = k_1(q_e - q_t) \quad (9)$$

where  $k_1$  is the rate constant of first order adsorption,  $q_e$  is the amount of metals taken-up by the adsorbent at equilibrium ( $mg/g$ ), and  $q_t$  ( $mg/g$ ) is the amount of metals adsorbed at any given time  $t$  (min).

The integrated expression of Eq. (9) by applying boundary condition of  $q_t = 0$  at  $t = 0$  can be written as follows;

$$\ln(q_e - q_t) = -k_1 t + \ln q_e \quad (10)$$

The pseudo-second-order kinetic model is given as (Ho and McKay, 1999; Ho, 2006);

$$\frac{dq_t}{dt} = k_2 (q_e - q_t)^2 \quad (11)$$

where  $k_2$  is the rate constant of pseudo-second-order adsorption ( $g/mg.min$ ). By integrating Eq.(11) over the boundary conditions of  $q_t = 0$  at  $t = 0$ , and  $q_t = q_t$  at  $t = t$ , and rearranging the following linear form of the pseudo-second-order kinetic model is obtained;

$$\frac{t}{q_t} = \frac{1}{q_e} t + \frac{1}{k_2 q_e^2} \quad (12)$$

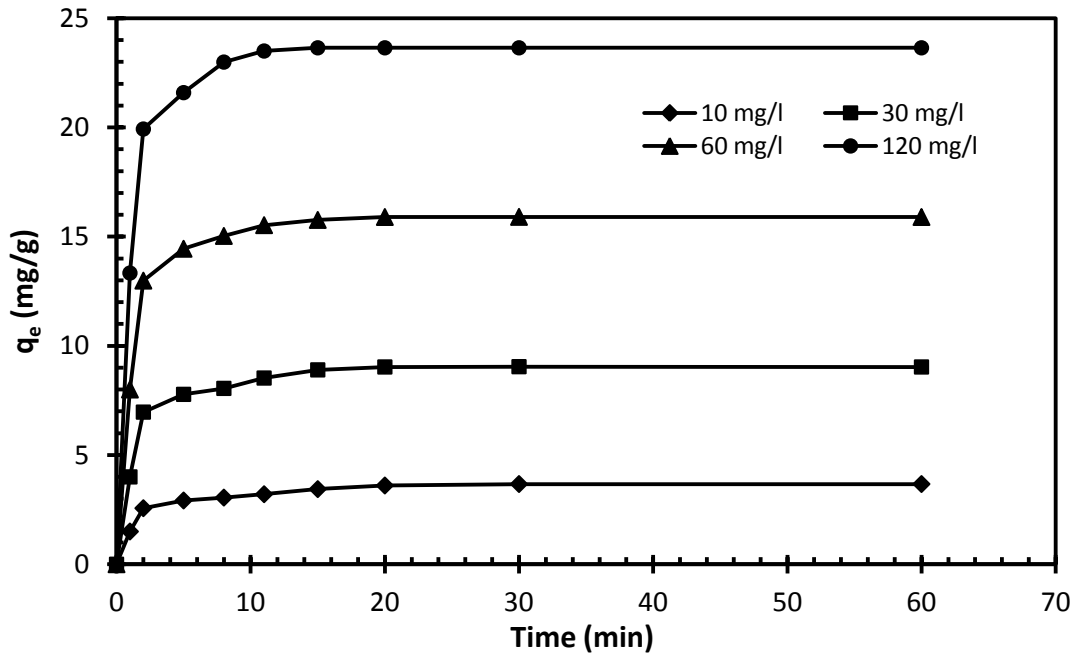


Figure 3.12. Time course of  $Cu^{2+}$  ions uptake by yeast cells at different metal concentrations (biomass concentration: 1.5 g/l).

The rate constants  $k_1$  and  $k_2$ , the predicted metal uptake values ( $q_{e(cal)}$ ) are presented in Table 3.3. It can be seen that the second order kinetics equation fitted the experimental data much better than the first order. For many adsorption systems, the pseudo-first order model found to fit the experimental data for an early stage of sorption (Ho and McKay, 1999), which was the case in this work.

As shown in Figure 3.13, pseudo-second order kinetics equation found to fit well in the whole range of metal-biomass interaction time as the values of  $q_{e(cal)}$  obtained from these plots correlated well with the values measured experimentally with high correlation coefficients  $R^2 > 0.99$  (Table 3.3). Similar results were reported by Chen and Wang (2010) for the removal of metals by biomass of *S. Cerevisiae*, as well as in studies by Gupta and Bhattacharyya (2011), and Malamis and Katsou (2013).

Table 3.3. Copper adsorption rate constants associated with pseudo-first-order and the pseudo-second-order kinetics equations.

<b>Metal Conc. (mg/l)</b>	<b><math>q_{e(exp)}</math> mg/g</b>	<b>Pseudo-second-order</b>			<b>Pseudo-first-order</b>		
		<b><math>k_2</math> (g.mg<sup>-1</sup>.min<sup>-1</sup>)</b>	<b><math>q_{e(Cal)}</math> mg/g</b>	<b><math>R^2</math></b>	<b><math>k_1</math> (min<sup>-1</sup>)</b>	<b><math>q_{e(Cal)}</math> mg/g</b>	<b><math>R^2</math></b>
10	3.67	0.2625	3.70	0.9999	0.1709	2.43	0.9455
30	9.03	0.1934	9.07	1	0.2446	5.82	0.9411
60	15.90	0.1779	15.95	1	0.3110	9.56	0.9242
120	23.65	0.1712	23.70	1	0.4202	9.73	0.9668

The rate constant values obtained from the plots varied between 0.1712 to 0.2625 g.mg<sup>-1</sup>.min<sup>-1</sup> for 120 and 10 mg/l Cu<sup>2+</sup> concentrations, respectively. The decrease in the rate constant  $k_2$  indicated that the biomass saturation time is slightly longer for the higher initial metal concentration (Gupta and Bhattacharyya, 2011). This can be due to

active adsorption by live yeast cells that can hinder the intracellular accumulation of metals at higher metal concentrations for survival. This may lead to the hypothesis of surface adsorption at all metal concentrations, which occurs during the initial fast adsorption stage, followed by an intracellular adsorption at lower metal concentration ( $\leq 50$  mg/L).

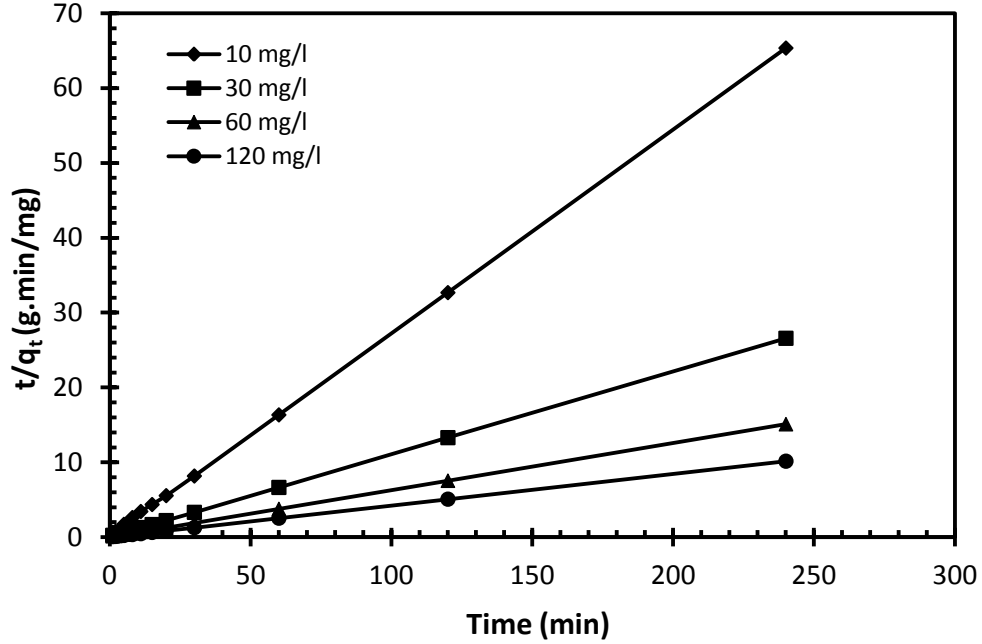


Figure 3.13. A pseudo-second-order kinetic model applied to examine the effect of initial metal concentration on rate constant (biomass dose 1.5 g/l).

### 3.3.9. Diffusion-based kinetics

The kinetic results were further analyzed by using Weber and Morris (1963) intraparticle diffusion model as in Eq. (13);

$$q_t = k_d t^{1/2} + I \quad (13)$$

where  $k_d$  is the inter-particle diffusion rate constant ( $\text{mg} / \text{g} \cdot \text{min}^{0.5}$ ), and  $I$  is the equation constant related to thickness of diffusion layer. Generally, as illustrated in Figure 3.14, there are three steps involved in adsorption of species from liquid phase on a solid phase adsorbent (Ofomaja, 2008; Kumar and Gaur, 2011) dictating the rate

of sorption process : (I) bulk diffusion; (II) external diffusion through liquid film layer around the sorbent particles; and (III) intraparticle diffusion.

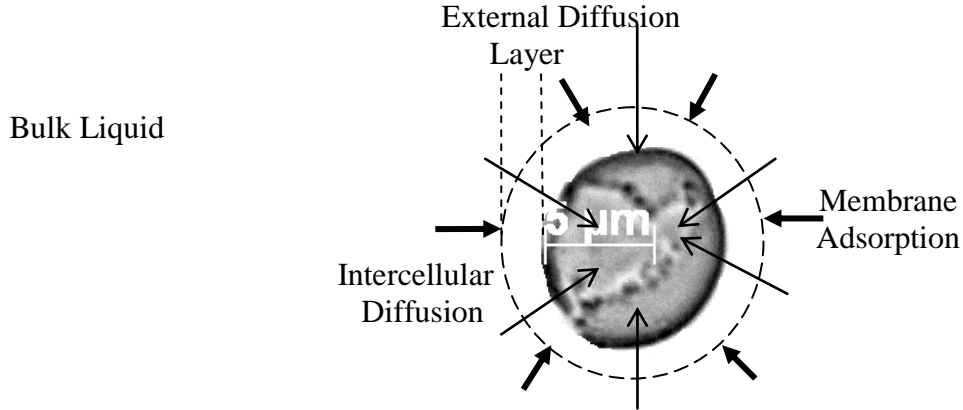


Figure 3.14 Schematic of the transfer of metals from the bulk liquid phase to a yeast cell.

In the metal-biomass contactor used in this work, the mass transfer step (I) was very rapid, attributed to a well-mixed biosorption system, and thus steps (II) and (II) played important role in overall mass transfer rate of metals from aqueous solution into the yeast cells. In order to evaluate the relative importance of these two steps, metal sorption kinetics were evaluated using the intraparticle (Eq. 13) and external mass transfer models.

At stage (II) of sorption, metals are diffused from the liquid phase through the external diffusion layer (Figure 3.14). The change in the adsorbate's concentration in liquid phase at this stage, which is the initial rate of sorption, is given by the following equation (McKay et al., 1988);

$$\frac{dC_t}{dt} = -k_E(C_t - C_s) \quad (14)$$

where  $k_E$  ( $\text{min}^{-1}$ ) is the external mass transfer rate constant, and  $C_s$  (mg/l) is the metal concentration at the surface of sorbate. Applying boundary conditions of  $t = 0$ ;  $C_s = 0$  and  $C_t = C_0$ , Eq.(14) becomes;

$$\left( \frac{d(C_t / C_0)}{dt} \right)_{t \rightarrow 0} = -k_E \quad (15)$$

Figures 3.15 and 3.16 are the plots of  $q_t$  vs.  $t^{1/2}$ , and the  $k_t$  and  $I$  parameters of Eq. (13), the intraparticle diffusion model, obtained from Figure 3.16 are listed in Table 3.4.

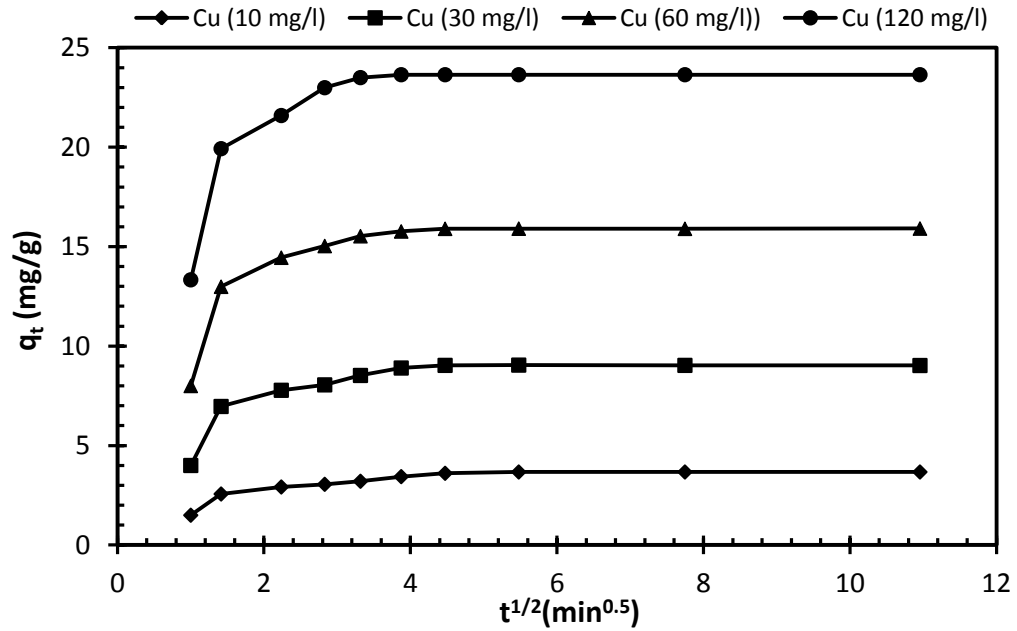


Figure 3.15. Intraparticle diffusion model for Cu (II) biosorption on yeast cells at different metal concentrations. Multi-linearity of plots (three distinct regions) was observed for metal uptake as the metal-biomass contact time increased.

As shown in Figure 3.15, the uptake of copper by yeast biomass at all metal concentrations followed three distinct stages. The metal uptake increased quickly at the beginning (0-5 min), which could represent the negligible bulk diffusion and start

of surface adsorption step. Then, the change in the adsorption capacity  $q_t$  slowed down (5- 20 min), which could be due to intraparticle diffusion, film diffusion, or both. Film diffusion could come into play when metal concentration difference (or mass transfer rate) between the bulk liquid and the surface of the adsorbent decreased as the contact time increased, which denoted that the number of remaining adsorption sites on the biomass surface for binding of metals became limited. Saturation of sorbent particles with metals occurred as the final plateau stage.

Values of  $I$  in Eq. (13) varied from 2.11 to 17.99 mg/g for 10 mg/l and 120 mg/l initial metal concentrations, respectively (Table 3.4). Low value of  $I$  ( $I \rightarrow 0$ ) at low metal concentrations indicates that the  $q_t$  vs.  $t^{0.5}$  plots should pass through the origin (Figure 3.16) and intracellular diffusion would control the adsorption of metals by yeast cells. On the contrary, the larger values of  $I$  means the greater boundary layer effect and therefore, the greater the contribution of the surface sorption in the rate controlling step. Furthermore, if the plots of Eq. (13) in all stages of adsorption do not go through the origin, it is an indicative of imprecision of the postulated intraparticle diffusion mechanism (Weber and Morris, 1963; Poots et al., 1976).

The second stage of biosorption in Figure 3.15 was used to obtain the intraparticle diffusion rate constant,  $k_I$ . The slopes of this stage are illustrated in Figure 3.16, and the  $k_I$  values with their correlation coefficients  $R^2$  (0.9328 - 0.9894) are tabulated in Table 3.4. Intra-particle diffusion rate constant of  $\text{Cu}^{2+}$  increased as the concentrations of metal in the liquid phase increased. This suggested that the intraparticle diffusion model (Eq. 13) predicts an increase in internal mass transfer of  $\text{Cu}^{2+}$  ions; however, due to active adsorption behaviour of live yeast cells, the natural resistance of the cells for internal uptake would be increased at higher metal concentrations.

In this study, the plots of metal uptake  $q_t$  against  $t^{0.5}$  were linear in the second stage (Figure 3.16), in which, the departure from the origin is larger at increasing metal concentrations. This reveals possible involvement of some other mechanism along with intraparticle diffusion in controlling the rate of sorption process. Such complex

mechanism have also been reported for biosorption processes by other researchers (Ahmad and Rahman, 2011; Deniz and Karaman, 2011).

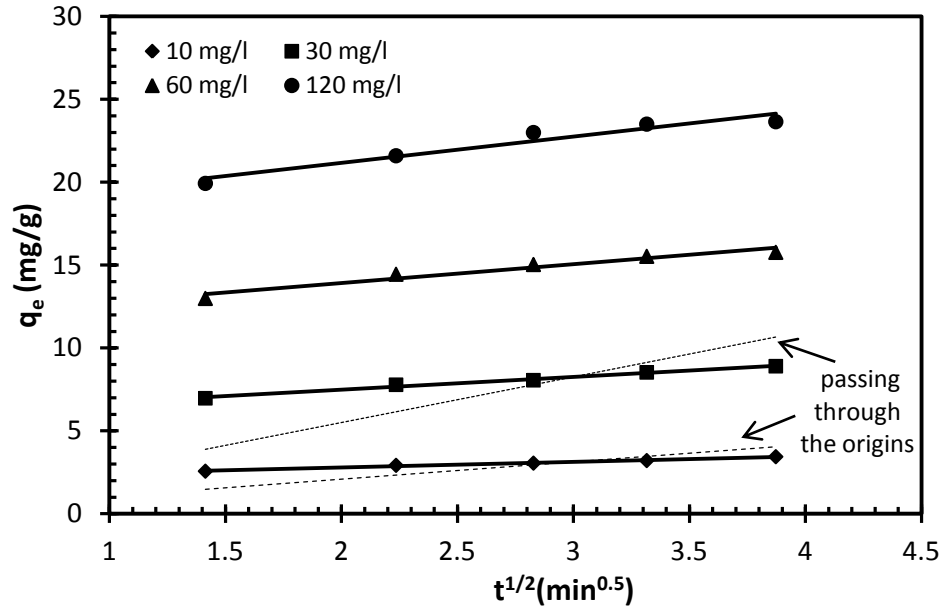


Figure 3.16. Slopes of second stage intraparticle diffusion plots ( $1 < t^{1/2} < 4$ ) to calculate the  $K_I$  coefficient values.

Graphical representations of Eq. (15), the external mass transfer model in liquid phase at different initial copper concentrations, are presented in Figure 3.16. At time zero,  $C_t/C_0 = 1$ , and then started to decrease with increasing the contact time. The slope of these plots was calculated for the initial external mass transfer period (0 –2 min), and the external mass transfer rate constants  $K_E$  for the tested metal concentrations ( $0.96 < R^2 < 0.99$ ) are listed in Table 3.4.

The external diffusion rate  $K_E$  of  $\text{Cu}^{2+}$  ions decreased with increasing metal concentration in the solution. Overall, the diffusion-based kinetics study revealed that the biosorption of  $\text{Cu}^{2+}$  ions with live yeast cells tended to follow both external and the intraparticle diffusion models, whereas intracellular diffusion was the presumptive dominant mean of adsorption at lower metal concentrations.



Table 3.4. External mass transfer and intraparticle diffusion parameters for biosorption of Cu ions on yeast cells (biomass concentration: 1.5 g/l)

<b>Metal Conc. (mg/l)</b>	<b>Intraparticle diffusion</b>			<b>External diffusion</b>	
	<b>K<sub>I</sub> (mg.g<sup>-1</sup>.min<sup>0.5</sup>)</b>	<b>I (mg/g)</b>	<b>R<sup>2</sup></b>	<b>K<sub>E</sub> (min<sup>-1</sup>)</b>	<b>R<sup>2</sup></b>
10	0.3406	2.11	0.9894	0.1925	0.9906
30	0.7731	5.93	0.9893	0.1742	0.9927
60	1.1321	11.66	0.9472	0.1623	0.9874
120	1.5906	17.99	0.9328	0.1245	0.9633

### 3.3.10. Biosorption mechanism – further insights

Fermentation processes are relied on viable yeast cells; however, biosorption of metals can be carried out by both living and non-living cells. A simple cell viability count method was performed using methylene blue stain to determine the viability of the cells in the continuous system before and after being exposed to metals (non-viable cells do not have the metabolic capability to degrade the intruding methylene blue so they are stained dark blue).

The test results showed that there was no significant difference in viability for cells within first hour of exposure to the metals. The results were in agreement with findings of Liang and Zhou (2007). They showed that yeast *S. cerevisiae* cells death under extracellular Cu stress starts at around 6 mM level, which was quite higher than concentrations used in the present study (< 2.9 mM). Thus, the biosorption process in this work was accomplished by live yeast cells.

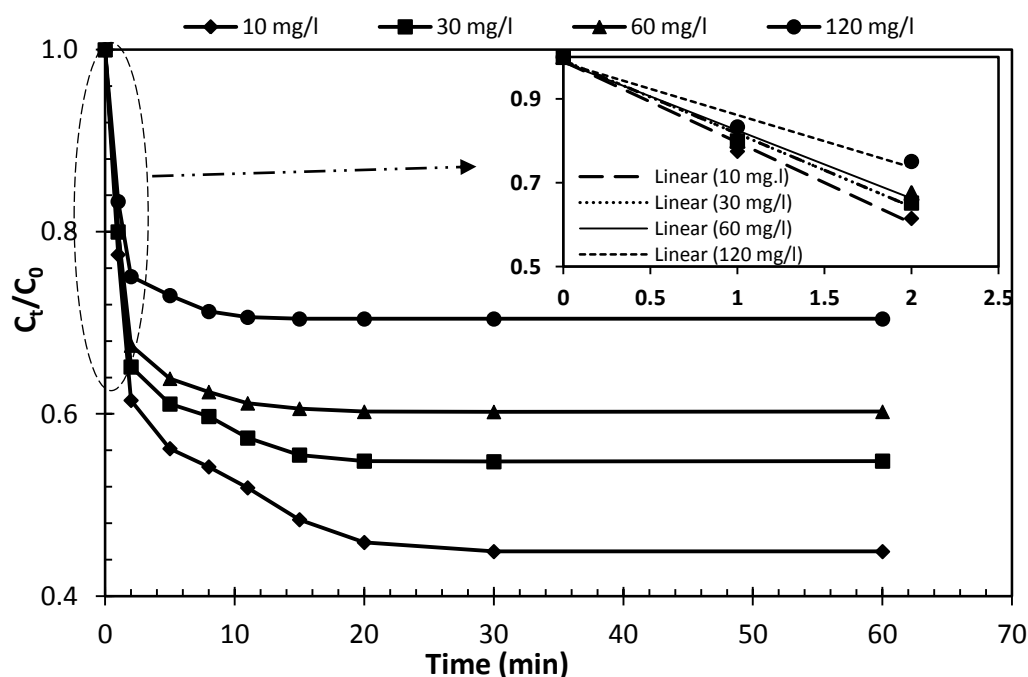


Figure 3.17. Time profile of  $\text{Cu}^{2+}$  ions dimensionless concentration  $C_t/C_0$  at different initial solute concentrations (biomass dose: 1.5 g/l). The external mass transfer constant ( $K_E$ ) for Cu adsorption on yeast cells was obtained from the initial slopes of the plots.

The metal biosorption mechanism is complicated and not fully-understood (Wang and Chen, 2006). The analysis of the FTIR spectra of yeast biosorbent showed the presence of several functional groups, such as carboxyl, hydroxyl, amino and carbonyl groups on the cell walls and their interaction with metal ions was responsible for metal binding (Amirnia et al. 2012; Wang 2002). Results of this work confirmed that biosorption of Cu ions by yeast cells was a combination of both intracellular metal accumulation and a metabolic-independent surface phenomenon. In contrast, comparison of passive biosorption results (Amirnia et al. 2012) with this work indicates that a non-metabolic biosorption occurred for  $\text{Pb}^{2+}$  (Figure 3.7) due to high toxicity of lead and the active defense mechanism of the cells prevented the intake of toxic lead, and reduced the amount adsorbed on the cell surface.

Although, the removal of  $\text{Pb}^{2+}$  in the continuous system was lower than that of in the batch system (Amirnia et al. 2012), maximum adsorption capacity of  $\text{Pb}^{2+}$  was still better than that of  $\text{Cu}^{2+}$ . This is probably due to the lower steric hindrance of  $\text{Pb}^{2+}$  due to smaller hydrated ionic radii of  $\text{Pb}^{2+}$  ions as compared to hydrated ionic radii of  $\text{Cu}^{2+}$  (Sengil and Özacar 2009).  $\text{Cu}^{2+}$  ions with higher free enthalpy of hydration than  $\text{Pb}^{2+}$  ions prefer to stay in the liquid rather than adsorbing onto the solid phase (Malamis and Katsou, 2013).

### **3.3.11. Large-scale applicability**

Assessing the potential of biosorption process by live yeast cells for removal of heavy metals in a continuous system, similar to conventional technologies such as ion exchange, is of paramount importance for large-scale design of this technology. The commercial development of this system can only be considered if its cost and efficiency are reasonably better than commercially available ion-exchange resins. In the lab-scale system, the major cost of the process was related to the nutrition feed used for growth and production of yeast cells. Replacing the nutrients with an inexpensive waste stream containing sugar used for the growth of the cells would improve the economic feasibility of the system.

The study by Machado et al. (2008) on cell separation after biosorption of metals by brewer's yeast strain of *Saccharomyces Cerevisiae* showed that the yeast strain was able to sediment in the presence of heavy metals acting as flocculants. Since the biosorption process is also rapid, removal of the heavy metals and cell separation can be simultaneously achieved. The concept that heavy metal adsorption facilitates separation of biomass could be used in large scale continuous systems.

The challenges of industrial application of biosorption process was addressed by Wang and Chen (2009) proposing the development of hybrid technologies for removal of pollutant, especially using living cells. In this study, an application of a continuous system for cell growth and metal biosorption combining physical adsorption and metabolic uptake of metals was demonstrated. This approach has a potential for

commercial application of biosorption as it may lead to simultaneous removal of organic pollutants and other inorganic impurities including heavy metals.

If biosorption is to be used in treatment of industrial wastewater effluents containing heavy metals ions, the regeneration process of biomass needs to be investigated to keep the operating costs down by opening the potential of metal recovery from biomass. Although, recovery of metal was not attempted in this work, due to low cost and abundance of biomass, recovery of metals from the spent biomass by acid wash is economically feasible.

### **3.4. Conclusions**

In this work, the possibility of using a continuous system for simultaneous production of yeast *S. cerevisiae* and removal of  $\text{Cu}^{2+}$  and  $\text{Pb}^{2+}$  ions from aqueous solutions by the produced biomass was investigated. The yeast cells showed a higher binding capacity for  $\text{Pb}^{2+}$  than  $\text{Cu}^{2+}$  ions. The biosorption data fitted Langmuir adsorption isotherm model and the kinetics of  $\text{Cu}^{2+}$  removal followed the pseudo-second-order model. The use of an air-lift bioreactor promoted efficient mixing and effective contact between the metal solution and the biomass. Though live cells were used, the biosorption on the cell surface was the major metal separation mechanism. Intracellular metal uptake represented  $< 10\%$  of the overall metal binding capacity for copper ions. The diffusion-based kinetics models suited well to the time-course metal adsorption by live yeast cells suggesting involvement of both extracellular and intracellular diffusion processes. The main finding of this work was that the continuous system is a practical, inexpensive, and self-contained method for removal of metals, where the adsorbent can be continuously produced and used for metal adsorption. Yeasts have minimal nutritional needs and they grow easily in simple medium; therefore, the cost associated with nutrient medium can be overcome by the use of waste agricultural material such as molasses as a hydrocarbon source. The large-scale application of continuous metal biosorption by yeast cells would be improved if the separation of metal-loaded biomass from solution is accelerated using a flocculent strain of *S. Cerevisiae*.

### 3.5. Acknowledgements

This work was supported by NSERC Discovery Grants awarded to Dr. A. Margaritis and Dr. M.B. Ray.

### 3.6. References

- [1] Ahmad M.A., Rahman N.K., Equilibrium, kinetics and thermodynamic of Remazol Brilliant Orange 3R dye adsorption on coffee husk-based activated carbon, *Chem. Eng. J.*, 170, 1 (2011) 154-161.
- [2] Amirnia S., Margaritis A., Ray M.B., Adsorption of mixtures of toxic metal ions using non-viable cells of *Saccharomyces cerevisiae*, *Adsorpt. Sci. Technol.*, 30, 1 (2012) 43-63.
- [3] Bashar H, Margaritis A, Berutti F, Maurice B., Kinetics and equilibrium of cadmium biosorption by yeast cells *S. cerevisiae* and *K. fragilis*, *Int. J. Chem. Reactor Eng.*, 1 (2003) 1-16.
- [4] Cassidy M.B., Lee H., Trevors J.T., Environmental applications of immobilized microbial cells: a review. *J. Ind. Microbiol.*, 16 (1996) 79–101.
- [5] Chen C., Wang, J., Removal of Heavy Metal Ions by Waste Biomass of *Saccharomyces cerevisiae* *J. Environ. Eng.*, 136, 1 (2010) 95–102.
- [6] Deniz F., Karaman S., Removal of Basic Red 46 dye from aqueous solution by pine tree leaves, *Chem. Eng. J.*, 170 (2011) 67–74.
- [7] Fomina, M., Gadd, G.M. Biosorption: current perspectives on concept, definition and application, *Bioresour. Technol.*, 160 (2014) 3–14.
- [8] Gonen F, Aksu Z., Use of response surface methodology (RSM) in the evaluation of growth and copper (II) bioaccumulation properties of *Candida utilis* in molasses medium, *J. Hazard. Mater.* 154 (2008) 731–738.
- [9] Gouveia C., Soares E.V., Pb<sup>2+</sup> Inhibits Competitively Flocculation of *Saccharomyces cerevisiae*, *J. Inst. Brew.*, 110, 2 (2004) 141–145.

- [10] Gupta S.S., Bhattacharyya K.G., Kinetics of adsorption of metal Ions on inorganic materials: a review, *Adv. Colloid Interface Sci.*, 162, 1-2 (2011) 39-58.
- [11] Hall K.R., Eagleton L.C., Acrivos A., Vermeulen T., Pore-and solid-diffusion kinetics in fixed-bed adsorption under constant-pattern Conditions, *I&EC Fundam.*, 5 (1966) 212–223.
- [12] Health Canada, Risk Management Strategy for Lead, available on Internet at: [http://www.hc-sc.gc.ca/ewh-semt/pubs/contaminants/prms\\_lead-psgr\\_plomb/index-eng.ph](http://www.hc-sc.gc.ca/ewh-semt/pubs/contaminants/prms_lead-psgr_plomb/index-eng.ph)”, ISBN: 978-1-100-21305-7 (2013).
- [13] Ho, Y.S., Review of second-order models for adsorption systems, *J. Hazard. Mater.*, 136 (2006) 681–689.
- [14] Ho Y.S., McKay G., Pseudo-second order model for sorption processes, *Process Biochem.*, 34, 5 (1999) 451-465.
- [15] Ho, Y.S., Chiang, T.H., Hsueh, Y.M., Removal of basic dye from aqueous solution using tree fern as a biosorbent, *Process Biochem.* 40, 1 (2005) 119–124.
- [16] Kapoor A., Viraraghavan T., Removal of heavy metals from aqueous solutions using immobilized fungal biomass in continuous mode, *Wat. Res.*, 32, 6 (1998) 1968-1977.
- [17] Kumar D, Gaur J.P., Chemical reaction- and particle diffusion-based kinetic modeling of metal biosorption by a *Phormidium* sp.-dominated cyanobacterial mat, *Bioresour. Technol.*, 102 (2011) 633–640.
- [18] Lagergren S., Zur theorie der sogenannten adsorption gelöster stoffe, *K. Sven. Vetenskapsakad. Handl.*, Band, 24, 4 (1898) 1–39.
- [19] Lesmana S.O., Febriana N., Soetaredjo F.E., Sunarso J., Ismadji S., Studies on potential applications of biomass for the separation of heavy metals from water and wastewater, *Biochem. Eng. J.* 44 (2009) 19–41.

- [20] Liang Q, Zhou B, Copper and Manganese Induce Yeast Apoptosis via Different Pathways, *Mol. Biol. Cell* 18, 12 (2007) 4741-4749.
- [21] Langmuir I., The adsorption of gases on plane surface of glass, mica and platinum, *J. Am. Chem. Soc.*, 40 (1918) 1361 – 1403.
- [22] Lokeshwari N. and Joshi K., Biosorption of Heavy Metal (Chromium) Using Biomass, *Global J. Environ. Res.*, 3-1 (2009) 29-35.
- [23] Machado MD, Santos MSF, Gouveia C., Soares H.M.V.M, Soares E.V., “Removal of heavy metals using a brewer’s yeast strain of *Saccharomyces cerevisiae*: The flocculation as a separation process”, *Bioresour. Technol.*, 99 (2008), 2107–2115.
- [24] Machado MD, Janssens S., Soares HM, Soares EV, Removal of heavy metals using a brewer's yeast strain of *Saccharomyces cerevisiae*: advantages of using dead biomass, *J. Appl. Microbiol.* 106, 6 (2009), 1792-804.
- [25] Malamis S., Katsou E., A review on zinc and nickel adsorption on natural and modified zeolite, bentonite and vermiculite: Examination of process parameters, kinetics and isotherms, *J. Hazard. Mater.* 252– 253 (2013) 428–461.
- [26] McKay G., El Geundi M., Nassar M.M., External mass transport processes during the adsorption of dyes onto bagasse pith, *Wat. Res.*, 22, 12 (1988) 1527–1533.
- [27] Marques P., Pinheiro H.M., Rosa M.F., Cd(II) removal from aqueous solution by immobilised waste brewery yeast in fixed-bed and airlift reactors , 214 (2007), 343-351.
- [28] Ofomaja, A.E., Sorptive removal of methylene blue from aqueous solution using palm kernel fibre: effect of fibre dose”, *Biochem. Eng. J.*, 40 (2008) 8–18.

- [29] Pilkington P. H., Margaritis A., Mensour N. A., Russell I., Fundamentals of Immobilized Yeast Cells for Continuous Beer Fermentation: A Review, *Inst. Brew.*, 104 (1998) 19-31.
- [30] Poots V.J.P., McKay G., Healy J.J., The removal of acid dye from effluent using natural adsorbents – I. Peat, *Wat. Res.* 10 (1976) 1061.
- [31] Reisman D.J., Peirano W.B, Lewis J.B., Basu D.k., Hohrseiter D., Summary Review of the Health Effects Associated with Copper: Health Issue Assessment, U.S. Environmental Protection Agency, Washington, D.C., EPA/600/8-87/001, NTIS PB87137733 (1987).
- [32] Selby, S.M. (Ed.), *CRC Standard Mathematical Tables*. Cleveland, Ohio: The Chemical Rubber Co., (1969), 14th ed., p496.
- [33] Sengil I.A., Özacar M., Competitive biosorption of  $Pb^{2+}$ ,  $Cu^{2+}$  and  $Zn^{2+}$  ions from aqueous solutions onto valonia tannin resin, *J. Hazard. Mater.* 166 (2009) 1488–1494.
- [34] Soares E.V., Mota M., Quantification of yeast flocculation. *J. Inst. Brewing* 103 (1997) 93–98.
- [35] Stratford M (1992) yeast flocculation: a new perspective. *Adv Microbiol Physiol* 33:2–71
- [36] Suh J. H, Yun J.W., Kim D.S., Comparison of  $Pb^{+2}$  accumulation characteristics between live and dead cells of *Saccharomyces cerevisiae* and *Aureobasidium pullulans*, *Biotechnol. Letters*, 20, 3 (1998) 247–251.
- [37] Tsezos M., Engineering aspects of metal binding by biomass, H.L. Ehrlich, C.L. Brierly (Eds.), *Microbial Mineral Recovery*, McGraw-Hill, USA (1990) 325–340 (Chapter 14).
- [38] Tobin J.M., White C., Gadd G.M., Metal accumulation by fungi: applications in environmental biotechnology, *J. Ind. Microbiol.*, 13 (1994) 126-130.



- [39] Volesky B., Advances in biosorption of metals: Selection of biomass types, FEMS Microbiol. Rev., 14 (1994) 291-302.
- [40] Volesky B., Sorption and Biosorption, BV-Sorbex, Inc., St.Lambert, Quebec, (2003).
- [41] Volesky B., Naja G., Biosorption technology: starting up an enterprise, Int. J. Technol. Transf. Commer., 6 (2007) 196–211.
- [42] Volesky B., Biosorption and me, Water Res., 41, (2007), 4017 – 4029.
- [43] Volesky B., May-Phillips H.A., Biosorption of heavy metals by *Saccharomyces cerevisiae*, Appl. Microbiol. Biotechnol., 42 (1995) 797-806.
- [44] Wang J., Chen C., Biosorption of heavy metals by *Saccharomyces cerevisiae*: A review, Biotechnol. Adv. 24 (2006) 427–451.
- [45] Wang J., Chen C., Biosorbents for heavy metals removal and their future, Biotech. Adv. 27 (2009) 195–226
- [46] Wang J., Biosorption of copper (II) by chemically modified biomass of *Saccharomyces cerevisiae*, Process Biochem., 37, 8 (2002) 847-850
- [47] Wehrheim B., Wettern M., Biosorption of cadmium, copper and lead by isolated mother cell walls and whole cells of *Chlorella fusca*, Appl. Microbiol. Biotechnol., 41 (1994) 725-728.
- [48] Walker, G.M., Yeast Physiology and Biotechnology, (1998), J. Wiley & Sons, 133-136.
- [49] Weber W. J., Morris, J. C., Kinetics of adsorption on carbon from solution, J. Sanitary Eng. Div., 89-2 (1963) 31-60.
- [50] White C., Gadd, G. M., Biosorption of radionuclides by fungal biomass, J. Chem. Tech. Biotechnol., 49 (1990) 331-343.

## **Chapter 4**

### **Copper Ions Removal by *Acer saccharum* Leaves in a Regenerable Continuous-flow Column**

## Abstract

Potential of waste *Acer saccharum* (Maple tree) leaves (MTL) for continuous removal of Cu (II) ions from aqueous solutions in a flow-through packed-bed was investigated. The effects of metal concentration (15 – 110 *mg/l*) and flowrate (5 - 30 *ml/min*) on breakthrough curves were investigated using the effluent concentration of 1 *mg/l* stipulated by the Canadian drinking water guidelines. Eight consecutive adsorption–desorption cycles were carried out with regeneration efficiencies of up to 98% using 0.1N H<sub>2</sub>SO<sub>4</sub>. Although the metal capacity of the biosorbent in the column remained constant at around 18.3 *mg/g*, shortened breakthrough times from 262 to 197 *min* was an indication of reduced column sorption performance with increasing cycles. Metal adsorption equilibrium data followed the two-constant isotherm models, Freundlich and Langmuir, and three-constant Sips model, and the kinetics data fitted well to a pseudo-second-order rate expression. Dynamic performance of the biosorption column for Cu (II) removal by MTL was predicted by numerically solving the second-order partial differential material balance equation of the developed non-linear local equilibrium model. The model breakthrough curves closely agreed with the column experimental data but overestimated the breakthrough times. The model dispersion coefficient was increased at higher metal flowrates and concentrations. The non-linear equilibrium model constants obtained from fitting the model to column sorption data conformed to the batch sorption values. The results showed that MTL as a local, abundant, and low cost biosorbent can easily be employed for metals removal from wastewaters in a packed bed column.

## 4.1. Introduction

Discharge of heavy metals into the environment from anthropogenic activities has resulted in adverse environmental and human health impacts (Volesky, 1994; Fu and Wang, 2011). Several technologies are in place to remove metals from wastewaters

before being released to the environment, but most of them are associated with high costs and inadequate efficiencies. Among the emerging technologies, biosorption of metals using natural biomass or agro-industrial wastes and by-products is known to be a feasible and efficient alternative (Volesky, 2003a; Abdolali et al, 2014).

Variety of biosorbents has been tested for their metal removal capacities; nevertheless, biosorption as a remediation process has not been utilized yet by metal industries for their effluents treatment (Wang and Chen, 2009; Park et al., 2010; Fomina and Gadd, 2014). A necessary aspect in success of biosorption technology for metal treatment is to be tested in continuous-flow mode similar to its competitive technologies such as ion exchange resins (Zang and Banks, 2006; Amirnia et al., 2015).

Another important factor for successful application of biosorption is selection of the best biomass type for metal adsorption, in which, other than effectiveness, easy availability and cost, and toxicity of the biosorbents should be taken into consideration (Kim et al., 2015). For this purpose, maple leaves as an agro-waste biomaterial found in abundance in temperate regions like Canada were selected. The main objective of this work was to examine the applicability and efficacy of MTL to remove metal cations in a flow-through column in continuous mode.

Maple trees are of deciduous tree species losing the leaves with the onset of fall season. Sugar maple or *Acer saccharum* is native to Canada and one of the most common maple trees in North America. Wood and sap from the tree are commercially valuable; however, fallen leaves, which are considered as yard waste in urban areas, are of none or low economic value and usually collected and dumped into the landfills. Centralized composting programs are being implemented in some communities across Canada for organic waste management including leaves and yard wastes.

In this study, we aim to evaluate the possibility of utilizing fallen maple leaves for metal adsorption as an environment-friendly waste management method. Copper removal from industrial wastewaters is of great importance as it is non-biodegradable

and toxic at high doses (Yu et al, 2000). It is also one of the most abundant hazardous metals found in the effluents of metal industry sources (Hossain et al., 2012), such as mining operations effluents in Canada.

So far, batch metal biosorption data have been extensively reported in the literature, which provides the basis for complex biosorption studies. Batch adsorption studies involving heavy metals and maple tree waste residues, such as maple wood sawdust and leaves have been studied, but their performance in continuous configurations was never evaluated. For instance, batch experiments were performed for chromium adsorption with maple sawdust by Yu et al. (2003); Rhaman and Islam (2009) studied the biosorption of copper (II) by maple wood sawdust; and Krishan and Gilbert (2014) tested maple leaves for removal of Ni (II) from aqueous solutions. Furthermore, batch biosorption of cationic dyes with Norway maple leaves was investigated by Witek-Krowiak et al. (2010). For practical applications in large scale, however, these biosorption systems need to be tested in continuous mode.

Use of a continuous-flow packed bed column for metal biosorption was reported as an effective and economic process engineering method for utilization of the maximum capacity of sorbents, and for design and scale up of the system (Volesky and Holan, 1995; Aksu and Gönen, 2004; Ramirez et al., 2007). To our knowledge, this is the first study where maple leaves are used for copper ions removal in a fixed-bed flow-through sorption column. In this work, we aimed to gain understanding of adsorption of copper to untreated MTL and quantify the dynamic operation performance of MTL in a continuous-flow column. The recovery of Cu (II) ions from exhausted MTL biomass by weak acid was also examined, which was an added value to the biosorption process economy allowing both the biomass and metals reuse in multiple sorption-desorption cycles.

Performance estimation, design, and optimization of a fixed-bed biosorption column for heavy metal removal can be conducted by an appropriate mathematical modeling and solving a series of nonlinear partial differential equations (Volesky, 2003b; Borba

et al, 2006). Such modeling approach for column biosorption is normally complicated; therefore, to achieve an analytical solution, it is desirable to use simplified assumptions and explicit mass transfer expressions (Aksu and Gönen, 2004; Chen and Wang, 2004). In this work, a mathematical model was developed to describe the column biosorption process based on material balance equations, involving solute movement by bulk flow, diffusion, and non-linear local equilibrium sorption.

## 4.2. Experimental

### 4.2.1. Sorbent preparation and analysis

Fallen native *Acer saccharum* (maple tree) leaves (MTL) were collected and washed twice with tap and distilled water to remove dirt, and dried in a convection oven (45°C) overnight. The biomass was subsequently ground and sieved to MTL particles between  $\approx 180 \mu\text{m}$  to 2.36 mm for biosorption studies.

### 4.2.2. Sorbate analysis

Cu (II) solutions were prepared using  $\text{CuSO}_4 \cdot 5\text{H}_2\text{O}$  in distilled water. Solution pH was adjusted before biosorption experiments by adding 0.5M HCl/NaOH. Metal analysis was carried out by ICP-OES (Varian Inc.). Biosorbent metal retention capacity  $q_t$  ( $\text{mg} / \text{g}$ ), and removal efficiency RE (%) at time 't' were calculated based on mass balance:

$$q_t (\text{mg/g}) = \frac{(C_0 - C_t)}{C_{\text{Biomass}}} \quad (1)$$

$$\text{RE (\%)} = \frac{(C_0 - C_t)}{C_0} \times 100 \quad (2)$$

where  $C_0$  ( $\text{mg} / \text{l}$ ) and  $C_t$  ( $\text{mg} / \text{l}$ ) are the initial metal concentration at the bulk solution and metal concentration at time  $t$ , respectively, and  $C_{\text{Biomass}}$  the concentration of

biomass ( $g/l$ ). At equilibrium,  $C_t = C_e$  and  $q_t = q_e$ . In continuous system, samples were collected from the outlet of the column to analyze for metal concentration.

#### **4.2.3. Biosorption column set-up and operation**

The experimental arrangement of the continuous biosorption system is shown in Figure 4.1. It included three parallel plexiglass columns with 27 cm length and 3.4 cm inner diameter, tanks containing metal feed stock and regenerant solutions connected to peristaltic pumps. Metal solution was pumped into the sorption columns from the bottom in an upward fashion providing higher bed utilization and uniform distribution of liquid with no channeling compared to downflow operation (Ko et al, 2001). The columns were packed with 40 g of dried maple leaves of the same size distributions. Foam stoppers were placed at the top and bottom of the column to screen and hold the biomass particles in the column, and for better flow distribution.

In continuous mode, although three columns were used, each column was operated sequentially as a single unit: when the first column was saturated with metals, the second column was put into operation with influent metal solution, while regeneration of the first column was carried out. Similarly, when the breakthrough occurred in the 2<sup>nd</sup> bed, the metal solution flow was diverted into the last column and the second column was put in regeneration mode, and so on. Each cycle ended with rinsing the column with DI water to remove the remaining of the regenerant acid in the bed, and also to stabilize the column pH to  $\approx 5$  measured by the wash water pH in the column outflow.

In column experiments, metal concentration at the column discharge contained very low amount of residual metals until the point that the exit concentration reached to the pre-defined allowable metal concentration, which is usually considered 1-5% of the inflow concentration. Duration of this step was represented as breakthrough time ( $t_b$ ), which is the basis for packed-bed adsorption column optimization under different operating conditions (Volesky, 2003b). In this work, breakthrough time ( $t_b$ ) was set to

be when the copper outflow concentration reached 1 mg/l to comply with the limit in the guidelines for maximum allowable copper concentration in Canadian drinking water (Health Canada, 2014). Samples were taken for metal analysis until the point in time that when the sorbate concentration in column outflow reached to 96% of that in column inflow (column exhaustion time,  $t_e$ ).

#### 4.2.4. Column bed void fraction

Bed void fraction  $\varepsilon_b$  of the column was measured following the work of Borba et al. (2006): biomass was loaded into the bed volume ( $V_b$ ) of  $248 \text{ cm}^3$  and DM water was passed through the bed to wet the packed sorbent. Then, the water was completely drained from the column for 24 h and the volume of water to fill up the void area  $V_v$  was measured.  $\varepsilon_b$  or wet-biomass porosity was calculated as follows;

$$\varepsilon_b = \frac{V_v}{V_b} \quad (3)$$

#### 4.2.5. Bed density

Density of the bed ( $\rho_b$ ) is defined as  $\rho_s(1 - \varepsilon_b)$  in which,  $\rho_s$  is the dry density of maple leaves. The bed density was obtained based on biosorbent mass packed in the column ( $m_b$ ) per unit bed volume. The MTL bed volume was the difference in volume of water needed to fill the column packed with dry biomass up to the bed height and empty bed volume ( $V_b$ ). It required 40 g of biomass to be packed into the column of volume  $248 \text{ cm}^3$  without changing the bed depth.

#### 4.2.6. Column biosorption capacity

Eq.(1) represented the metal sorption capacity ( $q_e$ ) of biomass when equilibrium had reached in batch systems. In column studies, the total bed biosorption capacity  $q_b(\text{mg/g})$  was calculated by mass conservation law from the area above the experimental breakthrough curve  $C_t \text{ vs. } t$ , which is the mass ratio of the metal adsorbed to the biomass used (mg adsorbed/g biomass);



$$q_b = \frac{F \int_0^t (C_0 - C_t) dt}{1000 m_b} \quad (4)$$

where  $C_0$  ( $mg/l$ ) is the metal feed concentration,  $C_t$  the metal concentration at the column outlet at time  $t$ ,  $F$  the volumetric flow rate of metal solution ( $ml/min$ ), and  $m_b$  is the dried  $g$  of packed biomass. Numerical integration of Eq. (4) was done using the trapezoidal rule in MATLAB and the experimental breakthrough data.

The percentage removal of metal  $(RE)_b$  was calculated by dividing the amount of metal ions removed by biomass in the column by total amount of the metal entered into the column ( $C_0 F \cdot t / 1000$ ) until the time  $t$ ;

$$(RE)_b \% = \frac{1000 q_b \cdot m_b}{C_0 \cdot F \cdot t} \times 100 \quad (5)$$

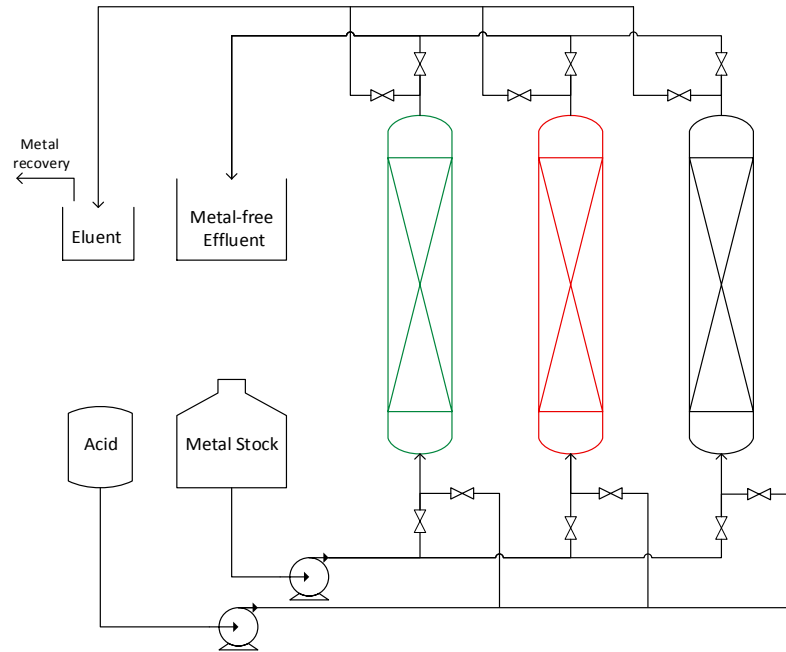


Figure 4.1. Schematic of triple column continuous-flow biosorption system (columns dimensions: 27 cm height and 3.42 cm base diameter).

The length of the adsorption zone ( $L_{ads}$ ) between  $t_b$  and  $t_e$  which is also called as the critical bed length (Volesky et al, 2003) was calculated by the following equation (Ruthven, 1984);

$$L_{ads} = L_b(1 - \frac{t_b}{t_e}) \quad (6)$$

where  $L_b$  (cm) is length of the bed.

The sorbent usage dose ( $g/l$ ) up to the breakthrough time in the packed-bed column was defined as  $g$  of biomass loaded in the column ( $m_b$ ) per volume of the metal solution treated. The volume of the treated metal solution was calculated by multiplying the column breakthrough time by the inlet volumetric flow rate ( $F$ ).

As mentioned earlier, natural form of crushed maple leaves was used without performing any pre-treatment or modification of biomass. Other than cost saving and environmental benefits, use of naturally abundant maple leaves without any pre-treatment steps yielded in simple continuous-flow column operation with mechanically stable adsorbent particles that can be easily packed in adsorption column without any immobilization techniques. Biomass immobilization techniques are generally applied on microbial biosorbents to improve packing and biomass separation from the effluent after adsorption. However, immobilization causes mass transfer limitations and reduces regeneration efficiency (Cassidy et al, 1996).

#### **4.2.7. Characterization of biosorbent**

Brunauer-Emmett-Teller (BET) surface area and Barrett-Joyner-Halenda (BJH) pore size and volume tests were performed on maple leaves using Accelerated Surface Area and Porosimetry analyzer (ASAP2010 Micromeritics) to measure the surface area and porosity of the biomass. Hitachi Scanning Electron Microscope SEM (S-4800) in conjunction with EDX (Energy Dispersive X-ray) was employed to analyze the structure of the leaves. Fourier Transform Infrared (FTIR) spectra of the leaves were

recorded using a FTIR- Bruker Spectrometer to identify the functional groups present on the surface of biomass.

#### 4.2.8. Modeling error analysis

To measure the degree of goodness-of-fit of the models to the experimental data used in this work, apart from the coefficient of determination ( $R^2$ ), the residual root mean square error (RMSE) and the sum of squares due to error of the fit (SSE) were also employed as follows (Ho et al., 2005);

$$RMSE = \sqrt{\frac{1}{n} \sum_{i=1}^n (q_{e,pred.i} - q_{e,exp.i})^2} \quad (7)$$

$$SSE = \sum_{i=1}^n (q_{e,pred.i} - q_{e,exp.i})^2 \quad (8)$$

where  $q_{e,exp}$  is the experimental uptake capacity of biomass, and  $q_{e,pred}$  is the uptake predicted from the model, and n is the number of measurements.

The models parameters were calculated by non-linear regression using Matlab.  $R^2$  values closer to 1 was an indicator that a greater proportion of variance was accounted for by the model, a SSE value closer to zero indicated a better fit, and RMSE closer to zero implied a fit that was more useful for prediction.

### 4.3. Results and discussion

Adsorption performance evaluation of any adsorbents relies on classical batch isotherm and kinetics experiments under controlled environmental conditions, supplemented by dynamic continuous-flow studies. The combined resulting data serves as a basis for the scale-up and sizing of the sorption contact systems (Volesky and Holan, 1995). In this work, the biosorption of copper by MTL were carried out in two parts: batch and column operations. The equilibrium and kinetics experiments

followed by breakthrough curves experiments and modeling of the fixed-bed column system.

#### **4.3.1. Batch Studies**

Adsorption of metals by biosorbents, in general, is a pH-dependent process as the surface charge of biosorbents is affected by the pH of solution and consequently their metal-retention performances. The variation of Cu (II) percentage removal and equilibrium uptake capacity of maple leaves with pH investigated (figure not shown). Copper biosorption increased with increase in solution pH, and maximum adsorption was achieved at pH 5.0. Low uptake values at lower pHs was possibly due to positive surface charge and of competition due to abundant hydrogen ions in the solution. The pH range was chosen according to our previous study of solution chemistry involving Cu (II) (Amirnia et al, 2012) to avoid metal precipitation at pH>6) so that biosorption remained the dominant removal mechanism, instead of surface precipitation.

##### **4.3.1.1. Effect of particle size**

Efficiencies of MTL with different particle sizes to remove Cu(II) ions from aqueous solutions are plotted in Figure 4.2. It was observed that as the particle size increased, the percentage removal decreased due to lower surface areas available for biosorption, however, the effect was not that significant.

All batch experiments were conducted with MTL particle sizes between 180 – 710  $\mu\text{m}$ . For column biosorption studies, particle sizes < 500  $\mu\text{m}$  was not selected to attain minimum biomass wash-out from the column due to attrition of fine MTL particles in water during the sorption-desorption cycles.

##### **4.3.1.2. Biosorption equilibrium isotherms**

Correlation of isotherm data ( $q_e$  vs.  $C_e$ ) by sorption isotherm equations are important for equilibrium modeling of biosorption systems and describing sorbate-sorbent interactions (Aygün et al., 2003). As summarized in Table 4.1, the equilibrium data of

$\text{Cu}^{2+}$  ions by MTL were fitted using three commonly used isotherm models; Freundlich (1906), Langmuir (1916), and Sips (1948).

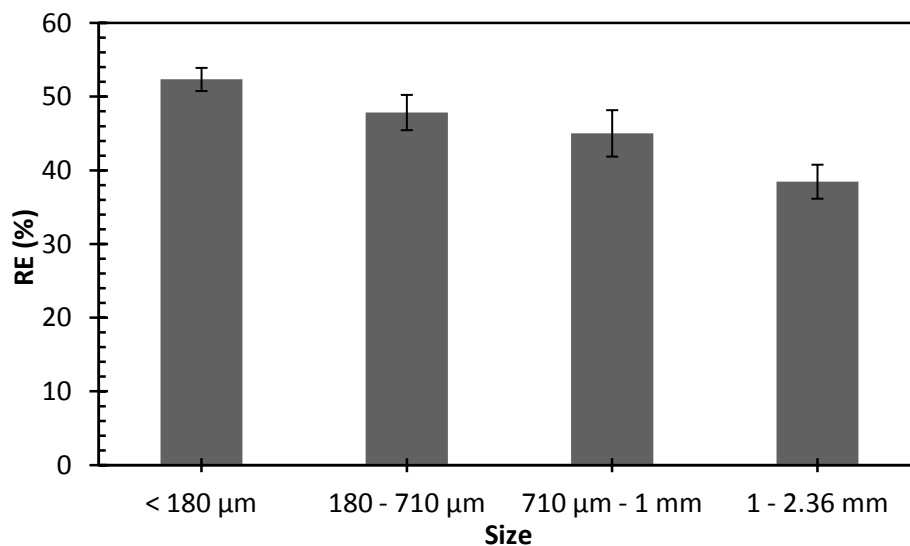


Figure 4.2. Influence of particle size on removal efficiency of Cu (II) ions by MTL biomass (dose: 1 g/l).

The isotherm parameters for 15 – 150 mg/l copper adsorption onto 1 – 8 g/l MTL given in Table 4.1 were determined by nonlinear regression analysis using CFtool in Matlab. For each biomass dry weight in isotherm experiments, initial Cu (II) concentrations were varied and equilibrium metal concentrations were analyzed. As expected, copper removal capacity was higher at higher MTL loading for the same initial concentration of Cu (II) due to a larger surface area being available for adsorption. Graphical observations of predictive performances of isotherm models in Figure 4.3 and fit quality parameters in Table 4.1 showed that although all three isotherms are suitable for predicting the  $\text{Cu}^{2+}$  equilibrium by the MTL biomass ( $R^2 > 0.98$ ,  $\text{RSME} < 1.4$ , and  $\text{SSE} < 5.4$ ), the data were best fitted by the monolayer Langmuir isotherm model in the studied concentration range as the other models had relatively higher RSME and SSE values.

According to  $R^2$  values, the Sips and Freundlich heterogeneous sorption models were found to be mathematically appropriate for describing the  $\text{Cu}^{2+}$  adsorption equilibrium

results. Similar results were reported by Hossain et al (2012) for copper sorption onto the palm oil fruit shells. Sips constant  $N$  was quite close to unity, which implied that biosorption of  $\text{Cu}^{2+}$  onto MTL could be reasonably described by the Langmuir model (Apiratikul and Pavasant, 2008). The dependence of adsorption data to different isotherms was related by Pierce and Moore (1982) to involvement of both strong and weak binding sites on the biomass surface for adsorption of metal ions at different environmental conditions.

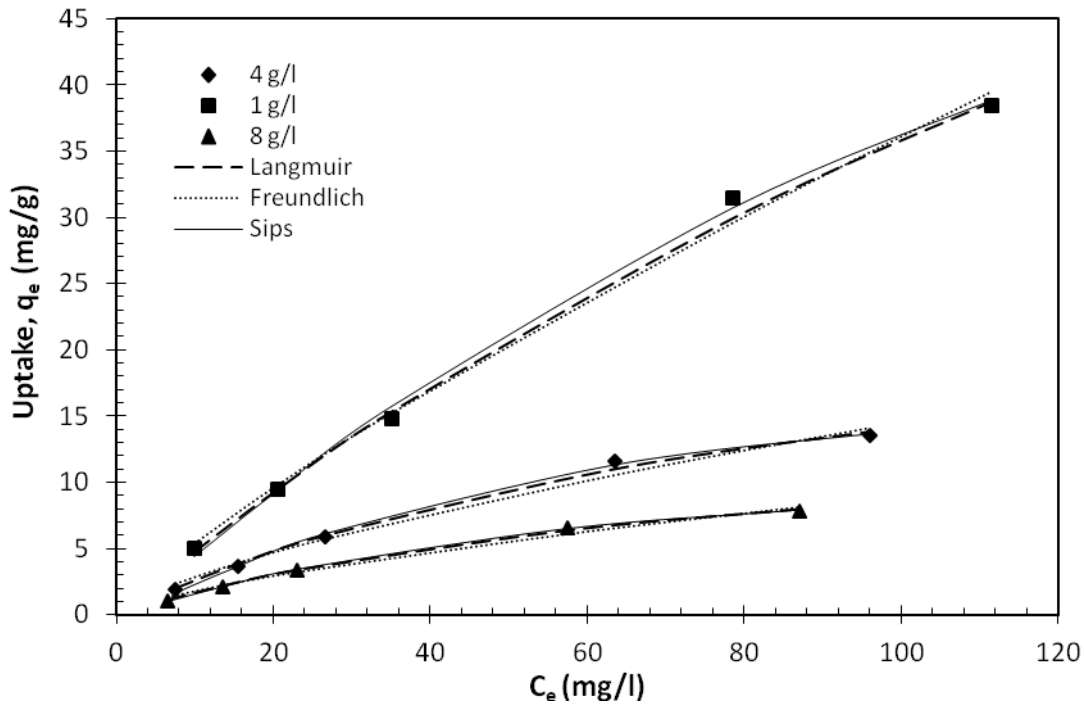


Figure 4.3. Cu (II) biosorption equilibrium data compared to of those predicted by isotherm models.

#### 4.3.1.3. Biosorption kinetics

##### 4.3.1.3.1. Effects of MTL dose and Cu(II) concentration

The time profiles of Cu (II) adsorption by MTL at different metal concentrations (Figure 4.4) showed that copper biosorption took place in three distinct stages: a rapid step within the first few minutes ( $< 2$  min) of sorbent-sorbate contact time representing

a negligible bulk mass transfer resistance and a surface adsorption mechanism, followed by a slow stage (2-10 min) which possibly is either controlled by an inter-particle diffusion or film diffusion, or both. A final plateau stage achieved when biomass binding sites became saturated with the metal ions. First biosorption kinetics stage ( $t < 2$  min) accounted for 82%, 85% and 90% of of sorption uptake in the studied metal concentrations of 15, 50, and 150 mg/l, respectively.

Table 4.1. Parameters in the isotherm equations for biosorption of copper with MTL.

Isotherm	Equation	Initial Metal Conc. (mg/l)	Parameters	Biomass Conc. (g/l)		
				1	4	8
Langmuir (1916)	$q = \frac{bq_{max}C}{1 + bC}$	15 - 150	b (l/mg)	0.0039	0.0103	0.0119
			$q_{max}$ (mg/g)	126.2	27.77	15.67
			$R^2$	0.9993	0.9944	0.9979
			RSME	0.4412	0.4364	0.1539
			SSE	0.584	0.5712	0.07105
Freundlich (1904)	$q = K_f C^{1/n}$	15 - 150	$K_f$	0.815	0.5719	0.3654
			n	1.214	1.423	1.438
			$R^2$	0.9936	0.9819	0.9875
			RSME	1.331	0.7843	0.3769
			SSE	5.315	1.845	0.4262
Sips (1948)	$q = \frac{b_s q_{max} C^N}{1 + b_s C^N}$	15 - 150	$b_s$	0.00399	0.00686	0.00956
			$q_{max}$	84.71	19.39	11.93
			N	1.136	1.281	1.192
			$R^2$	0.9975	0.9977	0.9995
			RSME	1.013	0.3429	0.09341
			SSE	2.053	0.2352	0.01745

The copper-MTL sorption kinetics was tested using a first-order equation (Lagergren, 1898) and a pseudo-second order rate equation developed by Ho and McKay (2000):

$$\ln(q_e - q_t) = -k_1 t + \ln q_e \quad (9)$$

$$\frac{t}{q_t} = \frac{1}{q_e} t + \frac{1}{k_2 q_e^2} \quad (10)$$

where  $k_1$  ( $\text{min}^{-1}$ ) and  $k_2$  ( $\text{g.mg}^{-1}.\text{min}^{-1}$ ) are the rate constants of first order and pseudo-second-order equations, respectively,  $q_e$  is the metal uptake at equilibrium ( $\text{mg/g}$ ), and  $q_t$  ( $\text{mg/g}$ ) is the amount of metal adsorbed at any given time  $t$  ( $\text{min}$ ).

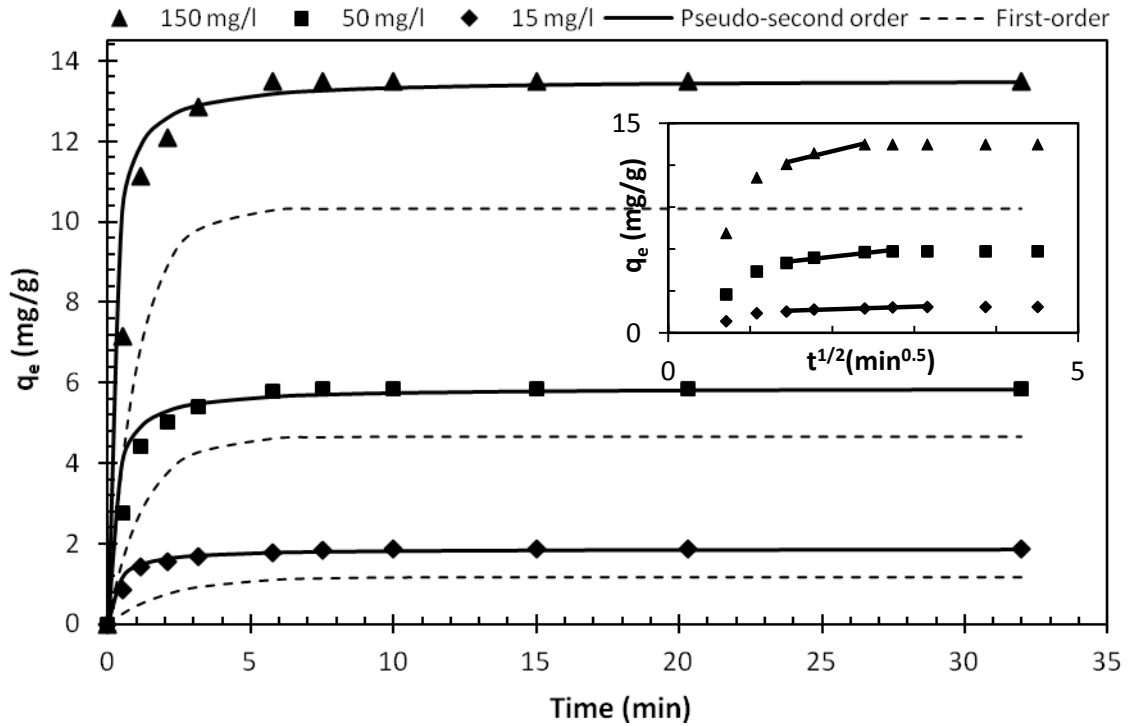


Figure 4.4. Influence of Cu (II) concentration on the kinetics of biosorption by MTL (biomass dose = 4 g/l). The slopes of the second stage of biosorption ( $q_t$  vs.  $t^{0.5}$ ) was used to obtain the intraparticle diffusion rate constants in Eq.(11).



Sorption kinetics data were also obtained when the MTL dosage was varied (Figure 4.5). The values of rate constants  $k_1$  and  $k_2$ , the predicted equilibrium sorption values,  $q_{e(cal)}$ , and the experimental uptake values  $q_{e(exp)}$  for different initial Cu (II) concentrations and MTL doses are given in Table 4.2. Based on the degree of agreement between the predicted and experimental uptake values and from the correlation coefficients ( $R^2$ ), it can be seen in Figure 4.4 that the pseudo-second order kinetics rate equation fitted the experimental data better than the first order.

The data in Table 4.2 and Figures 4.4 and 5 also showed that the MTL sorption capacity increased for the higher initial Cu (II) concentrations, and decreased with an increase in MTL dose. The increase in the rate constant  $k_2$  by increasing the MTL dose indicated that the biomass saturation time was slightly faster at higher biomass loads due to availability of more adsorption sites. On the contrary, slower uptake process with the decrease in  $k_2$  values at higher metal concentrations for the same biomass dose was not yielded from the experimental data. This may lead to the hypothesis of surface adsorption of metals at all concentrations, which is faster at higher concentration differences between the bulk and the biomass surface.

#### 4.3.1.3.2. Diffusion-based kinetics

The batch kinetics data were also analyzed by intraparticle diffusion (Weber and Morris, 1963), and external mass transfer (McKay et al., 1988) models as in Eqs. (11 and 12):

$$q_t = k_I t^{1/2} + I \quad (11)$$

$$\left( \frac{d(C_t / C_0)}{dt} \right)_{t \rightarrow 0} = -k_E \quad (12)$$

where  $K_I(\text{mg.g}^{-1}.\text{min}^{0.5})$  and  $K_E(\text{min}^{-1})$  are the inter-particle diffusion and external mass transfer rate constants, respectively, and  $I$  is a constant related to the thickness of diffusion layer. Slopes of the second stage intraparticle diffusion plots ( $1.4 < t^{1/2} < 3.2$ )

illustrated in Figure 4.4 was used to calculate the  $K_I$  coefficient values in Eq.(11). External mass transfer coefficient  $K_E$  was derived from the initial slopes of the  $C/C_0$  vs.  $t$  plots shown in Figure 4.5.

The large values of  $I$  indicated that the plots of Eq. (11) shown in Figure 4.4 did not go through the origin, and therefore, minimal contribution of intraparticle diffusion exists in biosorption of Cu (II) onto MTL (Weber and Morris, 1963; Poots et al., 1976) due to low pore area of MTL. Higher values of  $I$  denoted a greater boundary layer effect at higher metal concentrations and lower MTL doses, and therefore, a greater contribution of the surface sorption. Increase in the intra-particle diffusion rate constant  $k_E$  with the increase in concentration of Cu (II) in the liquid phase suggested an increase in the intraparticle diffusion of Cu (II) ions.

Table 4.2. Rate constants and parameters associated with chemical sorption and diffusion-based kinetics for biosorption of Cu (II) ions onto MTL.

Biomass dose (g/l)	Metal Conc. (mg/l)	Interparticle diffusion			External diffusion		Experiment $q_{e(\text{exp.})}$ (mg/g)	Pseudo-second-order			Pseudo-first-order		
		$k_I$ (mg.g <sup>-1</sup> .min <sup>0.5</sup> )	$I$ (mg/g)	$R^2$	$k_E$ (min <sup>-1</sup> )	$R^2$		$k_2$ (g.mg <sup>-1</sup> .min <sup>-1</sup> )	$q_{e(\text{Cal})}$ (mg/g)	$R^2$	$k_1$ (min <sup>-1</sup> )	$q_{e(\text{Cal})}$ (mg/g)	$R^2$
1	50	1.8027	9.14	0.9818	0.1812	0.9622	14.83	0.1752	14.90	1	0.3969	9.68	0.9583
									1.881	0.9			
4	15	0.1836	1.32	0.947	0.3188	0.9625	1.86775	1.6899	8	99	0.4904	1.1667	0.9588
4	50	0.6423	4.17	0.9413	0.2964	0.9489	5.85	0.8873	5.86	1	0.782	4.67	0.989
4	150	1.4135	10.17	0.9292	0.249	0.941	13.49125	0.4655	13.55	1	0.9389	10.334	0.9417
8	50	0.2118	2.86	0.9865	0.3549	0.9509	3.37	2.2256	3.37	1	1.1064	2.91	0.9739

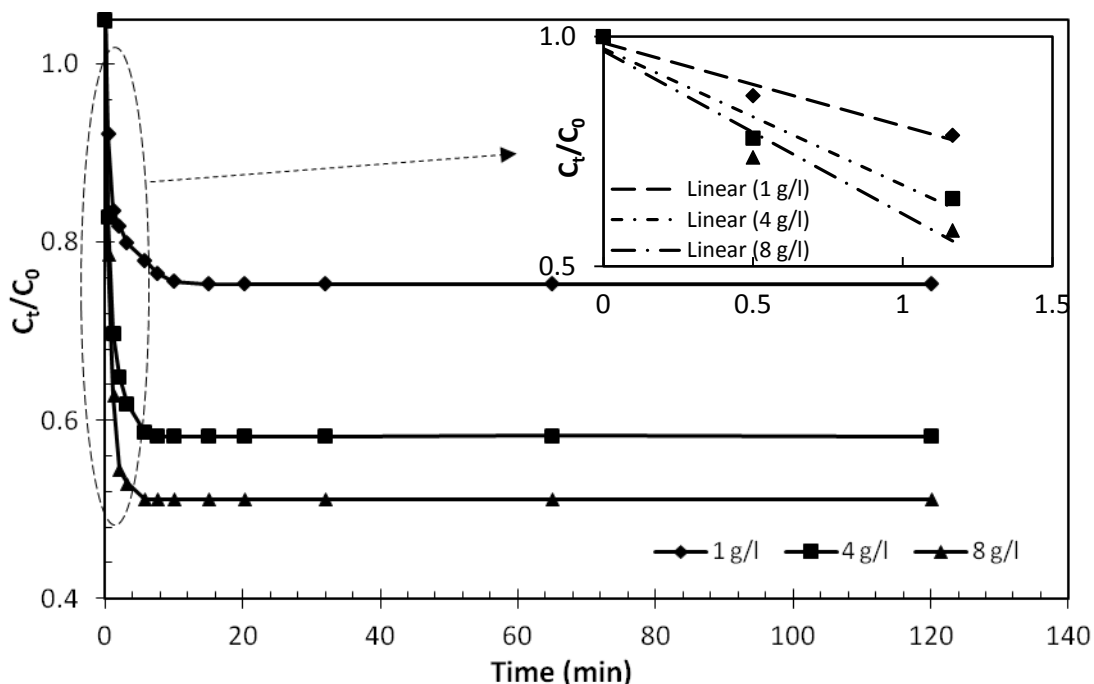


Fig. 4.5 Plot of dimensionless concentration vs. time for obtaining the external diffusion constant in Eq.(12) from the initial slopes for adsorption of Cu (II) ions onto MTL at different biomass doses (metal concentration 50 mg/l).

#### 4.3.1.4. Regeneration of MTL (Desorption of Copper form MTL)

Regeneration of separated MTL was conducted using a simple chemical treatment after adsorption. Five types of eluents, namely 0.1 N  $\text{H}_3\text{PO}_4$ , 0.1 N  $\text{H}_2\text{SO}_4$ , 0.1 N  $\text{HCl}$ , 0.1 N  $\text{CH}_3\text{COOH}$  and DI water were used to test the reusability of MTL as shown in Figure 4.6. MTL was easily regenerated for copper with low concentrations of acids (0.1N) and the maximum desorption happened with 0.1 N  $\text{H}_2\text{SO}_4$  solution (at pH 1.55). A 20% desorption with DI water (pH 6) was even occurred, which implies a weak biosorption mechanism.

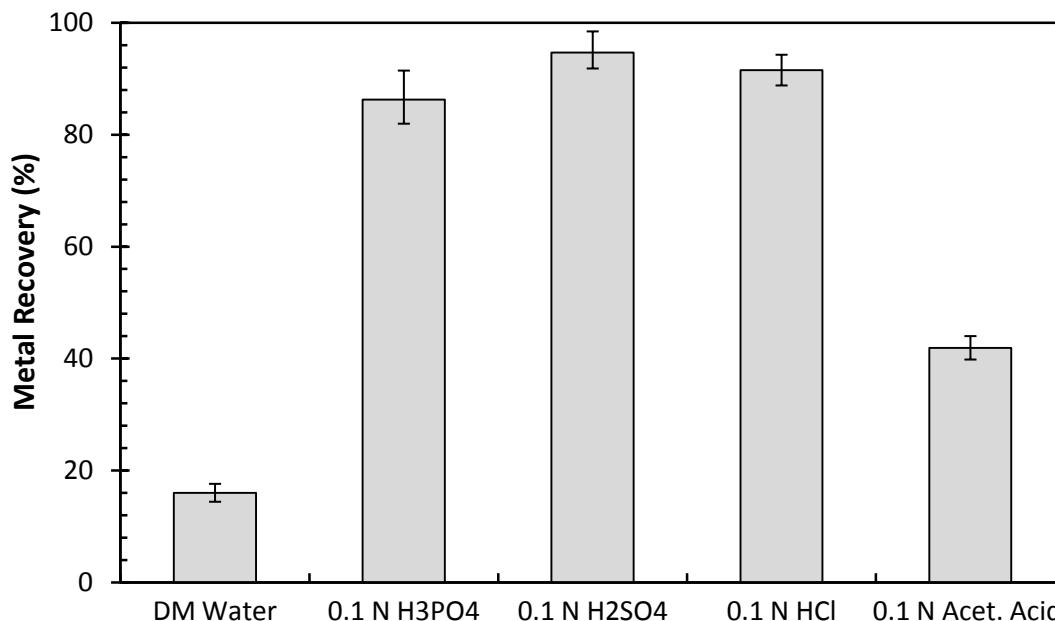


Figure 4.6. Regeneration of maple leaves with five types of eluents. Concentration of Cu (II) in the biomass (to be desorbed) was 25 ppm for all eluents (contact time 1 hour).

In column studies, the adsorbed  $\text{Cu}^{2+}$  ions were eluted from the biomass in eight cycles of adsorption-desorption using 0.1N sulphuric acid pumped upflow into the column. For regeneration, it was important to maximize the ratio of concentration between the initial metal-laden effluent and the final eluate (Tobin et al, 1994). The biomass regeneration produced small volumes of concentrated metals, which is potentially suitable for conventional metal reclamation processes (Kratochvil and Volesky, 1998).

#### 4.3.2. Column Studies

In column operations, in addition to the surface sorption and diffusion mechanisms discussed earlier, the process of metal biosorption is also influenced by macroscopic fluid flow pattern (e.g. advection and dispersion). The concept of breakthrough curve obtained from the operation of the fixed-bed biosorption column was used in describing the performance of the column (Volesky et al, 2003; Aksu and Gönen, 2004). All these factors were considered in simulating the dynamics of the fixed-bed column used in this study.

#### 4.3.2.1. Modeling (Modeling of biosorption process in a packed-bed column)

Batch sorption kinetics data in this work showed that a rapid metal equilibrium with MTL was achieved at the studied environmental conditions. This fact was applied for mathematical modeling of biosorption process in the packed-bed column. The principle of advection-dispersion-reaction (ADR) differential mass balance equation (Weber Jr et al., 1991) for transport of a solute from liquid phase to the solid phase was employed as the basis for modeling the column biosorption with the governing partial differential equation (PDE) as;

$$\frac{\partial C}{\partial t} = D_L \frac{\partial^2 C}{\partial z^2} - u_z \frac{\partial C}{\partial z} - \frac{\rho_b}{\varepsilon_b} \frac{\partial q}{\partial t} \quad (13)$$

where  $D_L$  is axial dispersion coefficient,  $u_z$  interstitial velocity,  $\rho_b$  is the bed density,  $C$  is the concentration of metal in the bulk liquid phase, and  $\varepsilon_b$  is the bed void volume calculated by Eq. (3).

The interstitial velocity of the bulk flow ( $u_z$ ) with a flowrate of  $F$  passing through the MTL particles with a diameter  $d_p$  packed in the column with a diameter of  $d_c$  was estimated using the following equation;

$$u_z = \frac{4F}{\pi d_c^2 \varepsilon_b} \quad (14)$$

Eq.(13) is the one-dimensional and non-steady state mass balance expression for a single sorbate being removed from a solution by a sorbent through diffusion, bulk movement, and sorption processes comprising the first, second, and third term in the right hand side of the equation, respectively. Such non-linear mathematical models representing the breakthrough curves and the dynamics of packed-bed columns are often complex and a general analytical solution is impossible to achieve without making some simplified assumptions (Hatzikioseyan et al., 2001; Borba et al, 2006).

The premise of a rapid local equilibrium derived from batch kinetics experiments implied that  $\partial q/\partial t$  at any point  $z$ , is reflected by the rate of change of the solute concentration in the liquid phase;

$$\frac{\partial q}{\partial t} = \frac{\partial q}{\partial C} \times \frac{\partial C}{\partial t} \quad (15)$$

Therefore, a rapid sorption reaction resulted in plausibility of negligible mass transfer resistances assumed in the liquid and solid phases. Similar modeling approach was used by Hatzikioseyan et al. (2001), with a difference that the axial dispersion coefficient, which is a key modeling parameter, was determined in this work by fitting the model data with the experimental data (Chen and Wang, 2004).

As batch experiments revealed (Table 4.1), the Langmuir isotherm adequately represented the biosorption of Cu (II) ions onto MTL. Therefore, for the rate of solute uptake term ( $\partial q/\partial C$ ) in Eq.(15), the derivative of Langmuir model was used;

$$\frac{\partial q}{\partial C} = \frac{b q_{max}}{(1+bC)^2} \quad (16)$$

where,  $q$  is the equilibrium uptake value,  $q_{max}$  is the total number of binding sites available for biosorption,  $C$  is the unadsorbed metal ion concentration in solution, and  $b$  is the Langmuir model constant. Substituting  $\partial C/\partial t$  in Eq.(13) by Eqs.(15, 16), we have;

$$\frac{\partial C}{\partial t} = D_L \frac{\partial^2 C}{\partial z^2} - u_z \frac{\partial C}{\partial z} - \frac{\rho_b}{\varepsilon_b} \frac{b q_{max}}{(1+bC)^2} \frac{\partial C}{\partial t} \quad (17)$$

$$\frac{\partial C}{\partial t} = (D_L \frac{\partial^2 C}{\partial z^2} - u_z \frac{\partial C}{\partial z}) / (1 + \frac{b \rho_b q_{max}}{\varepsilon_b (1+bC)^2}) \quad (18)$$

The boundary and initial conditions used to solve the ADR Eq.(18) are:

$$C = \begin{cases} 0 & t = 0, & 0 < z < L \\ C_0 & t > 0, & z = 0 \end{cases} \quad (19a)$$

$$\frac{\partial C}{\partial z} = 0 \quad t > 0, \quad z = L \quad (19b)$$

The first and second spatial derivatives in the above PDE system (Eq.(18)) were discretized using forth-order finite difference method (for boundary points, second-order forward and backward finite difference approximation were used), and the subsequent method of lines system of ordinary differential equations (ODE) was solved numerically in MATLAB for the given initial and boundary conditions. All model parameters were known based on column geometrics and operating conditions except for the dispersion coefficient  $D_L$  and the Langmuir constant  $b$ , which were determined by least square fitting of experimental data points using MATLAB.

#### 4.3.2.2. Column biosorption performance (multiple sorption-desorption cycles)

Figure 4.7 and Table 4.3 display the breakthrough data for eight biosorption cycles carried out with MTL particle sizes of  $500 \mu m - 1 mm$ , and inlet copper solution flowrate of  $21 ml/min$  containing  $55 mg/l$  Cu (II) at pH 5. The column void fraction ( $\epsilon_b$ ) and bed density ( $\rho_b$ ) for  $40 g$  of MTL was measured to be  $0.2621$  and  $555.2 g/l$ , respectively. Column service time  $t_b$  and exhaustion time  $t_e$ , when Cu (II) ions were detected at  $1 mg/l$  in the column effluent and at 96% of the breakthrough curves, respectively, are given in Table 4.3.

Breakthrough curves in the 2<sup>nd</sup> and 8<sup>th</sup> cycles were plotted in Figure 4.7. Generally, a steeper breakthrough curve is more favorable, indicating the effective utilization of biomass inside the column, whereas a flat curve shows long mass transfer zone in the column (Kratochvil and Volesky, 1998; Aksu and Gönen, 2004). The slopes of the subsequent curves at  $t_{50\%}$  (Table 4.3) varied slightly from  $0.0863$  to  $0.0883 mg/l/min$  up to the cycle#6, after which it slightly flattened until the 8<sup>th</sup> cycle which had the

lowest slope of 0.0727 mg/l.min. As shown in Table 4.3, the changes in the slopes yet were not significant over the first 6 cycles.

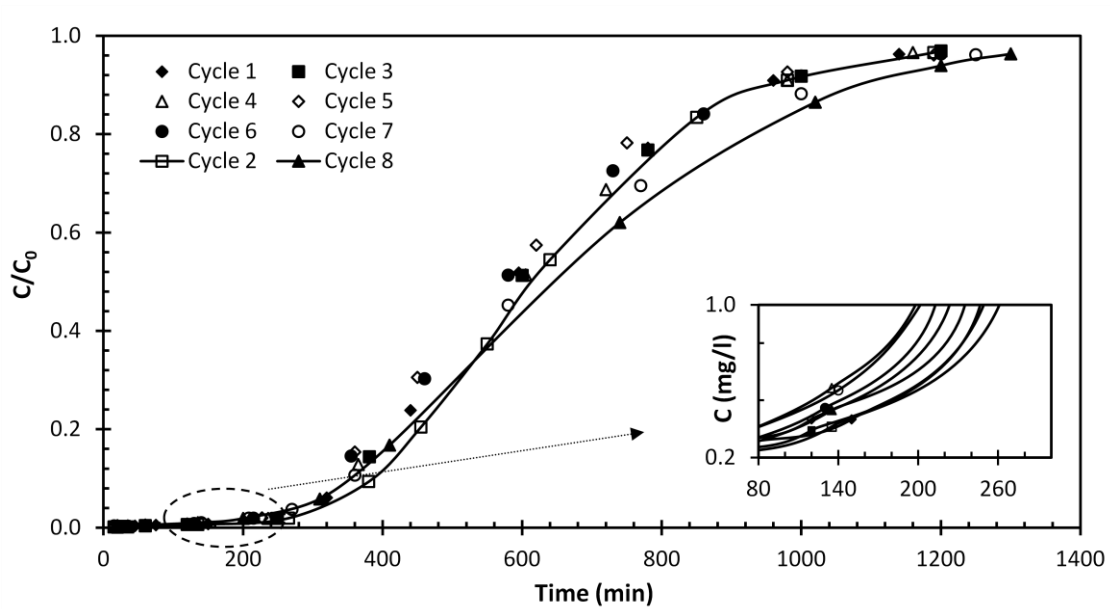


Fig. 4.7. Concentration profile of Cu (II) at the column outlet as a function of time for eight biosorption cycles ( $C_0 = 55 \text{ mg/l}$ ,  $F = 21 \text{ ml/min}$ ). Effluent concentration of  $1 \text{ mg/l}$  was used to obtain the column breakthrough time.

The breakthrough times ( $t_b$ ) were  $248 \text{ min}$  and  $197 \text{ min}$  in the first and last cycle, respectively. However, the maximum breakthrough time of the column was associated with the 2<sup>nd</sup> cycle ( $262 \text{ min}$ ), after which, there was a decreasing trend in  $t_b$  in average 8 min steps. It is possible with increasing cycles; there is a difference in metal biosorption mechanism between cycle 1 and the rest of the cycles.

As shown in Figure 4.8, during the first sorption cycle, some ions such as Ca(II) and Mg(II), K(I) and Na(I) were released from biomass to the liquid phase, which were significantly higher than leaching these ions to liquid phase without the presence of copper ions. Some trace amounts of Mn, Fe, and P were also released during the biosorption. This suggests that ion exchange could participate in sorption mechanism of Cu(II) ions by the MTL biomass. However, since the regeneration was performed



by acid (0.1N H<sub>2</sub>SO<sub>4</sub>), the desorbed metal ions in the 1<sup>st</sup> desorption cycle were not replaced by the same ions indicating that Cu(II) sorption mechanism after first cycle was less dependent on ion-exchange and was mainly based on adsorption on free binding sites of the biomass. Similar ion exchange mechanism was reported by Apiratikul and Pavasant (2008) for release of Ca(II), Mg(II), and Mn(II) from algal biomass *C. lentillifera* during biosorption of metals.

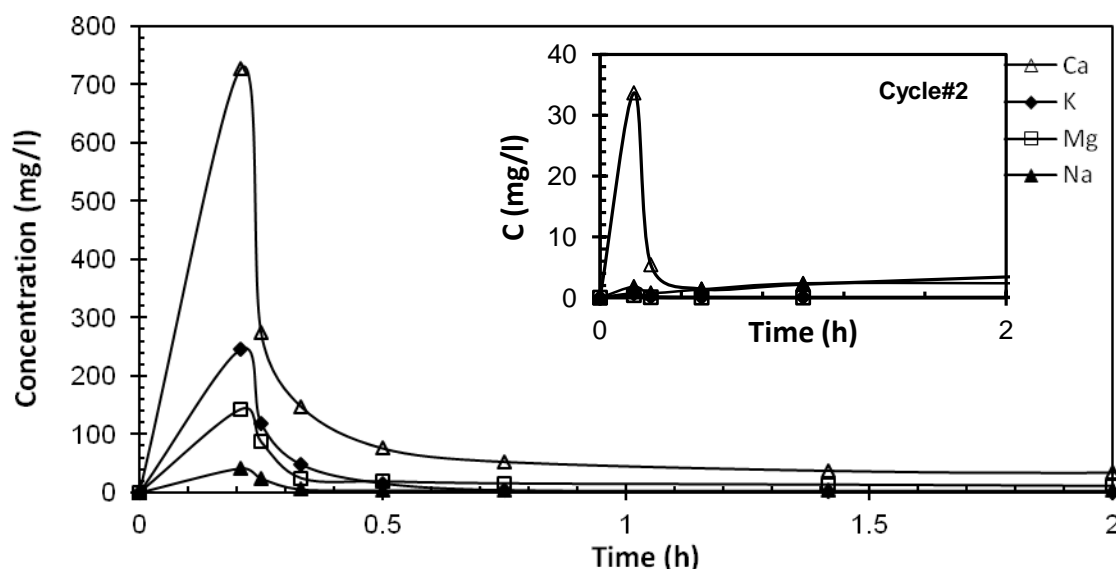


Figure 4.8 Metal ions released during the 1<sup>st</sup> and 2<sup>nd</sup> cycles of column biosorption. After the 2<sup>nd</sup> cycle, no significant amount of metal ions release was observed.

The breakthrough time enhancement in the 2<sup>nd</sup> cycle compared to the first cycle could also be due to the removal of all impurities from the surface of MTL particles after first acid wash acting as an involuntary biomass pretreatment step. The overall decrease in breakthrough times in each cycle with the increase in the cycle numbers (after cycle#2) could be because of not achieving 100% desorption efficiencies in the preceding cycle (Table 4.3).

The column biosorption capacity and removal efficiency were calculated for each cycle by solving Eqs.(4) and (5) and the results are summarized in Table 4.3. It was found that decreasing the breakthrough times showed no negative effect on column sorption capacity throughout the cycles. Similar results were reported by Volesky et al. (2003) for column biosorption of Cu (II) using seaweed *S. filipendula* biomass. The column overall adsorption rate even slightly elevated in the 2<sup>nd</sup> and last cycles, probably as a result of biomass acid wash in regeneration cycles. The average biosorption capacity and removal efficiency of MTL for Cu (II) ions were 18.3 mg/g and 53.5%, respectively.

Deterioration of sorption performance over multiple sorption-desorption cycles maybe caused by changes in chemistry and structure of adsorption sites on biomass surface as well as change in packed-bed density due to biomass weight loss during the cycles. After 8<sup>th</sup> cycle, the dry weight of biomass was measured and a weight loss of 5.4% was obtained, although there was no noticeable change in the bed length. However, some agglomeration of MTL particles was observed during the last sorption-desorption cycles causing unequal bed density.

Table 4.3. Column biosorption breakthrough parameters for eight sorption-desorption cycles (particle size 500  $\mu\text{m}$  - 1 mm;  $\varepsilon_b = 0.2621$ )

Cycle No.	Sorption									Desorption	
	$t_b$ (min)	$t_e$ (min)	$q_b$ (mg/g)	$(RE)_b$ (%)	$t_{50\%}$ (min)	$dc/dt$ (mg/l.min)	$L_{ads}$ (cm)	$D_L$ (cm <sup>2</sup> /min)	$b$ (l/mg)	$E$ (%)	$C_{2h}$ (mg/l)
1	248	1124	17.9	55.11	574	0.0863	21.0	50.05	0.010	95.36	34.52
2	262	1167	18.7	55.38	606	0.0873	20.9	40.33	0.010	94.52	30.04
3	246	1156	18.1	54.15	580	0.0862	21.3	53.71	0.011	96.93	28.54
4	234	1132	18.1	55.28	583	0.0868	21.4	55.59	0.011	98.21	24.25
5	223	1180	17.3	50.69	560	0.0883	21.9	63.30	0.012	94.03	16.51
6	212	1182	17.6	51.42	561	0.086	22.2	81.32	0.014	98.15	8.03
7	202	1242	19.0	52.92	601	0.0792	22.6	89.47	0.015	95.97	14.85
8	197	1285	19.8	53.45	638	0.0727	22.9	95.85	0.019	93.95	9.24

The length of adsorption zone defined in Eq.(6) for each cycle is presented in Table 4.3. It increased from 21 to 22.9 *cm* (~9%) from the 1<sup>st</sup> cycle to the 8<sup>th</sup> cycle reflecting a longer mass transfer zone at a higher cycle number. In each cycle, as the loading of metal solution to the column continued, the adsorption zone moved along the column until the breakthrough time that Cu (II) concentration at the column outlet began to increase constantly. From this point onward, although the bed is not fully saturated and the adsorption still kept occurred, the useful life of the bed was over (Kratochvil and Volesky, 1998). The results showed that a shorter length of sorption zone was associated with longer breakthrough times.

#### 4.3.2.3. Desorption

The elution curves for four consecutive cycles are shown in Figure 4.9, and desorption parameters of each respective cycle are summarized in Table 4.3. All desorption cycles conducted with 0.1N H<sub>2</sub>SO<sub>4</sub> at 35 ml/min for 2 h. As depicted in Figure 4.9, maximum desorption concentration of Cu (II) ions was reached within first 10 minutes of elution cycle. The highest elution peak of 2554 *mg Cu/l* was achieved for the cycle #5. The residual effluent concentrations at the end of desorption cycle (*C<sub>2h</sub>*) was between 34.52 and 9.24 *mg Cu/l* from desorption cycle#1 to cycle #8 (Table 4.3).

The elution efficiency *E*(%) was calculated based on the ratio of the metal mass desorbed (*m<sub>des</sub>*) to the mass of metal adsorbed (*m<sub>ads</sub>*):

$$E(\%) = \frac{m_{des}}{m_{ads}} \times 100 \quad (20)$$

$$m_{des} = F_e \int_0^t C_t . dt \quad (21)$$

where *F<sub>e</sub>* is the flowrate of the regenerant, and *m<sub>ads</sub>* is obtained based on column uptake capacity (*m<sub>ads</sub> = q<sub>b</sub>.m<sub>b</sub>*). The trapezoidal rule was used for numerical integration of Eq.(21). As illustrated in Table 4.3, elution efficiencies up to 98% were achieved similar to batch desorption experiments.

#### 4.3.2.4. Effect of process parameters

The effects of fluctuations in column inlet metal flowrate and concentration on breakthrough profiles are illustrated in Figures 4.10 and 4.11. The respective predicted breakthrough curves for different operational scenarios are also presented. The position of breakthrough curves changed along the time axis with respect to the influent concentration and flowrate: at higher flowrates, the column was saturated earlier resulting in relatively earlier breakpoint and exhaustion times as well as a wider adsorption zone ( $L_{ads}$ ), and a steeper breakthrough curve.

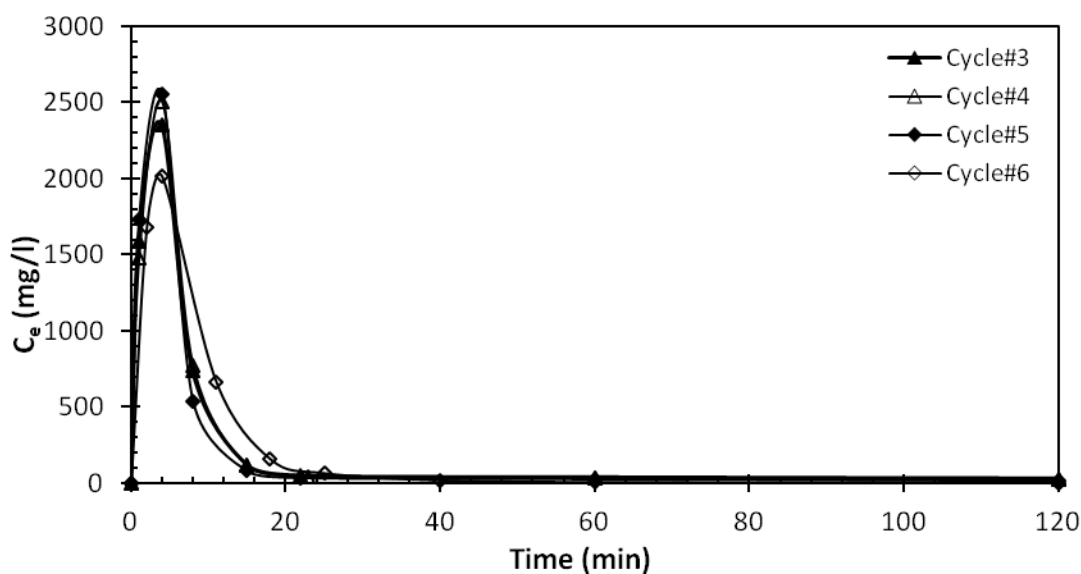


Figure 4.9. Cu (II) desorption concentration profile for regeneration cycles 3 to 6 (elute: 0.1N  $H_2SO_4$ , flowrate: 35 ml/min).

As shown in Table 4.4, the adsorption capacity of the column ( $q_b$ ) showed an increase up to 17.89 mg/g for flowrate of 21 ml/min, and then slightly declined to 16.57 mg/g as the flowrate increased to 30 ml/min. However, the highest metal concentration (110 mg Cu/l) at a constant feed flowrate of 21 ml/min produced the highest column uptake

capacity (28.64 mg/g). Lower inlet metal concentrations and lower flowrates resulted in delayed breakthrough and exhaustion times due to slower saturation of binding sites of the surface of biomass particles at lower metal flowrates and concentrations. Likewise, a shortened mass transfer zone ( $L_{ads}$ ) was observed at lower inlet flowrates and metal concentrations. Similar results in column performance were reported by Gokhale et al (2009), Vijayaraghavan et al. (2005), and Zümriye et al (2002).

The sorbent usage in the column was increased from 5.7 to 13.0 g/l by increasing metal load from 15 to 110 mg/l at a constant flowrate of 21 ml/min indicating a higher amount of biomass was consumed per liter of effluent treated when column inlet metal load was higher.

The dispersion coefficient ( $D_L$ ) obtained from modelling were significantly increased from 6.89 to 147.45  $cm^2/min$  as the feed flowrate increased from 5 to 30  $ml/min$ . Higher metal concentration also resulted in higher dispersion coefficient. The values of  $D_L$  are consistent with those reported by Chen and Wang (2004) for similar flowrates. It should be noted that the dispersion term in Eq. (18) estimated by best-fitting, was assumed to compensate for the flow non-idealities in case the metal biosorption is slow and mass transfer resistances are present in the liquid and solid phases, as noted earlier by Hatzikioseyan et al. (2001).

It can be seen in Tables 4.1 and 4.4 that the variations in  $b$  (Langmuir constant) values were matched to those obtained from batch experiment at similar operating conditions (e.g. at equivalent sorbent dosage vs. biomass dose, and similar metal concentrations), which validated the accuracy of the proposed model.

Vijayaraghavan et al. (2004) reported that a slower flowrate results in higher sorption capacity when the biosorption process is controlled by intraparticle mass transfer rate, while a higher flowrate would favor the sorption when the sorption is controlled by external mass transfer rate.

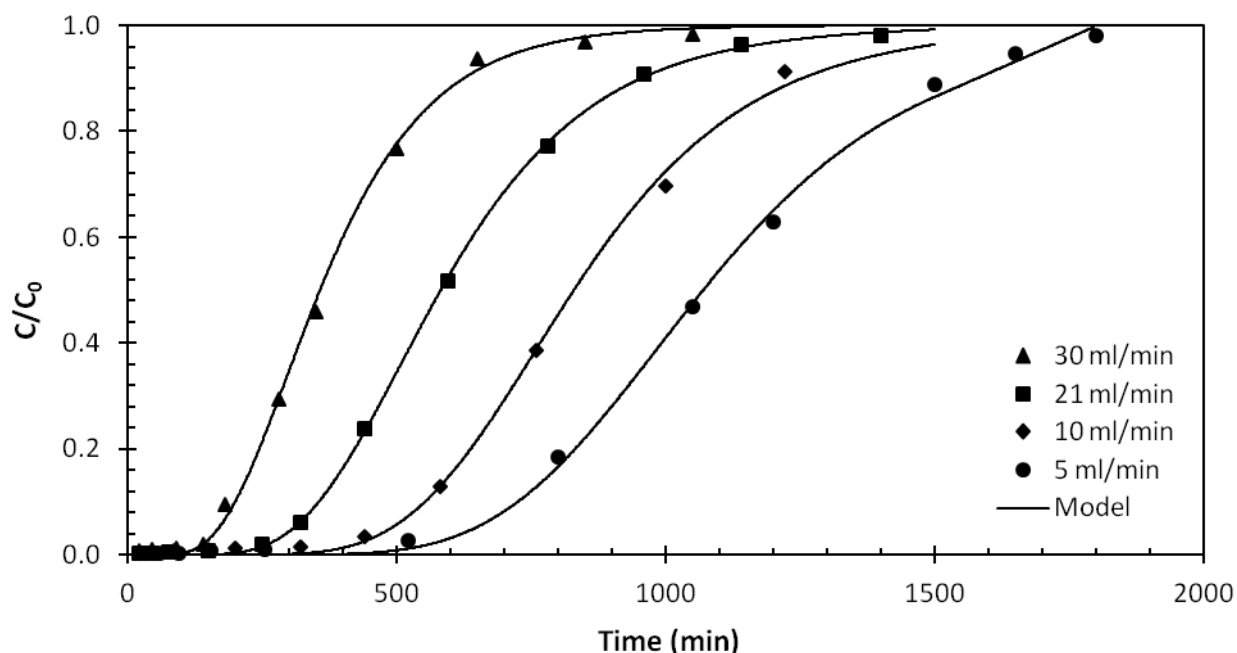


Figure 4.10. Experimental breakthrough curves and the simulated model results for different feed flowrates (Cu concentration at the inlet = 55 mg/l).

In this work, as shown in Table 4.4, there was no clear correlation between the sorption capacity and feed flowrates. Likewise, lower flowrates not always favored the biosorption. Hence, assuming a fast local equilibrium of the sorbate concentration with the sorbent due to negligible film and interparticle resistances in modeling the column sorption seems to be reasonable. Batch diffusion kinetics results (Table 4.2) are also in tandem with rapid local equilibrium assumption.

Table 4.4. Column performance data at different flowrates and inlet metal concentrations.

Operating parameters		Breakthrough analysis								
Flowrate	Feed Conc.	$t_b$	$t_e$	$q_b$	$L_{ads}$	Sorbent	$D_L$	$b$	Predicted	$\Delta t_b$
(ml/min)	(mg/l)	(min)	(min)	(mg/g)	(cm)	Usage (g/l)	(cm <sup>2</sup> /min)	(l/mg)	$t_b$ (min)	(%)
5	55	488	1700	7.46	19.2	16.4	6.89	0.009	556	13.9
10	55	372	1321	11.81	19.4	10.8	14.89	0.009	420	12.9
21	15	336	1438	6.18	20.7	5.7	85.59	0.054	387	15.2
21	55	248	1124	17.89	21.0	7.7	50.05	0.01	254	2.4
21	110	147	988	28.64	23.0	13.0	110.19	0.008	155	5.4
30	55	137	665	16.57	21.4	9.7	147.45	0.016	139	1.5

As shown in Figures 4.10 and 4.11, the developed model predicted the experimental sorption data well. Although the robustness and flexibility of the model were tested in simulating the column sorption performance at different operating conditions, the model overestimated the experimental breakthrough time by 2.4 – 15.2% (Table 4.4).

Comparing batch and column operations for Cu (II) biosorption by MTL, it is worth noting some of the process differences: in terms of metal concentration profiles in the liquid phase, it continuously decreased with time in batch system whereas continuously increased in the column system. The column adsorption system was also at non-steady-state in terms of metal concentration in liquid and solid phases, although a rapid equilibrium was reached at any point along the column length.

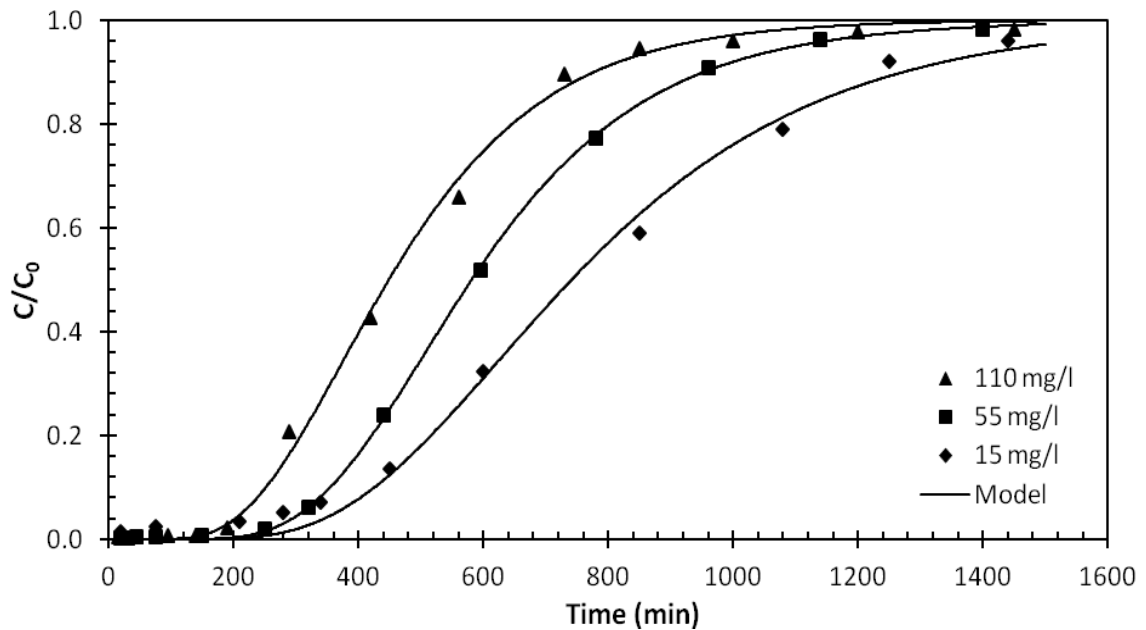


Figure 4.11. Plots of normalized Cu (II) concentration at the column outlet vs. time and simulated results at different metal concentrations in the column influent (flowrate: 21 ml/min).

#### 4.3.3. Characterization of MTL

Biosorption of metals is based on several mechanisms depending on the type and origin of the biomass, as well as the biomass processing methods (Volesky and Holan, 1995). The surface characterization of biomass is then of paramount importance in search for the dominant mechanism involved in biosorption. The BET test results (Table 4.5) provides information on pore size, area and volume of the MTL biomass. BET surface area of 11.59 m<sup>2</sup>/g (pore diameter 37.4 Å ) indicated that MTL biomass is not a highly porous material.

Table 4.5. BET surface properties and BJH pore size and volume of MTL (particle size < 250 µm)

	Method	Value
<b>Area</b> (m <sup>2</sup> /g)	BET	11.95
	External surface	13.17
	Pores BJH adsorption cumulative surface (17 Å < diameter < 3000 Å)	9.25
	Pores BJH desorption cumulative surface (17 Å < diameter < 3000 Å)	10.19
<b>Volume</b> (cm <sup>3</sup> /g)	Pores BJH adsorption cumulative volume (17 Å < diameter < 3000 Å)	0.031641
	Pores BJH desorption cumulative volume (17 Å < diameter < 3000 Å)	0.032366
<b>Pore size</b> (Å)	Adsorption avg. Pore diameter	37.40
	BJH adsorption avg. Pore diameter	136.90
	BJH desorption avg. Pore diameter	126.99



Infrared spectra of MTL can be seen in Figure 4.12(a, and b) for the metal-free and the metal-loaded biomass. The changes in absorption peaks were representative of a metal binding process on the surface of the biomass. The intense band peak at  $1028\text{ cm}^{-1}$  changed to  $1032\text{ cm}^{-1}$  may suggest involvement of phosphate or C-O groups in the biomass (C-O stretch between  $1000 - 1320\text{ cm}^{-1}$  for alcohols, carboxylic acids, esters, ethers), and the shift in the peak position from  $3342$  to  $3362\text{ cm}^{-1}$  could be attributed to the binding of Cu (II) with amino or hydroxyl groups (Pradhan et al., 2007; Rahman and Islam; 2009, Ramrakhiani et al., 2011; Gorgievski et al., 2013). Therefore, the identified functional groups of hydroxide, phosphorous, and carboxyl etc. present in the biomass contributed in Cu(II)-MTL interactions in addition to other biosorption mechanisms.

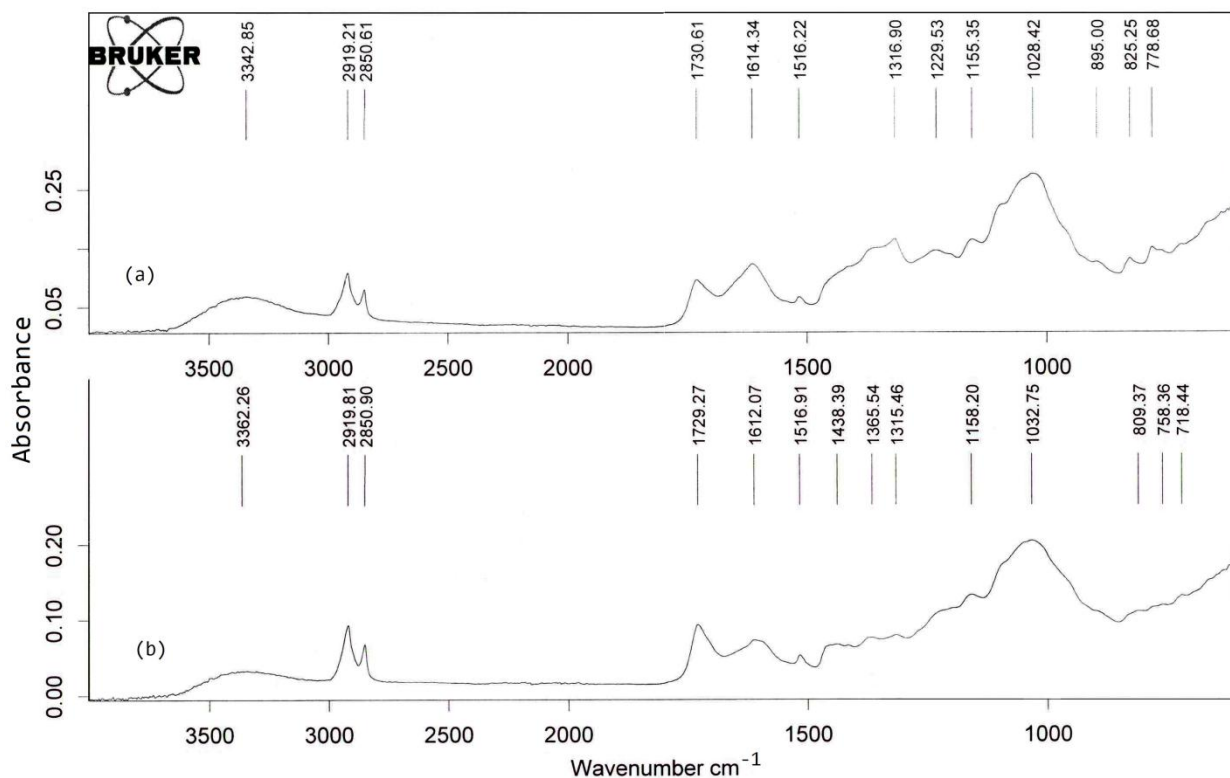


Figure 4.12. FTIR spectra of MTL (a) before and (b) after Cu (II) ions adsorption.

The SEM image of MTL in (Figure 4.13 a, and b) showed that biomass surface structure is irregular and rough containing open pores, which may promote the metal adsorption. Comparing the images of MTL before and after Cu (II) adsorption in Figure 4.13, Surface morphology of metal-loaded MTL became more homogenous containing dense pores, which may influenced by the presence of metal ions (Xiao-jing et al., 2014; Annadurai et al., 2002; Rahman and Islam, 2009).

Leaves are composed of variety of organic and inorganic compounds such as chlorophyll, carotene, anthocyanin, and tannins containing a variety of functional groups which can contribute to metal biosorption (Volesky, 2003a). As discussed earlier (Figure 4.8), MTL also contains Ca, K, Mg, and Na ions in the structure of these compounds in leaves, which can exchange with Cu (II) ions.

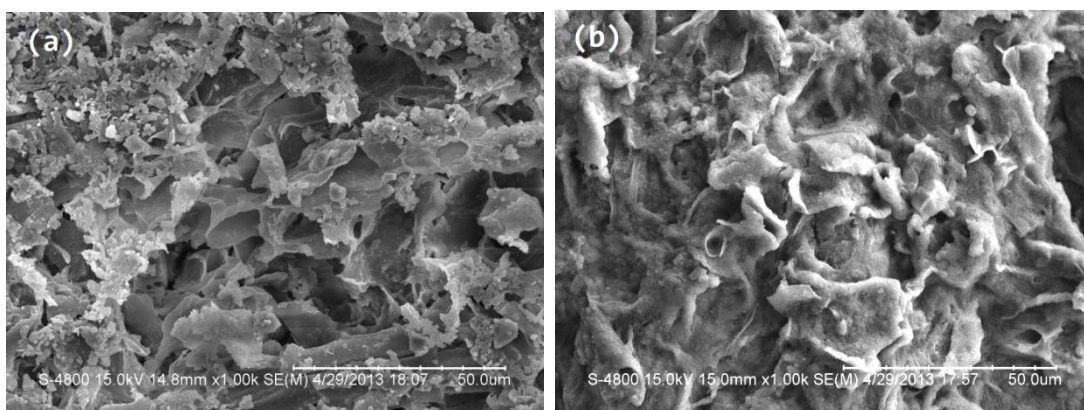


Figure 4.13. SEM images of Maple leaves powder (a) without metal (b) with metal.

Maple leaves contain a large amount of tannins as a natural organic materials, which altered the colour of the treated water after batch biosorption and caused an aesthetic water quality problem by giving it a brownish tea colour. However, this happened with only the first cycle of column operation, and the effluent colour from the 2<sup>nd</sup> sorption-desorption cycle was clear. Therefore, if biosorption of metals by maple leaves was

used for drinking water treatment in batch systems, some chlorination/filtration or ozonation/filtration must be used to remove tannins from water.

#### **4.4. Conclusions**

Plant wastes, such as maple tree leaves (MTL), are inexpensive and of low economic value, locally abundant and readily available in Canada. In this work, Cu (II) adsorption capacity of waste MTL was explored in a fixed-bed flow-through column. Ability of MTL biomass to be regenerated and reused was also examined. Multiple sorption-desorption cycles without reducing efficiency of MTL for metal biosorption was possible due to easy regeneration of MTL and resulted in low-volume high-concentration solutions ready for a conventional metal recovery operation. The shortening column service times did not coincide with altering the adsorption capacity of the column implying available but less accessible sorption sites throughout the sorption-desorption cycles.

The results of the kinetics experiments showed that the Cu (II) sorption process by MTL followed a pseudo-second order rate model. Chemical and diffusion-based kinetics data showed that intracellular diffusion did not control the adsorption of Cu (II) on MTL, and surface adsorption was the main mechanism of metal removal by the biomass.

Prediction of characteristic breakthrough curves is necessary for a successful design of a packed-bed sorption column. A theoretical model was developed based on the concept of rapid local equilibrium to describe the operation of the biosorption column. The breakthrough data was adequately described by the developed model. The column's deteriorating sorption performance with increasing number of sorption-desorption cycles was described by shortening breakthrough times, broadening mass transfer zones, changing chemistry of sorption sites of the aging biomass, and unequal packed-bed density for the last sorption runs.

Results in this work confirmed that biosorption of Cu (II) using MTL is a feasible method of heavy metal removal as the process is capable to be operated continuously, can handle fluctuations in operational flow rates, and a simple yet robust operating system. The selected column length was a representative of a lab-scale column studies and longer packed beds also could be tested. It is obvious that the increase in bed depth results in higher sorption capacity of the bed, and hence in a longer breakthrough time. Investigating MTL's selectivity to different types of metals in a packed-bed column would be worthwhile to discover the full potential of MTL biomass for heavy metals treatment. The presented model in this work for column biosorption of Cu (II) could serve as a basis for developing models for more complex metal biosorption processes involving multi-metals and other impurities in industrial effluents.

#### **4.5. Acknowledgements**

This work was supported by individual NSERC Discovery Grants awarded to Dr. A. Margaritis and Dr. M.B. Ray.

#### **4.6. References**

- [1] Abdolali A., Guo W.S., Ngo H.H., Chen S.S., Nguyen N.C., Tung K.L., Typical lignocellulosic wastes and by-products for biosorption process in water and wastewater treatment: a critical review, *Bioresour. Technol.*, 160 (2014) 57–66.
- [2] Aksu Z., Gönen F., Biosorption of phenol by immobilized activated sludge in a continuous packed bed: prediction of breakthrough curves, *Process Biochem.*, 39 (2004) 599–613.
- [3] Amirnia S., Ray M.B., Margaritis A., Heavy Metals Removal from Aqueous Solutions Using *Saccharomyces cerevisiae* in a Novel Continuous Bioreactor-Biosorption System, *Chem. Eng. J.*, 264 (2015) 863–872.

- [4] Amirnia S., Margaritis A., Ray M.B., Adsorption of Mixtures of Toxic Metal Ions Using Non-viable Cells of *Saccharomyces cerevisiae*, Adsorpt. Sci. Technol., 30, 1 (2012) 43-63.
- [5] Apiratikul R., Pavasant P., Batch and column studies of biosorption of heavy metals by *Caulerpa lentillifera*, Bioresour. Technol., 99 (2008) 2766–77.
- [6] Aygün A., Yenisoy-Karakaş S., Duman I., Production of granular activated carbon from fruit stones and nutshells and evaluation of their physical, chemical and adsorption properties, Microporous Mesoporous Mater., 66 (2003) 189–195.
- [7] Borba C.E., Guirardello R., Silva E.A., Veit M.T., Tavares C.R.G., Removal of nickel(II) ions from aqueous solution by biosorption in a fixed bed column: Experimental and theoretical breakthrough curves, Biochem. Eng. J., 30 (2006) 184–191.
- [8] Cassidy M.B., Lee H., Trevors J.T., Environmental applications of immobilized microbial cells: A review, J. Ind. Microbiol., 16 (1996) 79–101.
- [9] Chen J.P., Wang L., Characterization of metal adsorption kinetic properties in batch and fixed-bed reactors, Chemosphere, 54 (2004) 397–404.
- [10] Fomina M., Gadd G.M., Biosorption: current perspectives on concept, definition and application, Bioresour. Technol., 160 (2014) 3–14.
- [11] Freundlich HMF, Über die adsorption in Lösungen. Z Phys. Chem., 57 (1906) 385–470.
- [12] Gokhale S.V., Jyoti K.K., Lele S.S., Modeling of chromium (VI) biosorption by immobilized *Spirulina platensis* in packed column, J. Hazard. Mater. 170, (2009) 735–743.

- [13] Guidelines for Canadian drinking water quality, Health Canada, [http://hc-sc.gc.ca/ewh-semt/pubs/water-eau/sum\\_guide-res\\_recom/index-eng.php](http://hc-sc.gc.ca/ewh-semt/pubs/water-eau/sum_guide-res_recom/index-eng.php) (2014).
- [14] Gorgievski M., Božić D., Stanković V., Štrbac N., Šerbula S., Kinetics, equilibrium and mechanism of  $\text{Cu}^{2+}$ ,  $\text{Ni}^{2+}$  and  $\text{Zn}^{2+}$  ions biosorption using wheat straw, *Ecol. Eng.*, 58 (2013) 113–122.
- [15] Hatzikioseyan A., Tsezos M., Mavituna F., Application of simplified rapid equilibrium models in simulating experimental breakthrough curves from fixed bed biosorption reactors, *Hydrometallurgy* 59 (2001) 395–406.
- [16] Ho Y.-S., Review of second-order models for adsorption systems, *J. Hazard. Mater.*, 136 (2006) 681–9.
- [17] Ho Y.-S., Chiu W.-T., Wang C.C., Regression analysis for the sorption isotherms of basic dyes on sugarcane dust, *Bioresour. Technol.*, 96 (2005) 1285–91.
- [18] Hossain M.A., Ngo H.H., Guo W.S., Nguyen T.V., Palm oil fruit shells as biosorbent for copper removal from water and wastewater: experiments and sorption models, *Bioresour. Technol.*, 113 (2012) 97–101.
- [19] Hu L., Adeyiga A.A., Greer T., Miamee E., Adeyiga A., Removal of Metal Ions From Wastewater With Roadside Tree Leaves, *Chem. Eng. Commun.*, 189 (2002) 1587–1597.
- [20] Kim N., Park M., Park D., 2015. A new efficient forest biowaste as biosorbent for removal of cationic heavy metals. *Bioresour. Technol.* 175, 629–632.
- [21] Ko D.C.K., Porter J.F., McKay G., Film-pore diffusion model for the fixed-bed sorption of copper and cadmium ions onto bone char, *Water Res.*, 35 (2001) 3876–3886.

- [22] Kratochvil D., Volesky B., Advances in the biosorption of heavy metals, Trends Biotechnol., 16 (1998) 291-300.
- [23] Lagergren S., Zur Theorie der Sogenannten Adsorption Geloster Stoffe. K. Sven. Vetenskapsakad. Handl., 24 (1898) 1-39.
- [24] Langmuir I., The constitution and fundamental properties of solids and liquids, J Am Chem Soc., 38 (1916) 2221-95.
- [25] McKay G., El Geundi M., Nassar M.M., External mass transport processes during the adsorption of dyes onto bagasse pith, Wat. Res. 22, 12 (1988) 1527-1533.
- [26] Park D., Yun Y.-S., Park J.M., The past, present, and future trends of biosorption, Biotechnol., Bioprocess Eng. 15 (2010) 86-102.
- [27] Pierce M.L., Moore C.B., Adsorption of arsenite and arsenate on amorphous iron hydroxide, Water Res., 16 (1982) 1247-1253.
- [28] Poots V.J.P., McKay G., Healy J.J., The removal of acid dye from effluent using natural adsorbents – I. Peat, Wat. Res., 10 (1976) 1061-1066.
- [29] Pradhan S., Singh S., Rai L.C., Characterization of various functional groups present in the capsule of Microcystis and study of their role in biosorption of Fe, Ni and Cr, Bioresour. Technol., 98 (2007) 595-601.
- [30] Rahman M.S., Islam M.R., Effects of pH on isotherms modeling for Cu(II) ions adsorption using maple wood sawdust, Chem. Eng. J., 149 (2009) 273-280.
- [31] Ramirez C.M., Pereira da Silva M., Ferreira L.S.G., Vasco E.O., Mathematical models applied to the Cr(III) and Cr(VI) breakthrough curves, J. Hazard. Mater., 146 (2007) 86-90.

- [32] Ramrakhiani L., Majumder R., Khowala S., Removal of hexavalent chromium by heat inactivated fungal biomass of *Termitomyces clypeatus*: Surface characterization and mechanism of biosorption, Chem. Eng. J., 171 (2011) 1060–1068.
- [33] Ruthven D.M., Principles of adsorption and adsorption processes, John Wiley & Sons (1984).
- [34] Sips R., On the structure of a catalyst surface, Journal of Chem. Phys., 16 (1948) 490–495.
- [35] Tobin J.M., White C., Gadd G.M., Metal accumulation by fungi: applications in environmental biotechnology, J. Ind. Microbiol., 13 (1994) 126–130.
- [36] Vijayaraghavan K., Jegan J., Palanivelu K., Velan M., Batch and column removal of copper from aqueous solution using a brown marine alga *Turbinaria ornate*, Chem. Eng. J., 106 (2005) 177–184.
- [37] Vijayaraghavan K., Jegan J., Palanivelu K., Velan M., Removal of nickel(II) ions from aqueous solution using crab shell particles in a packed bed up-flow column, J. Hazard. Mater., 113 (2004) 223–30.
- [38] Volesky B., Sorption and Biosorption, BV-Sorbex, Inc., St.Lambert, Quebec. (2003a).
- [39] Volesky B., Biosorption process simulation tools, Hydrometallurgy, 71 (2003b) 179–190.
- [40] Volesky B., Weber J., Park J.M., Continuous-flow metal biosorption in a regenerable Sargassum column, Water Res., 37 (2003) 297–306.
- [41] Weber W.J., McGinley P.M., Katz L.E., Sorption phenomena in subsurface systems: Concepts, models and effects on contaminant fate and transport, Water Res., 25 (1991) 499–528.



- [42] Weber W.J., Morris J. C., Kinetics of adsorption on carbon from solution, J. Sanitary Eng. Div., 89, 2 (1963) 31-60.
- [43] Yu B., Zhang Y., Shukla A., Shukla S.S., Dorris K.L., The removal of heavy metal from aqueous solutions by sawdust adsorption — removal of copper, J. Hazard. Mater., 80 (2000) 33–42.
- [44] Yu L.J., Shukla S.S., Dorris K.L., Shukla A., Margrave J., Adsorption of chromium from aqueous solutions by maple sawdust, J. Hazard. Mater., 100 (2003) 53–63.

## **Chapter 5**

### **Evaluation and Selection of Biosorbents Based on the Use of Langmuir Isotherm**

## **Abstract**

Evaluating and comparing metal adsorption performance of different biosorbents in terms of their metals capacities and relative affinity to metals are important for selecting an adsorbent for large scale application. Majority of the biosorption equilibrium data have shown to be well-represented by Langmuir isotherm model. However, there are conflicting reports in the literature on the use and interpretation of the Langmuir model constants as a measure of selecting the most appropriate biosorbent. We aim to address this issue in this critical review. Dimensionless metal uptake  $\theta$  was used to better describe the Langmuir constants based on a dynamic equilibrium between the sorbate and biomass active sites for adsorption.

## **5.1. Introduction**

Quantifying biomass-metal interactions is essential for biosorbents comparisons in adsorbing metals. Like any other adsorbate-adsorbent systems, isotherms are regularly used to describe the metal biosorption data. Among them, Langmuir model (Langmuir, 1918) is commonly used by many researchers, and the adsorption equilibrium of metal ions is usually very well-described by this model. However, the challenge lies with identifying the most desirable biosorbents based on the information obtained from the Langmuir adsorption isotherm.

The biosorption performance comparisons can be accomplished in two ways: 1) which biosorbent is a better adsorbent for a selected metal; and 2) what is the relative performance of a biosorbent in adsorbing different types of metals (e.g. one biosorbents, different types of metals). The Langmuir isotherm is frequently applied to answer these two questions.

The essential assumption in Langmuir model which sets it apart from other equilibrium models is that a monolayer of adsorbate covers the surface of the adsorbent. Other assumptions are: each adsorption site accepts only one molecule, all

sites are energetically equivalent, and that there are no interactions between the sorbed molecules (Give references, although known). The mathematical expression of Langmuir equation is:

$$q = q_{\max} \frac{bC_e}{1 + bC_e} \quad (1)$$

where,  $q$  is the equilibrium value of metal uptake (mg metal/ g biosorbents),  $q_{\max}$  the total number of binding sites available for biosorption (mg/g),  $C_e$  equilibrium or unadsorbed metal ion concentration in solution (mg/l), and  $b$  is the Langmuir model constant, which is often called affinity coefficient. Langmuir sorption model was originally derived for adsorption of gases to activated carbon (Langmuir, 1918) and is based on simplistic assumptions, such as finite number of homogeneous binding sites with uniform affinity for adsorption to take place, which seems to be unrealistic for a biosorption system, where both physical and chemical sorption and ion-exchange may occur. Nevertheless, biosorption data usually fit the Langmuir model with a high rate of accuracy as can be seen with numerous publications in the field.

Generally, according to Langmuir model, a good adsorbent has a high number of monolayer sorption sites denoting a highest achievable metal adsorptive capacity,  $q_{\max}$  (mg / g), at a given environmental condition. This is known as the saturation isotherm plateau as shown in Figure 5.1. The Langmuir coefficient  $b$  is known to be a measure of bonding affinity between adsorbate and adsorbents. This concept is directly applied to biosorption systems.

Many studies reported the lowest values of  $b$  as an indicator of the highest affinity between the biosorbent and the metals (Kratochvil and Volesky, 1998; Jalili et al., 2002; Volesky, 2003; Qaiser et al., 2007; Narasimhulu and Rao, 2009; Shetty and Rajkumar, 2009; Patil and Shrivastava, 2010; Dawodu et al., 2012; Akpomie et al., 2013; Amegrissi et al., 2013). On the other hand, several other publications, reported

that a good biosorbent should have a higher value of  $b$  (Donmez et al., 1999; Sag and Kutsal, 2000; Aksu, 2001; Lodeiro et al., 2005; Aksu and Dönmez, 2006; Zhou et al., 2009; Vijayaraghavan and Yun, 2008; Naeem et al., 2009; Liu et al. 2009; Bertagnolli et al., 2014). Furthermore, there is uncertainty as to the possible physical meaning of this constant that could be used to quantify the metal-biomass affinity.

Other studies by Volesky's group (Davis et al., 2003; Davis et al., 2000) quantified the biomass-metal interactions using the Langmuir constant  $b$ , where higher  $b$  values indicated higher metal affinity. Vijayaraghavan et al. (2005) used a corrected definition of a steep initial isotherm slope (e.g. high  $b$ ) to characterize biosorbents performances, whereas Kratochvil and Volesky (1998) have used the opposite definition of  $b$ .

The main aim of this study is to offer an accurate interpretation of the shape of the Langmuir biosorption isotherm at a wide range of equilibrium sorbate (metal) concentrations used for biomass selection by quantifying and contrasting the performance of different biosorbents.

## 5.2. Discussion

As described earlier, the adsorption isotherm models, such as Langmuir model, have been widely used to determine the performance of an adsorbent. However, Kratochvil and Volesky (1998) demonstrated that this approach may not be relevant unless the equilibrium metal concentration is known (under the same environmental conditions). In other words, to predict different biosorbents behaviour with respect to a model metal, the sorption capacity ( $mg / g$ ) of biosorbents for the metal must be compared only at the same metal equilibrium concentrations.

Figure 5.1 shows the Langmuir isotherm plots for four different hypothetical biosorbents with the same maximum adsorption capacity of 100 mg/g for a metal. Different values of Langmuir constant  $b$  are presented by varying initial slope of the

adsorption isotherms. The biosorbent with lowest  $b$  (0.01 l/mg) represents a gradual increase in metal uptake by increasing metal equilibrium concentration until reaching the maximum adsorption capacity. By increasing the  $b$  values from 0.01 to 5 l/mg, the initial slope of the isotherm curve becomes steeper, where at  $b = 5$ , the maximum uptake capacity is reached at very low metal equilibrium concentrations.

Comparing the plots for the highest and lowest values of  $b$  in Figure 5.1, it can be inferred that biosorbents with higher  $b$  values (e.g.  $b > 0.5$  l/mg) reach to the full saturation metal capacity  $q_{\max}$  (100 mg/g in this example) at lower equilibrium metal concentrations ( $C_e < 50$  mg/l), whereas biosorbents with lower  $b$  values ( $b < 0.5$  l/mg) reach to  $q_{\max}$  at much higher residual metal concentrations.

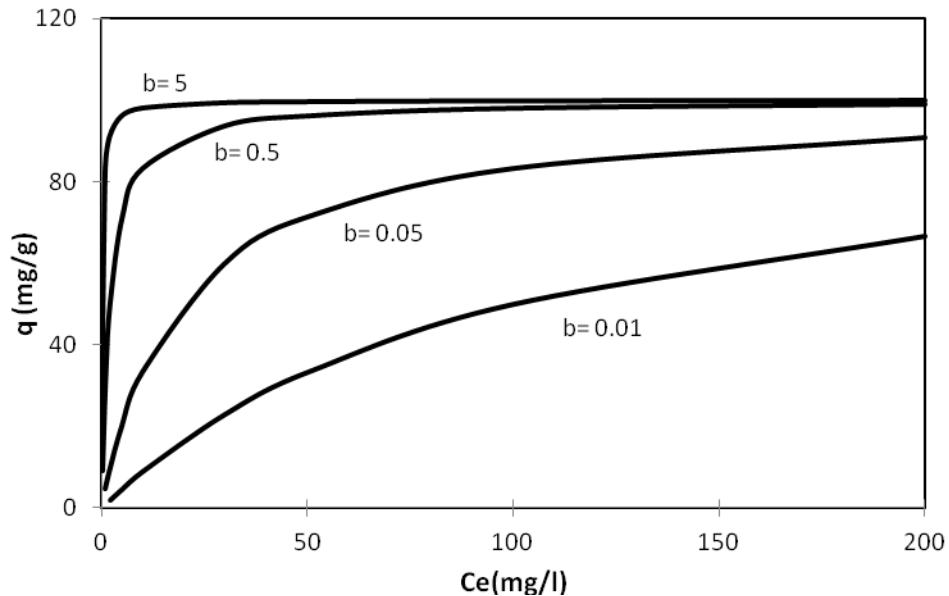


Fig. 5.1. Langmuir equation plots of metal uptake  $q$  versus equilibrium metal concentration with varying coefficient  $b$  (0.01 – 5 l/mg) and constant  $q_{\max} = 100$  mg/g.

Therefore, deduced from the Langmuir model's underlying assumptions, biosorbents with constant  $q_{\max}$  and higher  $b$  values have higher efficiencies in adsorbing metals as their adsorption sites on the biomass surface are easily accessible. Nevertheless,

Langmuir equation does not offer any mechanisms for adsorption of metals and it is just reflecting on the experimental data.

As shown in Figure 5.1, when  $b$  is low ( $b < 0.05$  l/mg),  $q_{\max}$  may not be well-defined as extrapolation is needed to obtain  $q_{\max}$  if a limited range of experimental data is available (e.g. limited metal concentrations tested).

Figure 5.2 shows the Langmuir isotherm curves generated by using Eq.(1) for different hypothetical biosorbents with varying maximum metal capacity  $q_{\max}$ , but the same Langmuir constant of  $b = 0.05$  l/mg. The graph also depicts the performance of a single biosorbent for different types of metals. It is obvious that the biosorbent with highest possible  $q_{\max}$  is desirable as it represents the practical limiting amount of sorbate that can be adsorbed per unit mass of biosorbent ( $mg$  metal/  $g$  biomass) where the adsorption sites on the biomass surface is fully covered by the metals.

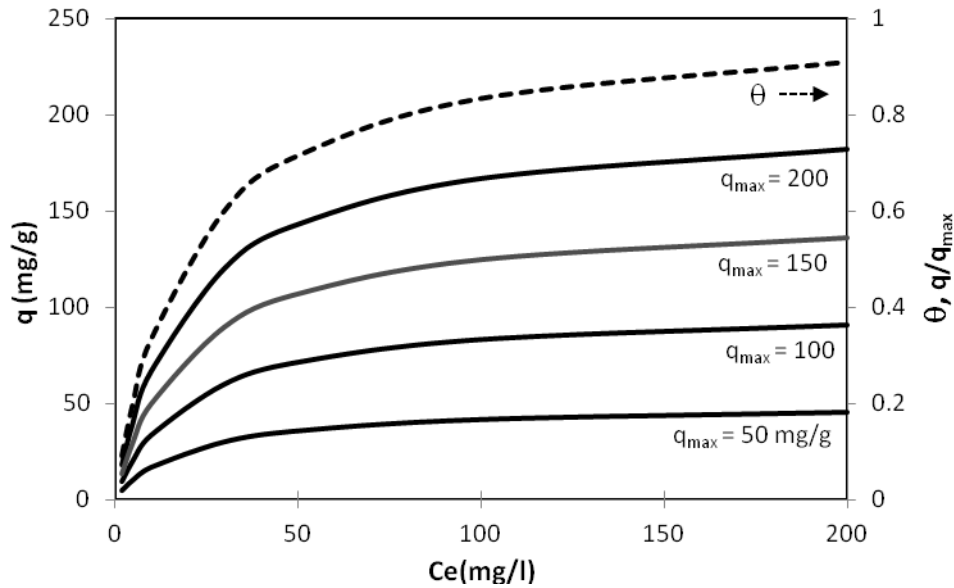


Fig. 5.2. Langmuir isotherm model plots for hypothetical biosorbents with constant  $b$  (0.05 l/mg) and varying  $q_{\max}$  (50 – 200 mg/g). The dashed line values shown on the

secondary vertical axis is the dimensionless metal uptake  $\theta$ , which overlaps for all range of  $q_{\max}$  (50 – 200 mg/g).

One interesting point in Figure 5.2 is that, although all four biosorbents have different practical max capacity for the metal, their dimensionless metal uptakes,  $\theta = q/q_{\max}$  values, surface coverage fractions, are exactly the same for all the biosorbents for the same equilibrium metal concentration. Surface coverage degree is the surface occupied with metal over total surface available for metal adsorption. Therefore, when the Langmuir constant  $b$  values are the same for different biosorbents, their dimensionless uptake capacity is constant regardless of having different maximum adsorption capacities. This implies that they have similar degree of affinity for the sorbate (metal).

### 5.2.1. Derivation of Langmuir Equation Constant

To better understand the Langmuir equation and its applicability in modeling of biosorption processes it is necessary to examine what happens when a biosorbent is brought into contact with metal solution. Unlike the Freundlich empirical equation, the Langmuir equation is based on the theoretical principle that sorbates are chemically/physically adsorbed on the adsorbent surface at a fixed number of vacant adsorption sites (Sag and Kutsal, 1995), and there is a dynamic equilibrium between the adsorbed and un-adsorbed species,



where  $k_{ads}$  is the equilibrium constant for forward reaction and  $k_{des}$  represents equilibrium constant for backward reaction,  $M^+$  is the un-adsorbed metal or sorbate, and  $B^-$  represents the biosorbent or unoccupied binding site, and  $MB$  is the adsorbed metal. At equilibrium, rates of forward and backward reactions are equal, and therefore the equilibrium constant  $K$  can be calculated based on the kinetic theory,

$$\text{Forward reaction rate} = k_{ads}[M^+][B^-] \quad (3)$$



$$\text{Backward reaction rate} = k_{des}[MB] \quad (4)$$

At equilibrium,

$$K = \frac{[MB]}{[M^+][B^-]} = \frac{k_{ads}}{k_{des}} \quad (5)$$

where  $[B^-]$  is the empty binding site concentration,  $[M^+]$  bulk concentration of sorbate,  $[B_0]$  total binding sites available, which defines the maximum adsorption capacity,  $q_{\max}$ , and  $[MB]$  is the amount of metal retained by the biomass at equilibrium, which is equilibrium adsorption capacity  $q$ . Thus,  $[B^-]$  will be equal to  $q_{\max} - q$  (the number of unoccupied sites at equilibrium),

$$[B_0] = [B^-] + [MB] = \text{constant} = q_{\max} \quad (6)$$

$$[B^-] = q_{\max} - q \quad (7)$$

As defined above, to derive Langmuir equation, we use the surface coverage fraction,  $\theta$ , and the fraction of surface unoccupied by sorbate as ' $1 - \theta$ '. Using Eqs. (6) and (7), we have,

$$\theta = \frac{q}{q_{\max}} = \frac{[MB]}{[B_0]} \quad (8)$$

$$1 - \theta = \frac{q_{\max} - q}{q_{\max}} = \frac{[B^-]}{[B_0]} \quad (9)$$

According to Eq.(6) at equilibrium,

$$k_{ads}[M^+][B^-] = k_{des}[MB] \quad (10)$$

By dividing both sides of Eq.(10) by  $[B_0]$ , and using Eq.(5) we get,

$$K \frac{[M^+][B^-]}{[B_0]} = \frac{[MB]}{[B_0]} \quad (11)$$

Using Eqs.(8) and (9), Eq.(11) becomes,

$$K[M^+](1-\theta) = \theta \quad (12)$$

Now, we can solve Eq.(12) to write it in terms of  $\theta$ ,

$$K[M^+] = K[M^+]\theta + \theta \quad (13)$$

$$K[M^+] = \theta(1 + K[M^+]) \quad (14)$$

$$\theta = \frac{K[M^+]}{1 + K[M^+]} \quad (15)$$

Eq.(15) is the same as Langmuir isotherm expression given by Eq.(1), where  $[M^+]$  is equal to  $C_e$  or bulk concentration of sorbate, and  $K$  is the adsorption-desorption equilibrium constant  $k_{ads} / k_{des}$  defined by Eq.(5). Comparing Eqs.(1) and (15), we can conclude that this is actually the Langmuir equation constant  $b$ ,

$$b = \frac{k_{ads}}{k_{des}} \quad (16)$$

Similar definition for the Langmuir rate constant  $b$  has been reported elsewhere by Chong and Volesky (1995) and Lee (2014) as well. Therefore, according to Eq.(16), higher values of  $b$  is associated with higher values of  $K$  or higher ratio of the adsorption rate constant to desorption rate constant; and thus, the biosorbent has higher

affinity to adsorption of metals. Langmuir model has also been reported using dissociation coefficient ( $K_d = 1/K$ ) in the following form (Lu et al., 2006),

$$q = \frac{q_{\max} C_e}{K_d + C_e} \quad (17)$$

Figure 5.3 shows the isotherm plots of the biosorbents  $A, B, C$  and  $D$  in contact with metal solutions at different equilibrium concentrations, and compares the cases that selected biosorbents have not yet reached their full saturation capacity in a biosorption experiment. In such cases, biosorption performance needs to be compared at  $q$  values less than  $q_{\max}$  ( $\theta < 1$ ).

The answer to the question that “which biosorbent should be selected” depends on what we want to achieve in a biosorption process. If interest is in reaching highest practical metal removal capacity, then the biosorbent with the highest values of  $q_{\max}$  should be chosen, and the favorable biosorbents in Figure 5.3 would be in the order of  $C > D > B > A$ .

However, if biosorbent selection criterion is the adsorption performance in terms of level of metal uptake capacity  $q$ , where the surface saturation of metals has not yet reached, the judgement should be at the same metal equilibrium concentrations for all biosorbents (e.g. vertical lines in Figure 5.3). For instance, at  $q_{150}$ , the sequence of the best biosorbent order is the same as those of  $q_{\max}$ . But, for  $q_{60}$ , the favourability sequence would be  $D > C > B > A$ . At  $q_{30}, q_{20}, q_5$ , the desirable biosorbent sequences would be  $D > B > C > A$ ,  $D > B > A > C$ ,  $D > A > B > C$ , respectively.

Therefore, if the goal in biosorbent selection is to achieve highest possible metal uptake irrespective of final residual metal concentration, the biosorbent with highest  $q_{\max}$  should be selected regardless of the  $b$  values. On the contrary, if only the residual

metal concentration in the solution after biosorption is important (e.g. environmental application for regulatory compliance of the metal concentration in effluents), the selected biosorbent should have a high  $q_{\max}$  as well as a high  $b$ .

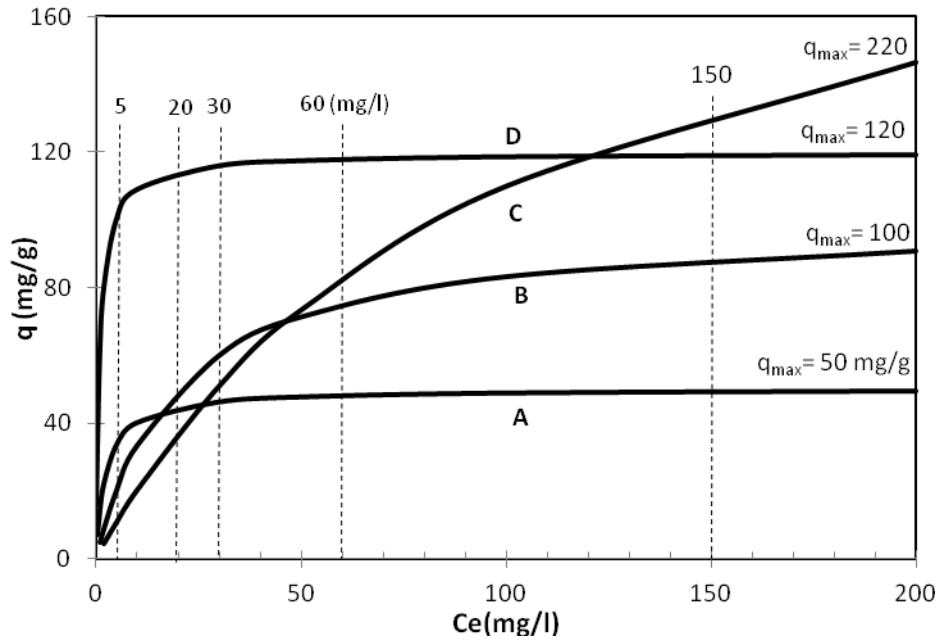


Fig. 5.3. Performance comparisons of 4 biosorbents in different residual metal concentrations where some biosorbents have not reached their full saturation ( $\theta < 1$ ).

Lodeiro et al. (2005) studied the ability of five different brown seaweeds to remove cadmium from aqueous solutions and their equilibrium data fitted well with the Langmuir model. The Langmuir isotherm constants were estimated to compare the metal adsorption performances of algae (Figure 5.4). As shown in Table 5.1, the lowest and highest values of  $q_{\max}$  correspond to *L. ochroleuca* and *S. polyschides*, respectively (64 and 95 mg/g), whereas *S. polyschides* had the lowest  $b$  value.

The maximum sorption capacity followed *S. polyschides* > *A. nodosum* > *P. caniculata* > *B. bifurcata* > *L. ochroleuca*; however, the Langmuir affinity constant  $b$  followed a different order: *A. nodosum* > *P. caniculata* > *L. ochroleuca* > *B. bifurcata* > *S. polyschides* conforming to the initial slopes of isotherm curves in Figure 5.4. Nevertheless, in low cadmium equilibrium concentration of 10 mg/l, *A. nodosum*,

which has the maximum value of  $b$ , showed the highest cadmium uptake ( $q_{10} = 38$  mg/g) followed by *P. caniculata* (32 mg/g).

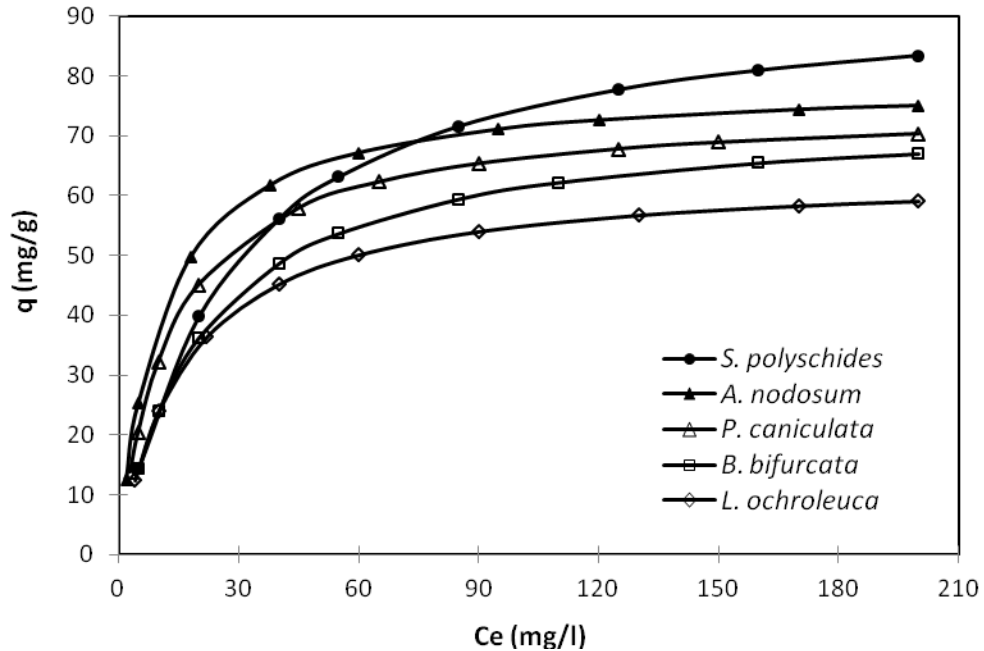


Fig. 5.4. Cadmium equilibrium fitted to Langmuir isotherm for five types of algae (2.5 g/l). Data adopted from Lodeiro et al. (2005).

The lowest  $q_{10}$  belonged to *B. bifurcata* (24 mg/g), as opposed to the order of biosorbents compared at the uptake values in higher metal equilibrium concentrations ( $q_{200}$  and  $q_{\max}$ ). Therefore, depending on the process goals for cadmium removal, the desirable biosorbent choices can differ amongst the 5 Algae biosorbents shown in Figure 5.4.

While many investigators have used Langmuir adsorption constant  $b$  as a measure of affinity of biosorbents for metals, there is a large number of publications on biosorption, in which a dimensionless number,  $R_L$ , referred to as separation factor or dimensionless equilibrium parameter, was derived based on the Langmuir constant  $b$  to work out the degree of favorability of the metals to biosorbents.

Table 5.1. Langmuir model parameters for Cd adsorption by 4 types of algae reproduced from Lodeiro et al. (2005).  $q_{10}$  and  $q_{200}$  are equilibrium uptake values at 10 and 200 mg/l Cd, respectively.

$q_{10}$		Algae	$q_{200}$	$q_{\max}$	$b$	
Algae	(mg/g)		(mg/g)	(mg/g)	Algae	(L/mg)
<i>A. nodosum</i>	38	<i>S. polyschides</i>	83	95	<i>A. nodosum</i>	0.094
<i>P. caniculata</i>	32	<i>A. nodosum</i>	75	79	<i>P. caniculata</i>	0.075
<i>S. polyschides</i>	25	<i>P. caniculata</i>	70	75	<i>L. ochroleuca</i>	0.06
<i>L. ochroleuca</i>	25	<i>B. bifurcata</i>	67	74	<i>B. bifurcata</i>	0.048
<i>B. bifurcata</i>	24	<i>L. ochroleuca</i>	60	64	<i>S. polyschides</i>	0.036

Hall et al. (1966) introduced the factor  $R_L$  for the first time, which was based on the Langmuir isotherm constant  $b$  and the initial metal concentration  $C_0$  to identify the favorable adsorption process,

$$R_L = \frac{1}{1 + bC_0} \quad (18)$$

Eq. (18) was used by Kiran et al. (2006), Chen and Wang (2010), Ahmad and Rahman (2011), Meitei and Prasad (2013), Gorgulu Ari and Celik (2013) and several other researchers to predict whether a sorption system is favourable ( $0 < R_L < 1$ ), or unfavourable ( $R_L > 1$ ). However, since  $b$  and  $C_0$  are both positive numbers (e.g. negative experimental values of  $b$  may imply that adsorption equilibrium data do not conform to a Langmuir isotherm), the  $R_L$  values seem to be always less than 1 ( $R_L < 1$ ) since  $1 + bC_0 > 1$ . Therefore, from Eq. (18), we can only come to the conclusion that the lower the  $R_L$  values ( $R_L \rightarrow 0$ ) the more favorable metal biosorption process is.

### 5.2.2. Estimation of biosorption thermodynamics by Langmuir isotherm constant

The Langmuir constant  $b$  has also been used by some researchers, such as Tewari et al, 2005; Kiran et al., 2006; Padmavathy, 2008, to calculate the thermodynamic parameters associated to metal-biosorbent interaction processes. The rate of adsorption and desorption in Eq.(2) are related to the energy of adsorption and desorption through the Arrhenius equation (Chong and Volesky, 1995). The Gibbs free energy change  $\Delta G$  is the activation energy differences of adsorption-desorption reaction equilibrium. The relation between  $\Delta G$  and the biosorption reaction constant  $K$  in Eq.(2) is given by the following equation,

$$\Delta G = -RT \ln K \quad (19)$$

with  $R$  being the gas constant and  $T$  is the temperature. The dependence of the equilibrium constant  $K$  to temperature can be used to determine the biosorption thermodynamic parameters using following equations,

$$\Delta G = \Delta H - T\Delta S \quad (20)$$

As shown in Eq. (16),  $K$  corresponds to Langmuir constant  $b$ ,

$$-RT \ln b = \Delta H - T\Delta S \quad (21)$$

$$\text{or } \ln b = -\frac{\Delta H}{R} \frac{1}{T} - \frac{\Delta S}{R} \quad (22)$$

The slope and intercept of the plot of  $\ln b$  vs.  $1/T$  give  $\Delta H$  and  $\Delta S$  values, respectively. Entropy decreases during the biosorption as the metal ions are being adsorbed on the solid surface from the aqueous solution ( $\Delta S < 0$ ). Negative Enthalpy of biosorption reaction ( $\Delta H < 0$ ) suggests that the biosorption process is exothermic

and thermodynamically plausible, and the negative values of  $\Delta G$  also implies that the biosorption of metals occurs spontaneously.

### 5.3. Conclusions

Although Langmuir model was originally derived based on adsorption of gases to activated carbon using simplistic assumptions, it has been widely used for modeling of complex biosorption processes as the metal adsorption equilibrium data shown to usually conform to it without describing any specific adsorption mechanism. In this study, Langmuir equation was characterized based on dynamic equilibrium between adsorbed and un-adsorbed metal ions, and the Langmuir equilibrium constant  $b$  was shown to be the ratio of the adsorption/desorption rates; therefore, the higher the  $b$  values of an adsorbent-adsorbate, the better the adsorption rate.

It seems that most of the papers using wrong interpretation of Langmuir constant have used the Kratochvil and Volesky (1998) as their reference, in which low values of  $b$  are connected with a desirable high affinity (or steep initial slopes of Langmuir isotherm curves), without attending this group's succeeding works (Davis et al., 2003; Davis et al., 2000) with corrected definition of Langmuir parameters.

The shape of the Langmuir isotherm curves was used to compare the biosorptive performance of different biosorbents when exposed to metal solutions. A high value of  $b$  was shown to be an indicator of strong bonding between the metal and biomass, but its magnitude solely did not provide sufficient and reliable information to select a highly desirable biosorbent for metal removal as it is rather a fitting parameter than an adsorption constant. The quality of a biosorbent is mainly judged based on  $q$  values which was defined as how much adsorbate could be practically adsorbed and retained at a given equilibrium metal concentration where the surface coverage fraction was less than 1 ( $\theta < 1$ ). This could be delineated by the Langmuir parameter  $q_{\max}$  when all active sites available on the biomass surface for metal adsorption are saturated with metal ions ( $\theta = 1$ ). Selection criteria in general for the most appropriate biosorbent could vary based on the application of the biosorbent and the process priorities, e.g. if



the priority is to reduce the effluent metal level to a standard range before being discharged to the environment, large values of  $b$  and  $q_{\max}$  are desirable.

## 5.4. Acknowledgements

This work was supported by individual NSERC Discovery Grants awarded to Dr. A. Margaritis and Dr. M.B. Ray.

## 5.5. References

- [1] Ahmad M.A., Rahman N.K., Equilibrium, kinetics and thermodynamic of Remazol Brilliant Orange 3R dye adsorption on coffee husk-based activated carbon, Chem. Eng. J., 170 (2011) 154–161.
- [2] Akpomie G.K., Abuh M.A., Obi N.D., Nwafor E.C., Ekere P. O., Onyiah I. M., Modelling on the equilibrium, kinetics and thermodynamics for zinc (II) ions removal from solution by “Aloji” Kaolinite clay, Int. J. Basic Appl. Sci., 2, 1, (2013) 173-185.
- [3] Aksu Z., Biosorption of reactive dyes by dried activated sludge: equilibrium and kinetic modeling, Biochem. Eng. J., 7 (2001) 79–84.
- [4] Aksu Z., Dönmez G., Binary biosorption of cadmium(II) and nickel(II) onto dried *Chlorella vulgaris*: Co-ion effect on mono-component isotherm parameters, Process Biochem., 41 (2006) 860–868.
- [5] Amegrissi F., Maghri I., Elkouali M., Kenz A., Salouhi M., Talbi M., Heavy metal uptake by agro based waste materials, Global J. Sci. Front. Res. (Environ. Earth Sci.) 13, 4 (2013) 1-5.
- [6] Bertagnolli C., da Silva M.G.C., Guibal E., Chromium biosorption using the residue of alginate extraction from *Sargassum filipendula*, Chem. Eng. J., 237 (2014) 362–371.

- [7] Chong K. H., Volesky B., Description of Two-Metal Biosorption Equilibria by Langmuir-Type Models, *Biotechnol. Bioeng.*, 47 (1995) 451-460.
- [8] Davis T.A., Volesky B., Vieira R.H.S.F., *Sargassum* seaweed as biosorbent for heavy metals. *Water Res.* 34, 17 (2000) 4270–4278.
- [9] Davis T.A., Volesky B., Mucci A., A review of the biochemistry of heavy metal biosorption by brown algae, *Water Res.*, 37 (2003) 4311–4330.
- [10] Dawodu F.A., Akpomie G.K., Ogbu I.C., Isotherm Modeling on the Equilibrium Sorption of Cadmium (II) from Solution by Agbani Clay, *Int. J. Multidisc. Sci. Eng.*, 3, 9 (2012), 9-14.
- [11] Donmez G.C., Aksu Z., Ozturk A., Kutsal T., A comparative study on heavy metal biosorption characteristics of some algae, *Process Biochem.* 34 (1999) 885 – 892.
- [12] Gorgulu Ari A., Celik S., Biosorption potential of Orange G dye by modified *Pyracantha coccinea*: Batch and dynamic flow system applications, *Chem. Eng. J.*, 226 (2013) 263–270.
- [13] Jalili R., Ghafourian H., Asef Y., Davarpanah S.J., Sepehr S., Removal and recovery of lead using nonliving biomass of marine algae., *J. Hazard. Mater.*, 2002, 92, 3 (2002) 253-262.
- [14] Hall K.R., Eagleton L.C., Acrivos A., Vermeulen T., Pore-and solid-diffusion kinetics in fixed-bed adsorption under constant-pattern Conditions, *Ind. Eng. Chem. Fundamen.*, 5, 2 (1966) 212–223.
- [15] Kiran I., Akar T., Ozcan A.S., Ozcan A., Tunali S., Biosorption kinetics and isotherm studies of Acid Red 57 by dried *Cephalosporium aphidicola* cells from aqueous solutions, *Biochem. Eng. J.*, 31 (2006) 197–203.
- [16] Kratochvil D., Volesky B., Advances in the biosorption of heavy metals, Review Article, *Trends Biotechnol.*, 16, 7, 1 (1998) 291-300.

- [17] Langmuir I., The adsorption of gases on plane surface of glass, mica and platinum, J. Am. Chem. Soc., 40 (1918) 1361 – 1403.
- [18] Lee H.S., Two Metal Biosorption of Chromium and Copper by Ca-Loaded *Laminaria japonica* Biomass, Biotechnol. Bioprocess Eng., 19 (2014) 696-702.
- [19] Liu Y., Cao Q., Luo F., Chen J., Biosorption of  $\text{Cd}^{2+}$ ,  $\text{Cu}^{2+}$ ,  $\text{Ni}^{2+}$  and  $\text{Zn}^{2+}$  ions from aqueous solutions by pretreated biomass of brown algae, J. Hazard. Mater., 163 (2009) 931–938.
- [20] Lodeiro P., Cordero B., Barriada J.L., Herrero R., Sastre de Vicente M.E., Biosorption of cadmium by biomass of brown marine macroalgae, Bioresour. Technol., 96 (2005) 1796–1803.
- [21] Lu W.B., Shi J.J., Wang C.H., Chang J.S., Biosorption of lead, copper and cadmium by an indigenous isolate *Enterobacter sp.* J1 possessing high heavy-metal resistance, J. Hazard. Mater., B134 (2006) 80–86.
- [22] Meitei M.D., Prasad M.N.V., Lead (II) and cadmium (II) biosorption on *Spirodela polyrhiza* (L.) Schleiden biomass, J. Environ. Chem. Eng., 1 (2013) 200–207.
- [23] Naeem A., Saddique M.T., Mustafa S., Tasleem S., Shah K.H., Waseem M., Removal of  $\text{Co}^{2+}$  ions from aqueous solution by cation exchange sorption onto NiO, J. Hazard. Mater., 172 (2009) 124–128.
- [24] Narasimhulu K., Rao P.S., Studies on removal of toxic metals from waste water using *pseudomonas* species, ARPN J. Eng. Appl. Sci., 4, 7 (2009) 58-63.
- [25] Padmavathy V., Biosorption of nickel(II) ions by baker's yeast: Kinetic, thermodynamic and desorption studies, Bioresour. Technol., 99 (2008) 3100–3109.
- [26] Patil A. K., Shrivastava V.S., Removal of Cu(II) Ions by *Leucaena Leucocephala* (Subabul) Seed Pods from Aqueous Solutions, E-J. Chem., (2010), 7(S1) 377-385.

- [27] Qaiser S., Saleemi A.R., Ahmad M.M., Heavy metal uptake by agro based waste materials, *Electron. J. Biotechnol.*, 10, 3 (2007) 409-416.
- [28] Sag Y., Kutsal T., Biosorption of heavy metals by *Zoogloea ramigera*: use of adsorption isotherms and a comparison of biosorption characteristics, *Chem. Eng. J.*, 60 (1995) 181-188.
- [29] Sag Y., Kutsal T., Determination of the biosorption heats of heavy metal ions on *Zoogloea ramigera* and *Rhizopus arrhizus*, *Biochem. Eng. J.*, 6 (2000) 145–151.
- [30] Shetty, R. and Rajkumar, Sh., Biosorption of Cu (II) by Metal Resistant *Pseudomonas sp.*, *Int. J. Environ. Res.*, 3, 1 (2009) 121-128.
- [31] Tewari N., Vasudevan P., Guha B.K., Study on biosorption of Cr (VI) by *Mucor hiemalis*, *Biochem. Eng. J.*, 23 (2005) 185-192.
- [32] Vijayaraghavan K., Jegan J., Palanivelu K., Velan M., Batch and column removal of copper from aqueous solution using a brown marine alga *Turbinaria ornate*, *Chem. Eng. J.*, 106, 2 (2005) 177–184.
- [33] Vijayaraghavan K, Yun Y.S., Bacterial biosorbents and biosorption, 26, 3 (2008) 266–291.
- [34] Zhou Y.T., Branford-White C., Nie H.L, Zhu L.M., Adsorption mechanism of  $\text{Cu}^{2+}$  from aqueous solution by chitosan-coated magnetic nanoparticles modified with  $\alpha$ -ketoglutaric acid, *Colloids Surf., B* 74, 1 (2009) 244–252.

## **Chapter 6**

### **Conclusions and Recommendations**

## 6.1. Conclusions

The adverse effects of heavy metals on human and environmental health are well known. Water quality and biological community in surface water are being affected by thousands of tons of toxic metals every year released by polluting industries. In the light of searching for effective, low-cost, and easily available alternative adsorbent for metal removal, the use of waste maple leaves and cells of *S. cerevisiae* was proposed and tested in batch and continuous systems.

The main conclusions drawn from this thesis are:

- Biosorbents used in this research showed external large surface areas with intrinsic functional groups which provided mass transfer of toxic metal ions from aqueous solutions to their surfaces due to chemical, physical and biochemical metal-biomass interactions in batch and continuous biosorption processes.
- Easy restoration of metals from the biomass after contact with weak acid suggested the adsorption of the metal ions onto the binding sites at the biomass surfaces is reversible.
- Although the continuous bioreactor-biosorption system had its own drawbacks (e.g. mass flowrate of biosorbent limited by growth rate of cells and long separation times), it was unique in showing that combined (on-line) biomass generation and metal biosorption is practical.
- This study confirmed that yeast cells are very efficient in removing  $\text{Pb}^{2+}$  ions from lead-bearing solutions with a capacity of adsorbing more than 98% of  $\text{Pb}^{2+}$  in optimum conditions. Removal efficiencies of  $\text{Cu}^{2+}$  and  $\text{Zn}^{2+}$  reached around 55% and 60%, respectively in the studied environmental conditions. In ternary metal system, yeast cells retained its overall metal uptake capacity,

although, a slight increase in  $\text{Pb}^{2+}$  ions uptake and a slight reduction in  $\text{Zn}^{2+}$  and  $\text{Cu}^{2+}$  ions uptake occurred.

- The yeast biomass used in this study was obtained from aerobic cultures and collected from the log phase of their growth. In all experiments, more than 90% of the adsorption capacity reached within first minutes of adsorption, which was an indication of fast adsorption kinetics, and the equilibrium data exhibited a good fit to Langmuir adsorption model.
- The yeast cells produced in the continuous bioreactor system provided continuously fresh surface for adsorption of the metals without the need for costly pretreatment steps, such as harvesting, separating, heat-killing, drying, and storage of biomass.
- The biosorbents tested in this study did not undergo any chemical or physical alterations, making them suitable for removal of metals from wastewaters. Other realistic aspects, such as employing continuous-flow biosorption systems, testing the removal of mixture of metals, using locally abundant biosorbents, combining living and non-living microbial biosorbents, and regenerating the used biomass, were addressed and tested in this research project as a step forward in improving the applicability of biosorption technology.
- Biosorption of heavy metals was a highly pH-dependent process, and pH control was imperative during the adsorption process to ensure that biosorption was the only mechanism responsible for metal removal.
- Surface adsorption, ion exchange, chemisorption, complexation, and interparticle sequestration were found responsible mechanisms in biosorption of metal ions in the tested biosorbents.

- Waste maple tree leaves were used in multiple sorption-desorption cycles without reduction in their sorption efficiency due to easy and highly efficient regeneration for multiple reuse, offering the metal recovery possibility from low-volume and high-concentration wash solutions.

Research performed in this work can serve as a potential incentive for promoting biosorption as a promising alternative to conventional metal treatment methods.

## **6.2. Recommendations for Future Work**

Biosorption is gaining increasing attention as a promising metal remediation method. More work is needed to improve our understanding of biosorption process, its complex mechanism, and its applicability in large-scale systems. The following recommendations are made for future work:

- In this study we found that using a continuous system for simultaneous production of yeast biomass and biosorption of metals by the produced biomass within the same system is possible. A waste stream containing necessary food source and nutrients can be used to cultivate the biosorbents, thereby reducing the environmental footprint of the process by resource recovery and waste reduction.
- The results of this research project showed that the yeast cells adsorb  $\text{Pb}^{2+}$  ions more than copper and zinc ions both in single and multi-metal solutions. We found a promising  $\text{Pb}^{2+}$  biosorption potential for yeast cells, which was quite encouraging to be tested in pilot-scale continuous systems using real industrial wastewater.
- The challenge of applying yeast biomass for continuous removal of heavy metals in this work lied with the efficient separation of metal-loaded biomass from the solution. The biotechnological application of continuous metal biosorption by yeast would be possible if the separation of biomass after the



metal biosorption is accelerated using a flocculent strain of *S. cerevisiae*. Additional work is recommended to be undertaken to determine this.

- What entice the industry to switch to Biosorption technology? To answer this questions, metal industry's perceived disadvantages or barriers for biosorption adoption needs to be evaluated, biosorption competitors needs to be identified - need to know who owns this market space, and if they have a strong position in the market. These market search criteria need to be analyzed to find out the potential opportunities for biosorption technology.
- This research showed that biosorption of metal-contaminated waters offers an inexpensive and environmentally-friendly technique that can have enormous advantages over traditional treatment methods. However, despite the advantages of biosorption method, its potential in treatment of real industrial wastewaters is yet to be fully discovered. Future research will require focus on removal of mixture of organics and metals using biosorption process.

Each of the chapters in thesis corresponded to a paper either published or submitted for publication.

# CURRICULUM VITAE

	<b>Shahram Amirnia</b>
<b>Education</b>	<ul style="list-style-type: none"> <li>▪ <b>Ph.D.</b>, Chemical &amp; Biochemical Engineering with Environment &amp; Sustainability, University of Western Ontario, Department of Chemical &amp; Biochemical Engineering, London, ON, 2015</li> <li>▪ <b>M.E.Sc.</b>, Chemical &amp; Biochemical Engineering with Environmental Science, University of Western Ontario, Department of Chemical &amp; Biochemical Engineering, London, ON, 2008</li> <li>▪ <b>B.Eng.</b>, Chemical Engineering – Gas Industries, Sharif University of Technology, Department of Chemical &amp; Petroleum Engineering, Tehran, (Summer co-op: Tabriz Refinery)</li> </ul>
<b>Honours and Awards</b>	<ul style="list-style-type: none"> <li>▪ <b>OGSST</b> (Ontario Graduate Scholarship in Science and Technology), The University of Western Ontario, 2010</li> <li>▪ <b>Award of Excellence</b>, Centre for Environment &amp; Sustainability, The University of Western Ontario, 2010</li> <li>▪ <b>Teaching Award</b>, Society of Graduate Student (SOGS), University of Western Ontario, 2009</li> <li>▪ <b>Julie Lassonde Scholarship</b>, Faculty of Engineering, The University of Western Ontario, 2008</li> <li>▪ <b>Ross &amp; Jean Clark Scholarship</b>, Faculty of Engineering, The University of Western Ontario, 2007</li> <li>▪ <b>Shell Sweeney Award</b>, GTA Union, The University of Western Ontario, 2007</li> </ul>

<b>Work Experience</b>	<ul style="list-style-type: none"> <li>▪ <b>Teaching/Research Assistant</b> - The University of Western Ontario, London, ON, 2007 – 2014</li> <li>▪ <b>Associate</b> – Western Regional Office of PEO (Professional Engineers Ontario), The University of Western Ontario London, ON, 2012 – 2015 (part-time)</li> <li>▪ <b>Business Analyst Intern</b> - Trojan Technologies (Business Development Department), London, ON, 2011</li> <li>▪ <b>Polypropylene Plant Supervisor – Process Engineer</b> (50 KT/y homo-polymer plant) - Polynar Polypropylene Plant, East Azerbaijan, Tabriz, 1999 – 2005</li> </ul>
<b>Publications and Conferences</b>	<ul style="list-style-type: none"> <li>▪ <b>Peer-Reviewed Journal Papers:</b> <ul style="list-style-type: none"> <li>[1] Amirnia S., Margaritis A., Ray M.B., Heavy metals removal from aqueous solutions using <i>Saccharomyces cerevisiae</i> in a novel continuous bioreactor–biosorption system, Chemical Engineering Journal, 264, (2015) 863–872.</li> <li>[2] Amirnia S., de Bruyn J.R., Bergougrou M.A., Margaritis A., Continuous rise velocity of air bubbles in non-Newtonian biopolymer solutions, Chemical Engineering Science, 94 (2013) 60-68.</li> <li>[3] Amirnia S., Margaritis A., Ray M.B., Adsorption of mixtures of toxic metal ions using non-viable cells of <i>Saccharomyces cerevisiae</i>, Adsorption Science &amp; Technology, 30, 1 (2012), 43-64.</li> </ul> </li> <li>▪ <b>Conference Papers:</b> <ul style="list-style-type: none"> <li>[1] S. Amirnia, A. Margaritis, M.B. Ray, Use of Yeast Cells of <i>S. cerevisiae</i> for Removal of Cu (II) Ions in a Continuous System: an Incentive for Promoting Biosorption Technology, Canadian Society of Chemical Engineering Conference (2014), Niagara Falls, Ontario, Canada.</li> <li>[2] Shahram Amirnia, A. Margaritis, M.B. Ray, “Biosorption Process for Simultaneous Removal of Coexistent Heavy Metals from Aqueous Solutions, Canadian Society of Chemical Engineering Conference (2011), London, Ontario, Canada.</li> <li>[3] Shahram Amirnia, A. Margaritis, M.B Ray, “Bio-adsorption, a method to remove heavy metals from industrial wastewaters”, 1st Annual</li> </ul> </li> </ul>

	<p>Colloquium of Water and Environmental Research, University of Western Ontario (2011), London, Ontario, Canada.</p> <p>[4] Shahram Amirnia, A. Margaritis, M.B. Ray, “Efficiency of Pb(II) Removal from Contaminated Waters by Yeast Species <i>Saccharomyces cerevisiae</i>”, 25th Annual Environmental Science &amp; Engineering Conference (2011), Cornwall, Ontario, Canada.</p> <p>[5] Shahram Amirnia, A. Margaritis, M.B. Ray, “Biosorption Process for Treatment of Heavy Metal Contaminated Waters”, Research Bridges (2011), Sarnia, Ontario, Canada.</p> <p>[6] Shahram Amirnia, A. Margaritis, M.B. Ray, “Adsorptive Performance of Yeast Cells to Remove Heavy Metals from Wastewaters”, 40th Annual WEAO Technical Symposium and OPCEA Exhibition, (2011), Westin Harbour Castle, Toronto, Ontario, Canada.</p> <p>[7] Amirnia S., Ray M.B., Margaritis A., (2010), “Adsorptive Performance of Yeast Cells to Remove Heavy Metals from Wastewaters”, 40th Annual WEAO Technical Symposium, Toronto, Canada.</p> <p>[8] Amirnia S., Margaritis A., Ray M.B., “Concentration, pH, and Surface Charge Effects on Copper Biosorption by <i>Saccharomyces cerevisiae</i>”, 7th Annual Earth Day Colloquium (2010), London, Ontario, Canada.</p>
--	--